JACOBS UNIVERSITY

Brian W. Alexander

Trace element analyses in geological materials using low resolution inductively coupled plasma mass spectrometry (ICPMS)

Technical Report No. 18
August 2008

School of Engineering and Science

Abstract

The benefits of inductively coupled plasma mass spectrometry (ICPMS) for geochemical studies include excellent instrument sensitivity for determining a large number of elements (<40) with high precision, and the ability to analyze numerous samples relatively quickly (minutes per sample). This study describes the ICPMS methods employed within the Jacobs University Bremen (JUB) Geochemistry Lab for determining the concentrations of 32 trace metals in different geological materials. The quality of the analytical data is discussed in the context of repeated analyses of certified reference materials (CRMs) commonly used in geochemical research.

The average analytical precision of the concentration measurements for all rock types discussed, reported as percent relative standard deviation, is better than ±3% for eleven elements (Ti, Co, Sr, Y, Zr, Ba, La, Ce, Pr, Nd, Pb), between ±3-5% for sixteen elements (Sc, Ni, Rb, Nb, Sm, Eu, Gd, Tb, Dy, Ho, Er, Tm, Yb, Lu, Th, U), and between ±5-8% for only five elements (Mo, Cs, Hf, Ta, W). The analytical accuracy of the data, determined from comparisons between measured elemental concentrations in various CRMs with published reference values, is considered excellent for 31 of 32 elements, with the exception being accurate measurements of Ti at high concentrations in the analytical solution (>10 mg/kg). However, some elements suffer from interferences due to the major element content of particular rock types, and are unlikely to be quantifiable when present at low concentrations. This includes Co in carbonate rocks, and Nb in Fe-rich rock types. The concentrations of many trace metals in some CRMs are poorly constrained, and early published datasets appear to frequently overestimate the abundances of these elements.

Table of Contents

List of Figures

List of Tables

1. Introduction

The advent of inductively coupled plasma mass spectrometry (ICPMS) has proven enormously beneficial to geochemical studies. Since commercialization of ICPMS technology in the early 1980's, ICPMS has become the method of choice for geochemical analyses, and is ideal for trace metal determinations and isotopic studies of many elements. The widespread implementation of ICPMS technology results from its ability to quickly quantify a large number of elements (>40) in geological samples on a routine basis. Additionally, ICPMS offers instrument sensitivity that permits quantification of ng/kg (parts-per-trillion, ppt) concentrations of many elements regardless of sample matrix, and as such is ideally suited for studies of geochemically diverse samples. This report describes the ICPMS analytical methods employed within the Geochemistry Lab at Jacobs University Bremen (JUB) and includes a critical discussion of the precision and accuracy of these methods.

The Geochemistry Lab at JUB is relatively new, with construction of the lab completed in the Summer of 2004. In the Fall of 2004 a PerkinElmer DRC-e quadrupole inductively coupled plasma mass spectrometer (ICPMS) was installed, which is the principal analytical instrument for determinations of trace metal concentrations. This report is not intended to provide detailed information regarding basic ICPMS principles and technology, and the reader is referred to Thomas (2003) for a thorough review. When samples are decomposed into liquid form, ICP instruments are ideal for multi-element geochemical analyses, as they allow relatively fast sample introduction into mass spectrometers, and are readily automated for the processing of large numbers of samples.

This report describes the steps utilized at JUB to obtain accurate trace metal concentration data in a variety of rock types, and proceeds from the processing of hand samples to the decomposition of sample powders, and finally to the methods employed to ensure the accuracy of the reported data. Sample preparation techniques are not the primary focus of this paper, and are only briefly discussed. Rather, considering the relatively short existence of the Geochemistry Lab at JUB and the necessary development of accurate and routine geochemical analytical techniques, most of the discussion will focus on a critical assessment of the methods employed in ICPMS trace metal determinations in a variety of geologic materials, and the relative precision and accuracy of these measurements.

2. Sample preparation

The majority of this report focuses on geochemical analyses of rock reference standards issued by governmental or research organizations. However, a brief description is given of the sample preparation methods used for natural rock samples that are collected as part of research studies at JUB. Rock samples, whether from outcrops or drillcores, are first processed by hand-trimming to avoid weathering rinds, quartz/calcite veining, or obvious alteration features. A geologist's hammer is used to produce roughly 50 g of small, 1-3 cm pieces that are crushed in a Fritsch Pulverisette 1 jaw crusher to obtain chips approximately 0.5 cm in size. Harder rock types (e.g., chert) are processed more finely to produce smaller sizes (≤0.3 cm chips). Sample chips are rinsed thoroughly with deionized water to remove dust and dried overnight in a laboratory oven at ~110 °C, after which approximately 20 g of chips are hand-picked to produce homogeneous samples devoid of secondary mineral veins. The sample chips are then powdered in a Fritsch Pulverisette 6 planetary mill using agate balls in a sealed agate mortar.

3. Sample decomposition

The ICPMS used in the JUB Geochemistry Lab is configured to accept samples in liquid form only, though ICP instruments with laser-ablation attachments for the analyses of solid samples are increasingly common. One advantage of converting samples to liquid form is that any effects due to heterogeneities within the sample (e.g., inclusions or minor mineral phases) are removed, and this approach is typically termed a 'whole-rock' analysis. The common method for rocks and minerals is to decompose the sample in strong mineral acids at elevated temperatures and pressures. The decomposition procedures used at JUB, and in fact, many of the ICPMS techniques as well, have been adapted from methods developed by P. Dulski at the GeoForschungsZentrum (GFZ) in Potsdam, Germany (see Dulski, 1994; Dulski, 2001).

Two sample decomposition methods are currently employed: the first is a high-temperature, high-pressure decomposition utilizing concentrated hydrofluoric (HF) and perchloric ($HClO_4$) acids that is suitable for the total dissolution of silicate-bearing samples (e.g., iron-formations, basalts), while the second method is a low-temperature nitric acid (HNO_3) decomposition used for dissolving carbonate samples such as limestones and dolomites. It is important to note that the HF-$HClO_4$

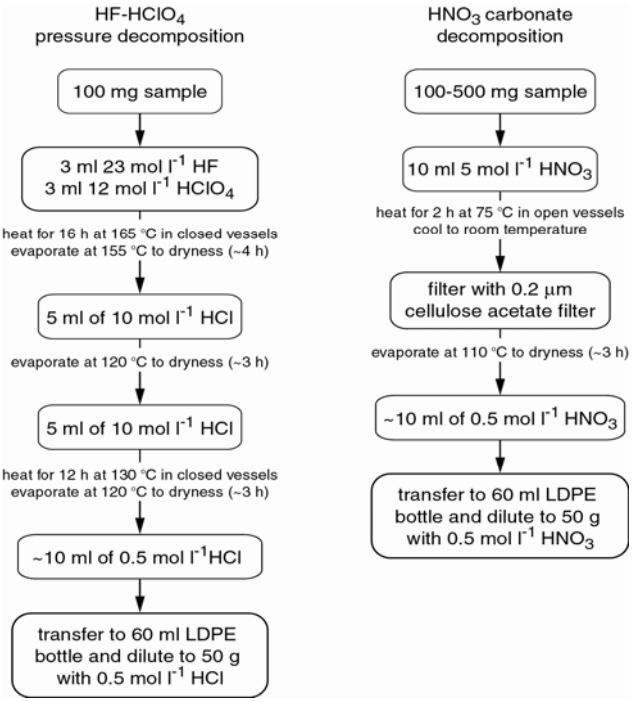

Figure 1. Flow-chart diagram of the two sample decomposition methods employed within the Geochemistry Lab at JUB for silicate-bearing samples (HF-$HClO_4$ pressure decomposition) and carbonate samples such as limestones and dolomites (HNO_3 carbonate decomposition). All reagents used are super-, ultra-pure grade and dilutions are performed with deionized water (18.2 MΩ). Modified after Dulski (2001).

decomposition provides complete dissolution of the sample powder, primarily due to the ability of HF to dissolve silicate minerals, whereas the low-temperature HNO_3 decomposition is considered to dissolve only the carbonate mineral fraction of the sample powder. The HNO_3 decomposition method, referred to as the 'carbonate decomposition', will not dissolve refractory organic carbon and/or primary silicate minerals. The carbonate decomposition will attack and leach secondary minerals such as clays, though the extent of this effect will vary as a function of sample composition. The two methods are schematically described in Figure 1, and most of the data and discussion presented here will focus on the HF-$HClO_4$ decomposition method. Regardless of the method chosen, every sample decomposition contains at least one certified reference material (CRM) which is treated analytically as an unknown sample, and which is considered to provide the best estimate of the accuracy of the complete decomposition method and ICPMS analysis. The CRMs commonly used in the Geochemistry Lab are listed in Table 1 and represent a variety of rock types, and for any individual sample decomposition a CRM is chosen that most closely resembles the rock type of the samples.

Table 1. Certified reference materials (CRM) used as quality assurance standards for routine sample decomposition and ICPMS measurements within the JUB Geochemistry Lab.

CRM	description	number of sample decompositions	issuing organization
FeR-2	Al-rich iron-formation	3	CCRMP Canadian Certified Reference Materials Project 555 Booth Street Ottawa, Ontario K1A 0G1 Canada
FeR-4	iron-formation	2	
IF-G[a]	Isua iron-formation	2 first lot 4 second lot	IWG-GIT International Working Group - Groupe International de Travail Service d'Analyse des Roches et des Minéraux, CPRG-CNRS, B.P. 20 Vandoeuvre-lés-Nancy Cedex, France
SCo-1	silty marine shale	4	USGS United States Geological Survey U.S. Geological Survey, Box 25046, MS 973 Denver, CO 80225, USA
SGR-1b	carbon-rich shale	3	
BHVO-2	Hawaiian basalt	7	
JMn-1	manganese nodule	4	GSJ Geological Survey of Japan available from: Seishin Trading Co., 1-2-1 Sanshin Bulding, Sannomiya, Tyuo-ku, Kobe, 650-0021, Japan
JCh-1	chert	3	
JDo-1	dolomite	12 (5 HF-$HClO_4$)[b] (7 HNO_3) [b]	

[a] original IF-G powder (first lot) no longer available, and newly processed IF-G powder (second lot) available 2006.
[b] refers to decomposition method used.

Sample decompositions were performed in 30 ml polytetrafluoroethylene (PTFE) vessels using a PicoTrace DAS acid digestion system (Bovenden**,** Germany). As the DAS system contains 16 PTFE vessels, routine sample decompositions consist of 14 samples, one CRM, and one method blank. Typically, these decompositions will convert 100 mg of sample powder into 50 g of a clear sample liquid, in a matrix of either 0.5 molar (moles/l, M) HCl or 0.5 M HNO_3. This dilution factor of 500 produces a total dissolved solid (TDS) content of 0.2% in the sample liquid (assuming no loss of volatiles such SiF_4 or CO_2), which is generally considered the maximum TDS content practical for routine ICPMS measurements. The ideal dilution factor for a particular rock or mineral reflects the balance between two competing effects; the minimization of matrix effects in the sample by utilizing high dilution factors, versus the detection and quantification limits imposed by the method and instrumentation. Typical dilution factors employed within the JUB Geochemistry Lab for ICPMS measurements range from 250 for very pure, trace metal-poor limestones and cherts, to ≥5000 for trace metal-rich samples such as marine ferromanganese crusts and nodules. The use of dilution factors <500 for cherts (SiO_2) and limestones ($CaCO_3$) is possible because much of the original sample powder is converted to volatile species

during decomposition (SiF_4 and CO_2, respectively), thereby reducing the total dissolved solid content of the ICPMS sample solution.

Cleaning of the DAS system between sample batches is accomplished by heating an acid mixture of 5 ml of 15 M HNO_3 and 1 ml 23 M HF in the sealed PTFE vessels for 12 hours at ~165 °C. Memory effects within the DAS system for the elements considered in this research have never been observed, and decomposition method blanks for these elements are essentially controlled by good laboratory practices and the purity of the reagents used in the decomposition.

4. ICPMS methods

4.1. Analyzed elements and mass interferences

Currently, the concentrations of 32 elements are determined during ICPMS analyses conducted within the JUB Geochemistry Lab. Initially, and until June 2006, concentrations of only 24 of these 32 elements were determined during routine ICPMS analyses, and the current element list and the scanned isotopic masses are presented in Table 2. Wherever possible, multiple isotopes are monitored for any given element, as the well-known abundances of natural isotopes provide a method for checking the quality of the analysis. This is accomplished by normalizing the signal intensity in cps (counts-per-second) for an isotope by its abundance. If no isotopic fractionation has occurred in the sample, and the measured intensities are not affected by interferences (e.g., interferences from isotopes of other elements), then these normalized intensities should be equivalent for all isotopes of an element.

For example, the rare earth element (REE) Yb is monitored at three isotopic masses, ^{171}Yb, ^{172}Yb, and ^{174}Yb, which have natural isotopic abundances of 14.3%, 21.9%, and 31.8%, respectively. If the following holds true:

$$\left(\frac{^{171}\mathrm{Yb}_{cps}}{0.143}\right) = \left(\frac{^{172}\mathrm{Yb}_{cps}}{0.219}\right) = \left(\frac{^{174}\mathrm{Yb}_{cps}}{0.318}\right) \qquad (1)$$

then these isotopes of are suitable for quantifying the concentration of Yb in the analyzed solution. The approach described by Eq. 1 is not suitable if some process, whether natural or analytical, has fractionated the monitored isotopes for a given element. Of the 32 elements quantified by ICPMS measurement, only Pb may be fractionated in such a manner due to natural processes occurring within the sample.

Table 2. Elements analyzed in routine ICPMS determinations, specific isotopes measured, interfering polyatomic species, and instrument quantification limits (IQLs) in HCl and HNO_3 acid matrices. See text for details. The eight elements in bold type were added to the routine ICPMS analysis in June 2006.

				average instrument quantification limit in rock/mineral samples (mg/kg)	
	element	monitored masses	observed/corrected interferences	0.5 M HCl matrix (n = 22)*	0.5 M HNO_3 matrix (n=4)*
1	**Sc**	^{45}Sc	$^{12}C^{16}O_2{}^{1}H^+$, $^{13}C^{16}O_2{}^+$	0.758	0.233
2	**Ti**	^{47}Ti, ^{49}Ti	$^{14}N^{16}O_2{}^{1}H^+$, $^{12}C^{35}Cl^+$, $^{14}N^{35}Cl^+$	1.94	0.284
3	**Co**	^{59}Co	$^{42}Ca^{16}O^{1}H^+$, $^{43}Ca^{16}O^+$, $^{24}Mg^{35}Cl^+$	0.009	0.020
4	**Ni**	^{60}Ni, ^{62}Ni	$^{14}N_2{}^{16}O_2{}^+$, $^{44}Ca^{16}O^+$, $^{25}Mg^{35}Cl^+$, $^{25}Mg^{37}Cl^+$, $^{27}Al^{35}Cl^+$	0.077	0.168
5	Rb	^{85}Rb	$^{48}Ca^{37}Cl^+$	0.019	0.009
6	Sr	^{88}Sr	$^{48}Ca^{40}Ar^+$	0.047	0.280
7	Y	^{89}Y	$^{54}Fe^{35}Cl^+$	0.003	0.004
8	Zr	^{90}Zr, ^{91}Zr	$^{55}Mn^{35}Cl^+$, $^{40}Ar^{16}O^{35}Cl^+$, $^{40}Ca^{16}O^{35}Cl^+$, $^{56}Fe^{35}Cl^+$	0.018	0.012
9	**Nb**	^{93}Nb	$^{40}Ar^{16}O^{37}Cl^+$, $^{40}Ca^{16}O^{37}Cl^+$, $^{56}Fe^{37}Cl^+$	0.014	0.015
10	**Mo**	^{95}Mo, ^{97}Mo	$^{55}Mn^{40}Ar^+$, $^{44}Ca^{16}O^{35}Cl^+$, $^{44}Ca^{16}O^{37}Cl^+$	0.069	0.076
11	Cs	^{133}Cs		0.004	0.004
12	Ba	^{135}Ba, ^{137}Ba		0.017	0.055
13	La	^{139}La		0.003	0.006
14	Ce	^{140}Ce		0.003	0.005
15	Pr	^{141}Pr		0.002	0.004
16	Nd	^{145}Nd, ^{146}Nd		0.005	0.007
17	Sm	^{147}Sm, ^{149}Sm		0.005	0.005
18	Eu	^{151}Eu, ^{153}Eu	$^{135}Ba^{16}O$, $^{134}Ba^{17}(OH)$, $^{137}Ba^{16}O$, $^{136}Ba^{17}(OH)$	0.002	0.004
19	Gd	^{158}Gd, ^{160}Gd	$^{142}Nd^{16}O$, $^{142}Ce^{16}O$, $^{141}Pr^{17}(OH)$, $^{144}Nd^{16}O$, $^{144}Sm^{16}O$, ^{160}Dy, $^{141}Pr^{19}(OH)$, $^{143}Nd^{17}(OH)$	0.003	0.005
20	Tb	^{159}Tb	$^{141}Pr^{18}O$, $^{143}Nd^{16}O$, $^{142}Nd^{17}(OH)$, $^{142}Ce^{17}(OH)$	0.002	0.004
21	Dy	^{161}Dy, ^{163}Dy	$^{145}Nd^{16}O$, $^{144}Nd^{17}(OH)$, $^{144}Sm^{17}(OH)$, $^{147}Sm^{16}O$, $^{146}Nd^{17}(OH)$	0.003	0.004
22	Ho	^{165}Ho	$^{149}Sm^{16}O$, $^{148}Nd^{17}(OH)$, $^{148}Sm^{17}(OH)$	0.002	0.004
23	Er	^{166}Er, ^{167}Er	$^{150}Nd^{16}O$, $^{150}Sm^{16}O$, $^{149}Sm^{17}(OH)$, $^{151}Eu^{16}O$, $^{150}Nd^{17}(OH)$, $^{150}Sm^{17}(OH)$	0.002	0.006
24	Tm	^{169}Tm	$^{153}Eu^{16}O$, $^{152}Sm^{17}(OH)$, $^{134}Ba^{35}Cl$	0.002	0.003
25	Yb	^{171}Yb, ^{172}Yb, ^{174}Yb	$^{155}Gd^{16}O$, $^{154}Gd^{17}(OH)$, $^{154}Sm^{17}(OH)$, $^{134,136}Ba^{37,35}Cl$, $^{135,137}Ba^{37,35}Cl$, $^{156}Gd^{16}O$, $^{155}Gd^{17}(OH)$, $^{158}Gd^{16}O$, $^{157}Gd^{17}(OH)$, $^{137}Ba^{37}Cl$	0.002	0.005
26	Lu	^{175}Lu	$^{158}Gd^{17}(OH)$, $^{159}Tb^{16}O$, $^{138}Ba^{37}Cl$	0.002	0.004
27	Hf	^{178}Hf, ^{179}Hf	$^{162}Dy^{16}O$, $^{161}Dy^{17}(OH)$, $^{163}Dy^{16}O$, $^{162}Dy^{17}(OH)$	0.004	0.005
28	**Ta**	^{181}Ta	$^{165}Ho^{16}O$	0.008	0.011
29	**W**	^{182}W, ^{183}W	$^{166}Er^{16}O$, $^{167}Er^{16}O$, $^{166}Er^{17}(OH)$	0.196	0.067
30	Pb	^{206}Pb, ^{207}Pb, ^{208}Pb		0.022	0.035
31	Th	^{232}Th		0.003	0.005
32	U	^{238}U		0.002	0.004

* n equals the number of separate ICPMS runs which contained at least one Certified Reference Material (CRM), with each run consisting of a separate acid decomposition of a mixed batch of samples and CRMs, and from which the average instrument quantification limits (IQL) for solid samples were calculated. See text for details regarding the calculation of detection and quantification limits.

Fractionation between the three isotopes of Pb monitored during ICPMS analyses, ^{206}Pb, ^{207}Pb, and ^{208}Pb, will occur due to radioactive decay of U and Th within the sample. The half-lives of the respective decay series, $^{238}U \rightarrow {}^{206}Pb$, $^{235}U \rightarrow {}^{207}Pb$, and $^{232}Th \rightarrow {}^{208}Pb$, range between ~700 million to ~14 billion years (Faure, 1986). Therefore, changes in the natural modern abundances of the Pb isotopes (^{206}Pb = 24.1%, ^{207}Pb = 22.1%, ^{208}Pb = 52.4%), due to the generation of radiogenic Pb within the sample may be significant, particularly in the geologically old (>2.5 Ga) samples commonly analyzed at JUB. Therefore, only in the case of Pb is Eq. 1 not used to monitor agreement between the concentrations determined from individual isotopes for a given element. For the remaining elements with more than one atomic mass available for monitoring, the application of Eq. 1 also provides a method for identifying interferences that may be affecting isotopes of a particular element.

The issue of ions with masses similar to the isotopes of interest producing undesirable interferences in ICPMS analyses is common. The elements in geological materials most suitable for routine ICPMS analyses have masses greater than 80 atomic mass units (amu). This primarily results from the fact that lower mass elements (e.g., many transition metals) may suffer severe interferences from polyatomic species generated within the plasma during ionization of the sample. Many of these polyatomic interferences result from the use of argon as the plasma source gas in most ICPMS instruments, and the subsequent formation of Ar-oxides and Ar-hydroxides (ArO^+ and $ArOH^+$), though other interfering species may be significant due to the choice of acid used for decomposing and diluting samples (e.g., chloride and nitrogen species).

A common example of the difficulties such polyatomic interferences present is evident in determinations of Fe, in which the isotope of choice for analysis is the most abundant one, ^{56}Fe (91.72%). However, within the plasma large numbers of $^{40}Ar^{16}O^+$ ions are produced which are indistinguishable from ^{56}Fe in low-resolution ICPMS analyses. High-resolution ICPMS instruments are capable of distinguishing between the $^{40}Ar^{16}O^+$ and ^{56}Fe peaks, but can only achieve this peak resolution at the expense of ion-beam transmission efficiency and a consequent reduction in instrument sensitivity. As a result high-resolution ICPMS methods are generally not suitable for element determinations in the sub-ppb (parts-per-billion, μg/kg) range necessary for analyses of many trace metals in geological samples, unless intensive

sample preparation methods are employed which isolate and concentrate the elements of interest from undesirable matrix elements.

Table 2 contains interferences commonly observed in ICPMS analyses performed within the JUB Geochemistry Lab. The inability of the low-resolution DRC-e ICPMS to resolve interferences from the isotopes of interest does not significantly inhibit the accurate determination of the 32 elements routinely analyzed, as correcting for these interferences is possible through careful characterization and quantification of the interfering polyatomic species. The majority of these corrected interferences are for the REE (Table 2), as the REE can form significant amounts of oxide and hydroxide species during ionization. For example, at typical instrument settings as much as 3% of the Ce present in the sample solution will be ionized to $^{140}Ce^{16}O^{+}$, and the $^{140}Ce^{16}O^{+}$ ion will consequently contribute to any Gd determinations that utilize the ^{156}Gd isotope. The isotopes monitored for quantification of the REE are therefore carefully selected to minimize these effects and maximize analytical accuracy, though as seen in Table 2 a significant number of corrections are necessary. While implementing such corrections is not trivial, uncorrected values may result in reported concentrations for REE elements that are erroneously high by as much as several percent, as illustrated by the example with CeO^{+}.

Corrections for polyatomic interferences are performed mathematically, typically offline using commercially available spreadsheet software such as Microsoft Excel (the approach followed at JUB). Interferences are identified and quantified by analyzing solutions that contain relatively high concentrations (50-1000 μg/kg) of a single element, and surveying the range of masses that might be affected by interferences produced by oxide, hydroxide, chloride, or nitrogen species of that particular element. For the REE, the most significant interferences are generated by REE-oxides or -hydroxides, and therefore are found at 16 and 17 amu above the interfering element (i.e., $REE^{16}O^{+}$ and $REE^{16}O^{1}H^{+}$). The measured intensities of the interfering element, and the various interferences it produces, allow calculation of ratios expressing the relative amount of interfering species generated as a function of the concentration of the interfering element. For example, if as mentioned above, 3% of ^{140}Ce in the sample is ionized to $^{140}Ce^{16}O^{+}$ (i.e., $^{140}Ce^{16}O^{+}/^{140}Ce$ equals 0.03), and if the Ce concentration in the sample corresponds to a measured intensity of 100,000

cps, then 3000 cps must be subtracted from any signal intensity measured at mass 156 (e.g., ^{156}Gd or ^{156}Dy). For a detailed treatment of possible REE interfering species and examples of calculations of the appropriate correction ratios the reader is referred to Dulski (1994). Considering the number of isotopically different REE-oxyhydroxide species that may be generated (Table 2), such corrections may seem unwieldy, but determination of these correction ratios is not necessary with each individual ICPMS analysis. The approach adopted here, and following the methods of Dulski (1994), requires periodic determination of these correction ratios at very specific ICPMS instrument settings which consistently produce similar $REEO(H)^+/REE^+$ values, and then ensuring that sample analyses are always performed at identical ICPMS instrument settings. For the analyses performed within the JUB Geochemistry Lab this entails tuning and optimization of the ICPMS so that CeO^+/Ce^+ does not deviate from 0.029 ±0.001.

4.2. External calibration

The determination of trace metal concentrations in sample solutions is performed using laboratory prepared external calibration standards. This procedure consists of using commercially available 1000 mg/l single element standards (Inorganic Ventures, USA) that are combined to form 1 mg/kg (parts-per-million, ppm) multi-element stock solutions. The 1 mg/kg stock solutions are prepared in acid matrices that are similar to those present in the 1000 mg/l single element standards, which are typically ~0.5 M HNO_3 (2.2% v/v). These multi-element stock solutions are further diluted immediately prior to an individual ICPMS analysis to produce 10 and 20 μg/kg calibration standards, which are analyzed in conjunction with the sample solutions. Preparation of these external calibration standards is presented schematically in Figure 2.

Ideally, the determination of elemental concentrations in sample solutions would proceed using the highly accurate method of standard addition, in which the sample solutions are split into a minimum of three aliquots, two of which would be spiked with the elements of interest at different concentrations. By comparing the ICPMS response for these three solutions it is possible to calculate the concentrations of the spiked elements in the non-spiked sample solution. The greatest advantage of the standard addition method is that it minimizes effects caused by matrix differences

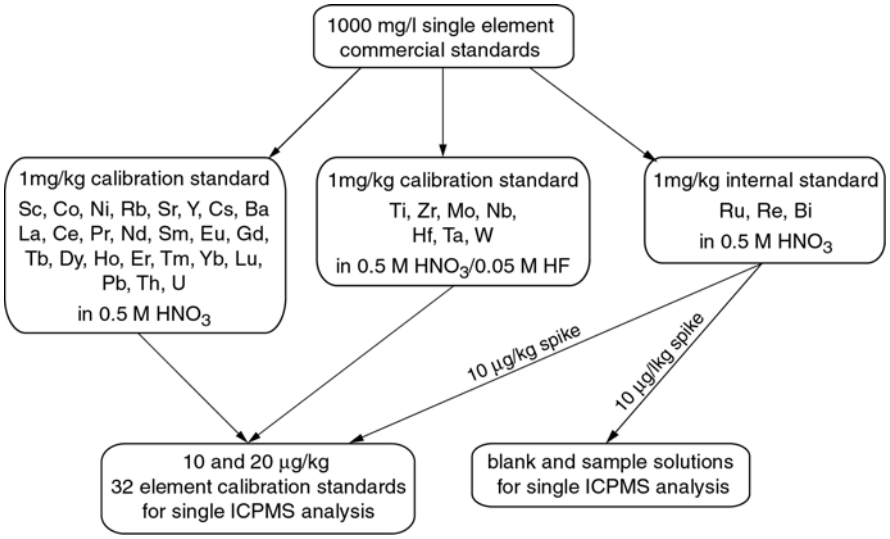

Figure 2. Diagram showing preparation of multi-element standards used for ICPMS external calibration and internal standardization. Note that immediately prior to an ICPMS analysis, all solutions receive 10 µg/kg of the Ru, Re, Bi internal standard (see text for details). Trace amounts of HF (0.05 M) are used to stabilize high field strength elements (Ti, Zr, Nb, Ta, etc.).

between samples and calibration standards, as the standards used for calibration are incorporated directly into aliquots of the sample solution itself. The greatest drawback to the standard addition method is that it does not lend itself to multi-element analyses, as it is most accurate when the spike concentrations for an individual element are similar to the unknown concentration in the sample. For geological samples, in which concentrations of trace metals routinely range over three orders of magnitude, this would necessitate the creation of calibration standards containing 32 potentially different, customized element concentrations, which assumes some pre-existing knowledge of these elemental concentrations in the unknown sample. Combined with the fact that every sample would require at least triple the ICPMS analysis time, the standard addition calibration method is generally not recommended for routine, multi-element ICPMS analyses of geological samples.

However, the external standard calibration method suffers from the aforementioned 'matrix effects'. These matrix effects are particularly troublesome for analyses of geological materials which contain significant amounts of dissolved solids at typical ICPMS dilution factors. For example, an iron-formation with 90% Fe_2O_3 that is diluted 1000x would produce a solution containing more than 600 ppm Fe, and this is generally the maximum dilution suitable for pure iron-formation samples. High dissolved metal concentrations tend to suppress ICPMS instrument sensitivity in a

variety of ways. These range from reductions in ionization efficiency within the plasma to the deposition of ion-beam inhibiting sample material (e.g., salts or metal-oxides) in the interface region between the plasma source and mass spectrometer. Therefore, there are two sample dependent matrix effects which need to be addressed for routine geochemical analyses, one of which may suppress analyte intensities within an individual sample (e.g., ionization efficiency), and a second effect which may induce a time-dependent signal drift due to high TDS content in the samples.

Correcting for these sample matrix effects is achieved by using internal standardization, in which *all* ICPMS solutions (blanks, external calibration standards, CRMs, and samples) are spiked with an equivalent amount of an internal standard. The applicability of this method is critically dependent upon the condition that the chosen internal standard must not be present in appreciable amounts in any of the ICPMS solutions (blanks, standards, or samples). For this purpose three elements are used for internal standardization following the methods of Doherty (1989); Ru, Re, and Bi. These three elements are ideal as they have low blank values for the reagents used in the decomposition and ICPMS methods, are present at very low concentrations in the majority of geological materials, produce no significant interference effects for the elements of interest, and are themselves free of significant interferences for their monitored isotopes (^{101}Ru, ^{187}Re, and ^{209}Bi).

The default ICPMS analysis consists of running samples in small batches bracketed by calibration standards and blanks, and is described in Figure 3. A typical ICPMS analysis consists of four to six of these small sample batches run consecutively in a single day, and is called an *ICPMS run*. Prior to analysis, appropriate sample dilution factors are determined based upon the sample type, and samples are diluted either in 0.5 M HCl for HF-$HClO_4$ pressure decompositions, or in 0.5 M HNO_3 for carbonate decompositions. Acid and method blanks, calibration standards, as well as CRMs are diluted in the same acid matrix as the samples, and all solutions are spiked with 10 μg/kg of the Ru, Re, Bi internal standard. Matching the acid matrix of the samples and calibration standards is crucial, as calibration standards prepared in HNO_3 typically display ~10% greater instrument response than calibration standards prepared in HCl. While HNO_3 is more commonly used for preparation of ICPMS solutions as a result of this improved instrument response (as well as fewer interfering polyatomic species at low masses), it does not produce

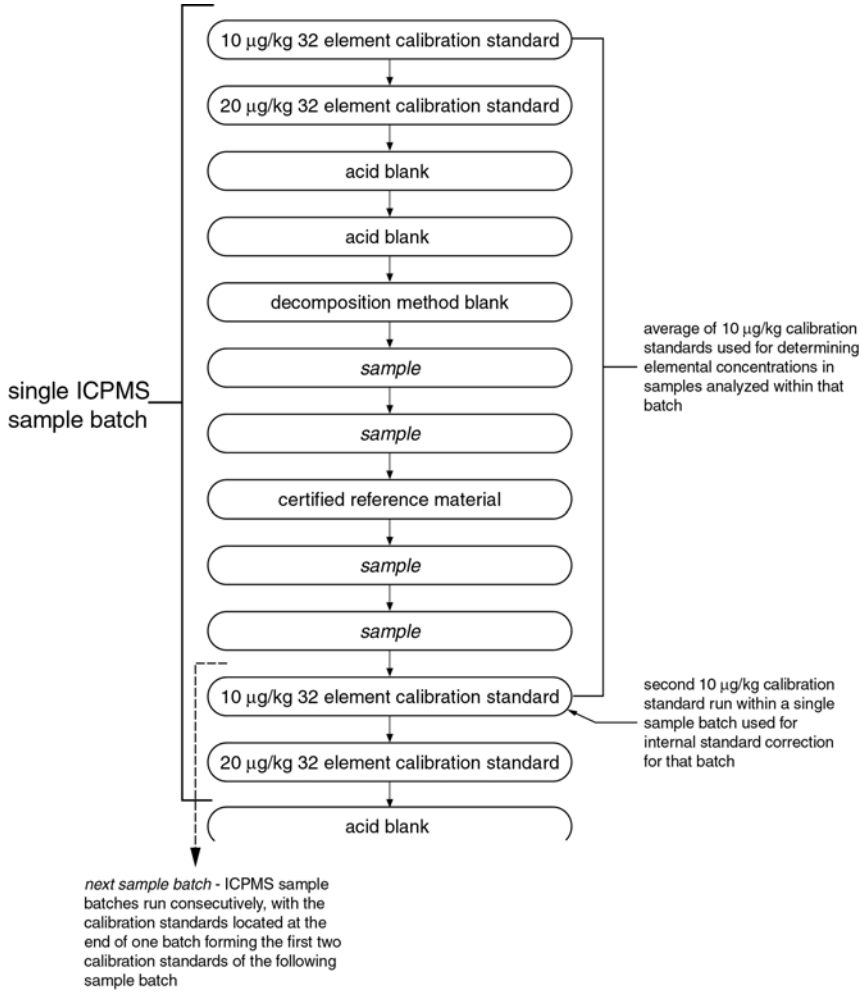

Figure 3. Diagram depicting the order in which various blanks, calibrations standards, and samples are analyzed for a single ICPMS sample batch. A typical ICPMS analysis consists of four or more sample batches run consecutively. The acid blank refers to the 0.5 M HCl or HNO_3 acid matrix used for diluting *all* ICPMS solutions for a given analysis. Note that *all* solutions are spiked with 10 μg/kg of the internal standard, and that Ru, Re, and Bi in the second 10 μg/kg 32 element calibration standard within a batch are used for application of internal standard corrections for that batch. The certified reference material is a commercially available geostandard that is included within every sample decomposition and run repeatedly with every sample batch. See text for details.

stable solutions with respect to high field strength elements (HFSE) such as Zr, Nb, Hf, and Ta (Münker, 1998), and therefore these elements are stabilized using trace amounts of HF in the stock 1 mg/kg calibration solutions. This stability issue for HFSE in dilute HNO_3 (0.5 M) means that samples processed using the carbonate decomposition method should be analyzed by ICPMS within 24 hours following completion of the sample decomposition. For samples processed using the HF-$HClO_4$ pressure decomposition and diluted in 0.5 M HCl, samples are also analyzed immediately, though this acid matrix appears sufficient for stabilizing HFSE on

Table 3. Change in HFSE concentration in IF-G iron-formation stored in 0.5 M HCl over a period of ~11 months.

mg/kg	IF-G 27-Oct-06*	IF-G 16-Sep-07	% difference 2007/2006
Ti	23.9	23.5	-1.88
Zr	0.903	0.865	-4.24
Nb	0.914	0.876	-4.12
Mo	0.562	0.604	7.50
Hf	0.0246	0.0227	-7.57
Ta	0.168	0.157	-6.71
W	251	248	-1.35

* date of ICPMS analysis.

longer time scales, as measured HFSE values in the IF-G geostandard change by less than 8% over a period of ~11 months (Table 3).

4.3. Data collection

Unknown samples that are analyzed within an ICPMS run (i.e., in a single day, as part of one or more sample batches that are analyzed consecutively), are generally measured once, whereas blanks, calibration standards, and CRMs are measured repeatedly. Prior to beginning any ICPMS measurements, the instrument is prepared by performing three consecutive analyses of the CRM solution to be used during that ICPMS run. This has the primary effect of conditioning the cones located in the interface region between the plasma and the mass spectrometer. These cones are instrumental in shaping the ion beam and must be periodically cleaned, and this pre-treatment significantly stabilizes signal intensities. A rinse solution is pumped through the sample introduction system before the measurement of any solution, be it a blank, standard, or sample. Nitric acid (0.5 M) is the typical rinsing agent, and a six minute rinsing step has been found effective for minimizing memory effects. An ICPMS measurement of any single solution consists of 60 individual scans through the mass range ^{45}Sc to ^{238}U using peak hopping mode and a peak dwell time of 50 ms. For any individual element, these 60 scans are then averaged to produce the raw ICPMS data in cps. Scanning time for a single solution is approximately 3.5 minutes, and when rinsing time, the time required for the autosampler to move to a different

solution, etc., are considered, the total amount of time necessary to measure any single solution is ~10 minutes.

4.4. Internal standardization

After an ICPMS analysis, the raw data in cps are transferred to an Excel spreadsheet for the application of three separate mathematical corrections. These corrections are applied to *all analytical solutions* (blanks, calibration standards, samples) in the following order: 1) internal standard corrections; 2) corrections for interfering polyatomic species; and 3) blank corrections. The internal standard (IS) correction using ^{101}Ru, ^{187}Re, and ^{209}Bi follows the method of Doherty (1989). The general application of the internal standard correction method is illustrated by the following equation, where Ru is used to correct the signal intensity of Sr:

$$I_{Sr,sample}^{corr} = I_{Sr,sample} * \left(\frac{I_{Ru,std}}{I_{Ru,sample}} \right) \quad (2)$$

where I is raw intensities in cps, $I_{Ru,std}$ is the measured intensity for the second 10 μg/kg calibration standard within an ICPMS sample batch (see Fig. 3), and I^{corr} is the corrected intensity. The term in parentheses in (2) is the *IS correction factor*. This approach assumes that any matrix or instrument drift effects that suppress or enhance the signal intensity for Sr proportionally affect the Ru signal intensity, and internal standard corrections are most effective when the element of interest and the IS are of similar mass (Thompson and Houk, 1987). Therefore, ^{101}Ru is used as an internal standard for all elements with atomic masses lower than 101 (Sc, Ti, Co, Ni, Rb, Sr, Y, Zr, Nb, and Mo), and ^{209}Bi is used for elements with masses greater than 209 (Th and U). For analytes with masses between Ru and Re, the IS correction factor term in (2) is expanded to a mass-dependent linear function between ^{101}Ru and ^{187}Re:

$$IS\ correction\ factor = \left(\frac{I_{Re,std}}{I_{Re,sample}} - \frac{I_{Ru,std}}{I_{Ru,sample}} \right) * \frac{\left(M_{analyte} - M_{Ru}\right)}{\left(M_{Re} - M_{Ru}\right)} + \frac{I_{Ru,std}}{I_{Ru,sample}} \quad (3)$$

where M is the atomic mass number for Ru, Re, and the analyte of interest. This treatment provides an IS correction factor that varies smoothly as a function of mass between ^{101}Ru and ^{187}Re. Internal standard correction factors typically range from

0.90, corresponding to an anomalous increase in measured analyte intensities in the sample, to 1.10, indicating an anomalous decrease in measured analyte intensities. Experience has shown that analytical accuracy is often compromised when IS correction factors deviate from unity by more than ~15% (i.e., <0.85 or >1.15), and it may be necessary to re-analyze the samples using a different dilution factor to minimize matrix and/or drift effects.

Following internal standard corrections, interference corrections for polyatomic species are applied to the sample data. These interference corrections are applied only to elements with atomic masses between 151 (Eu) and 183 (W). A detailed treatment of the determination and application of these interference corrections is beyond the scope of this discussion, and the reader is referred to Dulski (1994). The last correction applied to the sample data before calculating elemental concentrations involves subtracting the internal standard and interference corrected blank contribution, which would be due to the reagents used in preparing the samples, and/or from any laboratory procedures.

4.5. Analytical blanks and quantification limits

Two blank contributions may be defined for the described ICPMS methods. The first is the *acid blank* value, which is used for calculating the instrument detection and quantification limits (IDLs and IQLs). As all ICPMS solutions are analyzed in a 0.5 M acid matrix (either HCl or HNO_3), the acid blank is simply the purest 0.5 M acid solution that is capable of being produced within the JUB Geochemistry Lab. Analyses of the acid blank allows the calculation of IDLs and IQLs for any given element, which represent the best achievable (ideal) ICPMS sensitivity using the available laboratory reagents. The IDL and IQL equal 3x and 10x the standard deviation of the acid blank, respectively (MacDougall and Crummett, 1980), and are best characterized through long term, repeated analyses of the acid blank, as daily fluctuations in instrument sensitivity are common. It is important to note that IDLs and IQLs calculated from the acid blank are *not* equivalent to detection and quantification limits in a solid sample, that is, in a rock or a mineral. As all solid samples are highly diluted before ICPMS analyses, IDLs and IQLs determined for solid samples equal the acid blank multiplied by the appropriate dilution factor. Table 2 lists long term average IQLs in *solid samples* for 0.5 M HCl and 0.5 M HNO_3 acid matrices.

The second blank contribution to ICPMS analyses is the *method blank*. The method blank is a solution that has been processed in exactly the same manner as a sample during the decomposition method, and represents the contamination added to a sample as a result of the decomposition method and subsequent dilution in acid. While significant amounts of concentrated acid are used in the decomposition methods, these acids (in combination with contamination from labware) contribute insignificant amounts of trace metals to rocks typically analyzed, even for trace metal-poor samples like iron-formations and dolomites (Fig. 4). Method blank values are determined for every ICPMS analysis to monitor possible contamination sources, but as a result of the above observations, ICPMS data are blank corrected by subtracting the *acid blank* intensities. Only in instances where method blank values are significantly higher than those observed in Fig. 4 are blank corrections performed using the method blank intensities. The reasoning for this approach is as follows; since the method blanks are typically below the IQLs determined from the acid blanks, the method blank is not quantifiable. Only when method blanks exceed the acid blank IQL are they used for the blank correction. It should be noted that with regard to the carbonate decomposition method, many refractory elements (e.g., Ti, Nb, Ta) are not suitable for quantification, as they are expected to be primarily hosted in silicate-bearing phases that are resistant to dissolution with nitric acid, and in particular the poor IQLs for Sc mean that it is generally not quantifiable in trace metal-poor samples regardless of the decomposition method used (Fig. 4).

5. Analytical precision

For the analyses conducted within the Geochemistry Lab at JUB, analytical precision may be defined in different ways. The highest degree of precision is expected when considering only the 60 mass scans performed during ICPMS analysis of a single sample solution. If this sample solution is periodically re-measured with time during an ICPMS run, i.e., by occasionally returning the autosampler probe to the vial containing the solution, then analytical precision would be expected to decrease. Further decreases in analytical precision should occur if one considers repeated analyses of the same sample solution on different days, or repeated acid decompositions of the same sample powder, with the decreasing precision reflecting

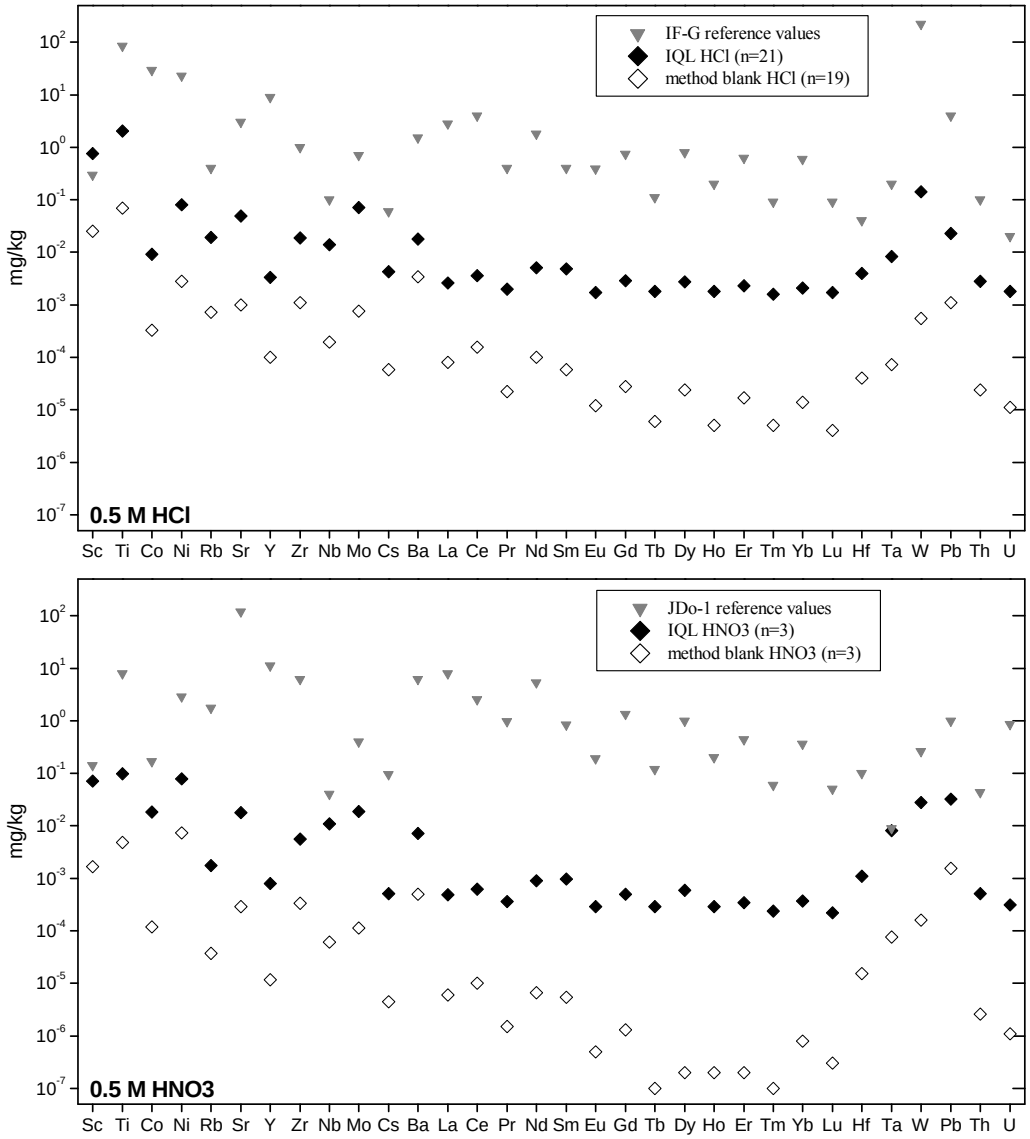

Figure 4. Long term average instrument quantification limits in mg/kg for solid samples (i.e., accounting for dilution factors) as determined from acid blanks, and average method blanks. Data for acid blank IQLs are also presented in Table 2. The top figure corresponds to a 0.5 M HCl acid matrix, and includes average method blanks for the HF-$HClO_4$ pressure decomposition method as well as reference data for the iron-formation IF-G, which represents a rock type that contains very low trace metal contents typically dissolved using the HF-$HClO_4$ method. The bottom figure corresponds to a 0.5 M HNO_3 acid matrix and the carbonate decomposition method, and includes reference data for the dolomite JDo-1, which represents a very low trace metal content rock typically dissolved using HNO_3. Regardless of decomposition method, the method blanks are at least 1 order of magnitude lower than IQLs for all elements, and generally 3-6 orders of magnitude lower than concentrations observed in the very trace metal-poor rocks typically analyzed. Method blanks and IQLs are significantly lower in 0.5 M HNO_3. Note that some elements are likely to be unquantifiable in many trace metal-poor rock samples due to concentrations close to or below the IQL (e.g., Sc, Nb, Ta).

error propagation during the complete sample decomposition and ICPMS analytical procedure. However, for many elements, in particular Y, Ba, the REE, and U, limits of precision appear to be controlled by the ICPMS measurement, and not by the sample decomposition method.

For the discussion of precision, three types of analytical precision are defined: 1) *sample precision*, calculated from the 60 mass scans of a single solution and representing raw, uncorrected data; (2) *run precision*, calculated from element concentrations determined by repeated analyses of a single solution over the duration of an ICPMS run (typically 6-12 hours); and (3) *method precision*, calculated from element concentrations determined from repeated acid decompositions and ICPMS analyses of a sample powder. The three types of precision and their relationships are illustrated in Figure 5. Note that sample precision reflects uncorrected intensities (cps), whereas run and method precision incorporate internal standard, interference, and blank corrections. To provide the best estimate of precision for analyses of rocks and minerals, these three types of precision are calculated using data obtained for the certified reference materials listed in Table 1. The discussion of sample, run, and method precision is limited to those analyses where the CRM was run repeatedly as part of every sample batch (see Fig. 3). Data are discussed as percent relative standard deviation (%RSD), though it must be stressed that standard deviations themselves usually vary significantly (±50% relative), so that an average RSD of 2% is expected to typically range as low as 1% and as high as 3%.

Sample precision in ICPMS determinations for common rock types is presented in Figure 6, along with the average sample precision for the 10 μg/kg calibration standard. As the 10 μg/kg calibration standard represents a solution free of the matrix effects typical of dissolved rock samples, it is expected to display the best RSD values, which are ~2% for almost all monitored isotopes. However, the 10 μg/kg calibration standard sample precision is indistinguishable from the sample precision determined for dissolved rock solutions, particularly for rock types that are not trace-metal poor, such as basalt and shale. Only for rock types that are very low in trace metals (e.g., JDo-1 dolomite), are sample precisions worse than those observed in the 10 μg/kg calibration standard, and only then for certain elements (e.g., Rb, Mo, Cs, Hf, Th, U). The run precision, where measurements of a CRM solution are periodically repeated over the course of an ICPMS run, is generally ~2%, similar to

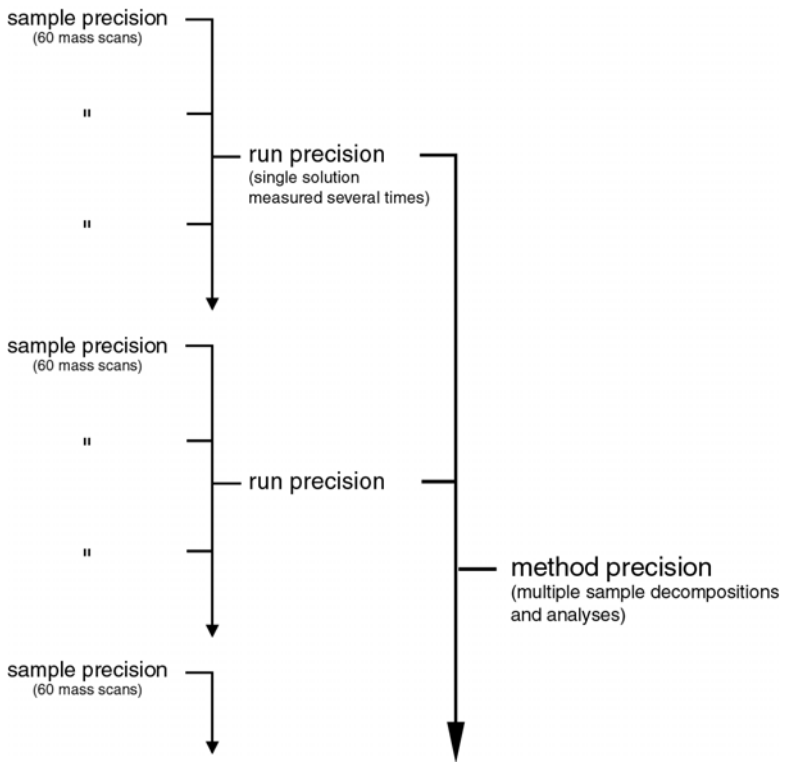

Figure 5. Diagram depicting various types of precision that may be defined for sample decompositions and ICPMS analyses. Note that sample precision reflects raw uncorrected intensities (cps), while run and method precision are calculated from corrected concentration data.

that of the sample precision for many elements, and also varies as function of rock type (Fig. 7). Shales display slightly poorer run precision (3-5%), though this might reflect the limited number of analyses where these CRMs were measured repeatedly. For purposes of long term reproducibility, the method precision is the most suitable measure of the standard deviation expected for a complete sample decomposition and ICPMS analyses, as it describes the variability expected in concentration data when a sample powder is dissolved numerous times over a period of months or years. Comparisons of the three types of precision discussed here (*sample*, *run*, and *method*) are presented in Figure 8 for CRMs of four different rock types. Of the 32 elements analyzed, the method precision RSD is better than 5% for 25 elements in BHVO-2 (basalt), 31 elements in SGR-1b, 26 elements in FeR-2 (iron-formation), and 22 elements in JDo-1 (dolomite). The method precision is also comparable to the sample and run precision, suggesting that any error associated with the HF-$HClO_4$ sample decomposition method (e.g., weighing and/or dilution errors) is small compared to the error inherent in the ICPMS analysis.

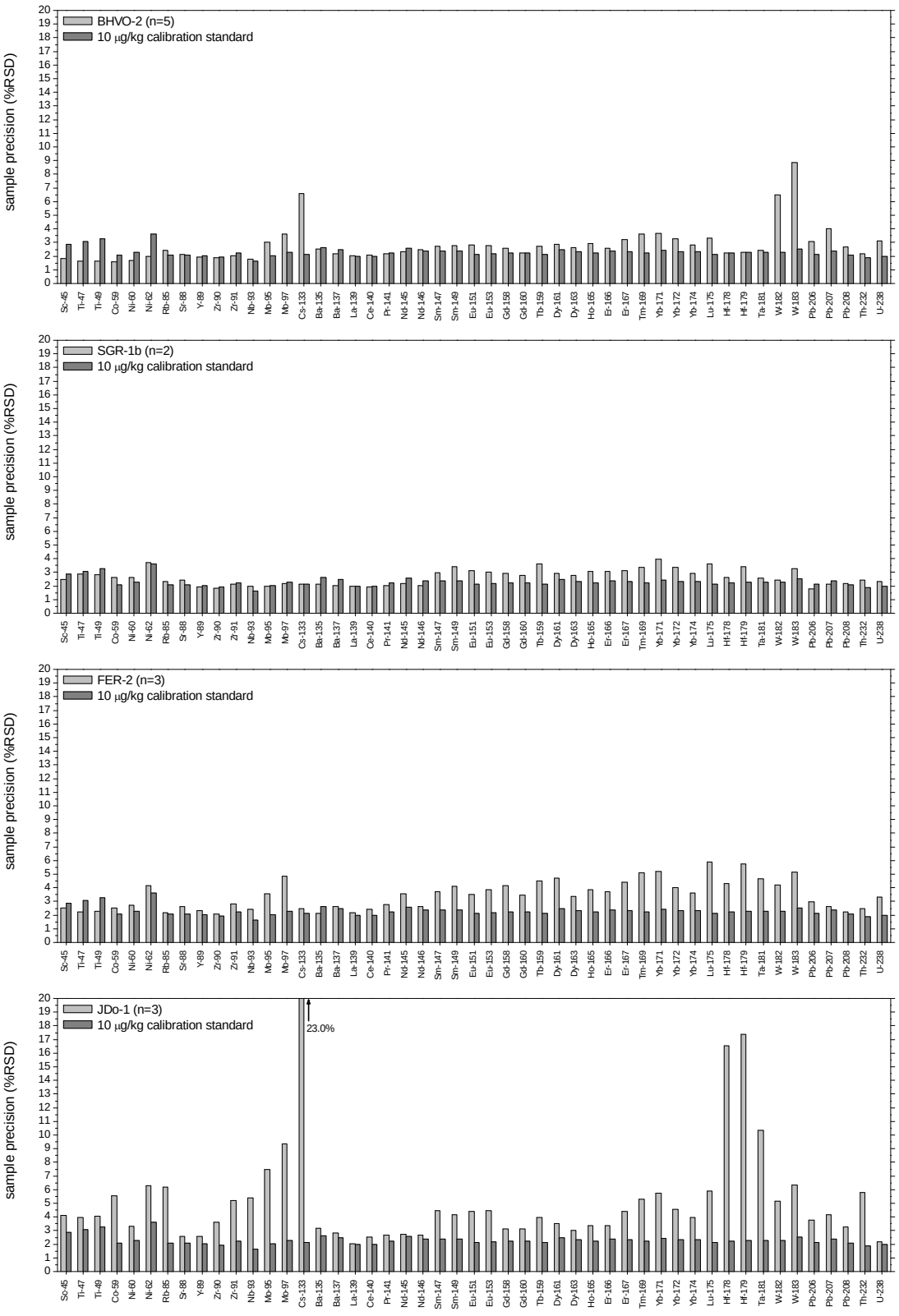

Figure 6. Average sample precision (see text for definition) for different rock types dissolved using the HF-$HClO_4$ decomposition, as calculated from the number (n) of decompositions where the CRM was measured repeatedly. The average 10 μg/kg calibration standard is presented for comparison (n=19). Precision is generally very similar between the rock solutions and the calibration standard, except for elements that are present at low concentrations in trace-metal poor rocks such as the JDo-1 dolomite (e.g., Rb, Mo, Cs, Hf, Th, U). This suggests that the standard deviation of ICPMS measurements is controlled by inherent instrument precision rather than by sample matrix effects.

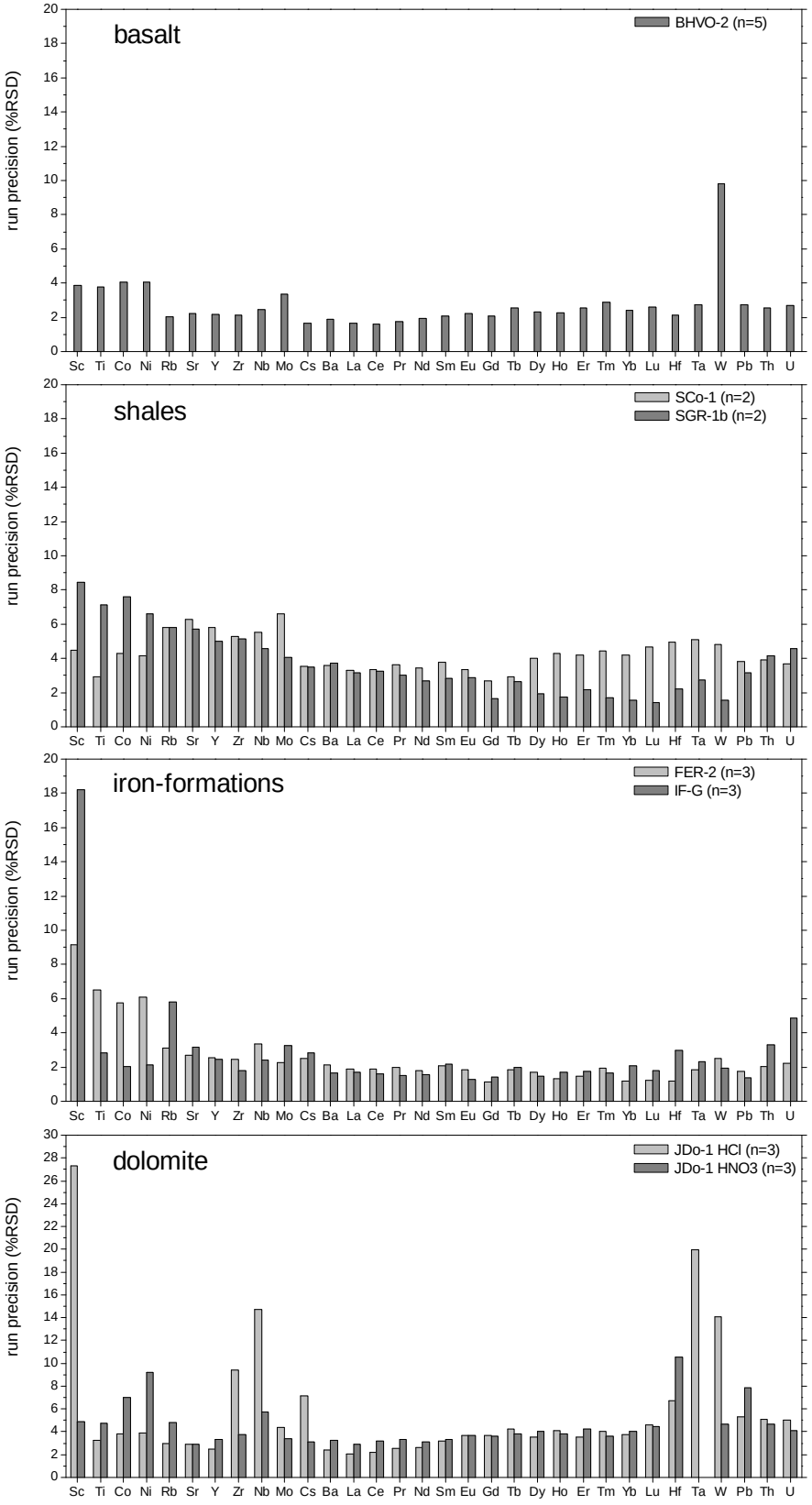

Figure 7. Average run precision for multiple (n) sample decompositions of certified reference materials that were analyzed repeatedly within a single ICPMS run (see text for details). All data for HF-$HClO_4$ sample decompositions, except for JDo-1 dolomite, which includes data for three carbonate (HNO_3) decompositions. Note bottom figure (dolomite) uses different scale. Poor RSD values are generally due to element concentrations approaching the instrument quantification limit (e.g., Sc, see Fig. 4).

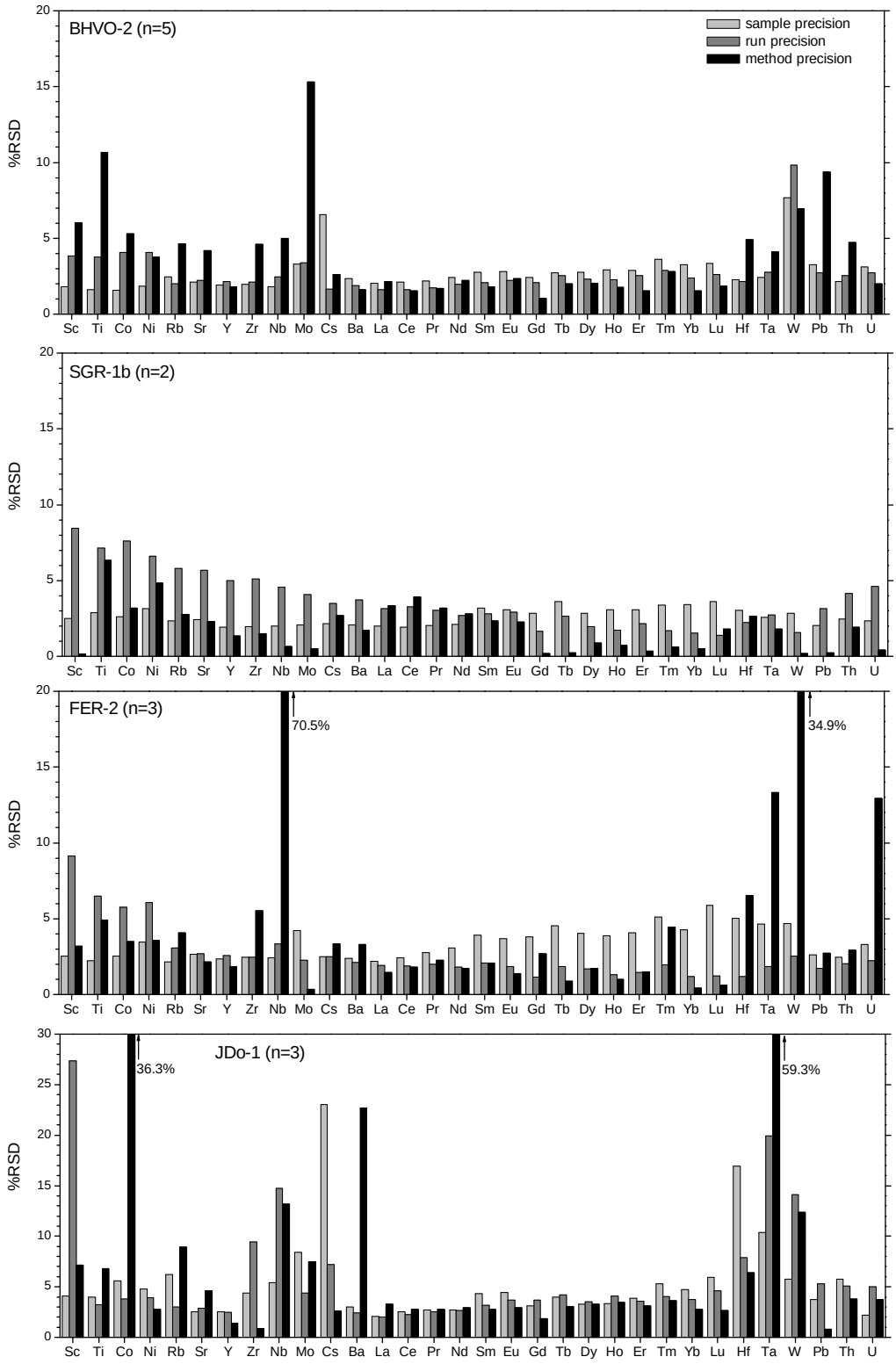

Figure 8. Comparison of average sample, run, and method precision for various CRMs, where n refers to the number of HF-$HClO_4$ sample decompositions and ICPMS runs in which the CRM was measured repeatedly. For most elements method precision is better than 5%, and is similar to, or even lower than, the sample or run precision. This suggests that for these elements the standard deviation of the data is primarily controlled by the inherent precision of the ICPMS instrument, and not by the decomposition method. Poor method precision is also due to low abundances for some elements that approach the IQL, e.g., Nb, Ta, and W in FeR-2 and JDo-1, as well as Co in JDo-1.

The method precision for elements present at low concentrations, particularly in FeR-2 and JDo-1, is typically poorer (e.g., Nb, Ta, W, as well as Co in JDo-1). However, some elements that are abundantly present at concentrations ranging from several mg/kg to several percent also display poor RSD values. The BHVO-2 basalt contains >1.5% Ti, yet suffers from a method precision of >10%, whereas Ba in JDo-1 is present at a concentration (6.14 mg/kg) well above the quantification limit and has an RSD above 20%. In the case of Ti, it is suspected that the poor ionization efficiency of this metal may mean that the 10 μg/kg calibration standard is not appropriate for quantification, as it produces a signal intensity that is not sufficiently greater than that observed for the background acid matrix, and this will be discussed in greater detail in the section regarding analytical accuracy. The poor method precision observed for Ba in the JDo-1 dolomite (22.7%) results from an 'outlier' for one of the three decompositions used in the calculation of the RSD value, as measured Ba in two decompositions is 5.32 and 5.63 mg/kg, while Ba measured in the third decomposition is 8.61 mg/kg.

To this point the discussion of analytical precision has been limited to the HF-$HClO_4$ decomposition method, as much of the research conducted within the JUB Geochemistry Lab focuses on whole-rock trace metal analyses, which necessitate complete dissolution of all mineral phases within the sample powder. However, with regard to analytical precision it is necessary to discuss the HNO_3 carbonate decomposition as well. As the carbonate decomposition is used for limestone and dolomite samples, the JDo-1 dolomite is the typical CRM included in decompositions and analyses of these rock types.

Sample and method precision for JDo-1 using the carbonate decomposition method are presented in Figure 9, and these measures of precision are comparable for most elements. This suggests that the carbonate decomposition method does not significantly increase the error budget for these elements, similar to that observed for the HF-$HClO_4$ decomposition. The method precision is better than 5% (RSD) for 25 of the 32 elements analyzed, and several elements displaying poor method precision (e.g., Rb, Cs, and Hf) are expected to be hosted in refractory mineral phases that would be resistant to dissolution by nitric acid. Elements at or near the IQLs and unlikely to be quantifiable in carbonate rocks at concentrations observed in JDo-1 include Sc, Nb, and Ta (see Fig. 4). For many elements the method precision as

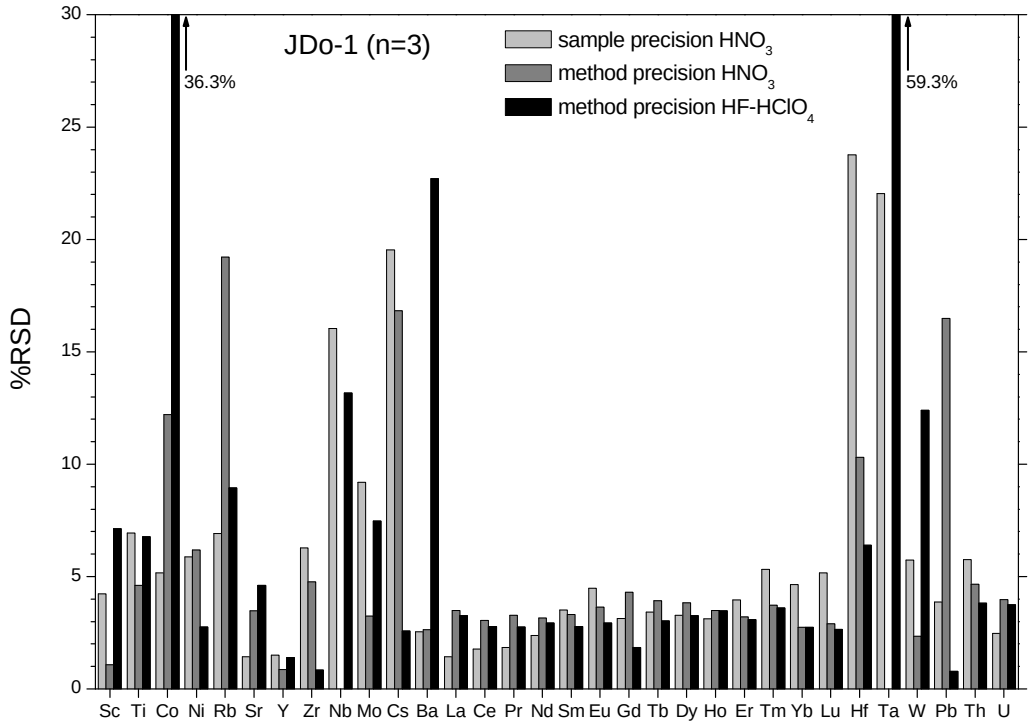

Figure 9. Average sample and method precision for the HNO_3 carbonate decomposition of the JDo-1 dolomite CRM (for run precision see Fig. 7). Method precision for the carbonate decomposition is better than 5% for 25 of the 32 elements analyzed, and poorer precision is generally restricted to elements typically hosted in refractory silicate minerals (Rb, Cs, Hf).

determined for the carbonate decomposition is quite similar to that observed for the HF-$HClO_4$ decomposition method, though the HF-$HClO_4$ decomposition results in significantly better precision for elements typically hosted by silicate minerals (e.g., Rb, Zr, Cs, Hf), due to the complete dissolution of refractory Si-bearing phases.

6. Analytical recovery

The relative precision for most elements analyzed is quite good, but this provides no information regarding potential loss of these elements as a consequence of the sample decomposition or ICPMS measurement. Some elements can exist as a volatile chemical species at some point during the decomposition process, and therefore may exhibit non-conservative behavior during sample preparation. The best example of this is Si, which is converted to volatile SiF_4 during HF dissolution of silicate minerals, and is consequently lost from the sample during evaporation of HF early in the HF-$HClO_4$ decomposition method. The ability of the sample treatment and ICPMS measurements described here to conserve the elements of interest throughout the decomposition and analytical procedure is termed *analytical recovery*.

Two approaches may be utilized to determine and quantify non-conservative behavior of the elements of interest. The first involves preparing artificial laboratory solutions that contain known quantities of the elements of interest, and then simply treating these artificial solutions as if they were unknown samples by subjecting them to a full sample decomposition and ICPMS analysis. This characterization of analytical recovery is discussed here, while the second approach, which involves determining elemental concentrations in a CRM and comparing these data with the reference values, is discussed below in the section regarding analytical accuracy.

Analytical recoveries of multi-element spikes (10 μg/kg) for the carbonate and HF-$HClO_4$ decomposition methods are presented in Figure 10. Recoveries for most elements are excellent, particularly for the carbonate decomposition, in which 27 of 32 elements have measured concentrations between 97-103% of the expected values. However, measured Ni in the carbonate digestion spike solution is ~30% too high, whereas Ta and W exhibit quite low recoveries of ~24% and ~80%, respectively. The anomalously high Ni recovery is attributed to contamination, as method blanks for the carbonate decomposition typically contain 2-5 μg/kg Ni. The significant loss observed for Ta and W is likely due to the filtration procedure performed for the carbonate decomposition. During the filtration step, the sample solution (10 ml of 5 M HNO_3) is passed over a 0.2 μm cellulose acetate filter (Fig. 1), which is subsequently rinsed with ~20 ml of 0.5 M HNO_3. Whereas this rinse step appears sufficient for most elements, Ta and W (and to a lesser extent Nb) are apparently retained, and may only be quantitatively rinsed from the filter by adding trace amounts of HF (0.05 M) to the rinsing solution (K. Schmidt, personal communication). The addition of HF to the rinsing solution should only be utilized if information regarding W is critical, as HF can form unstable complexes with other trace metals, particularly the rare earths, potentially limiting quantitative recovery of these elements. With regard to Nb and Ta, the use of HF during the filter rinse step is not particularly informative , as these are immobile elements expected to be hosted in refractory aluminosilicate phases, which are resistant to dissolution by the carbonate decomposition method.

For the HF-$HClO_4$ decomposition, analytical recovery for the 32 elements in the spike solution is more variable than that observed for the carbonate decomposition. Low mass elements tend to have slightly low recoveries around 95%,

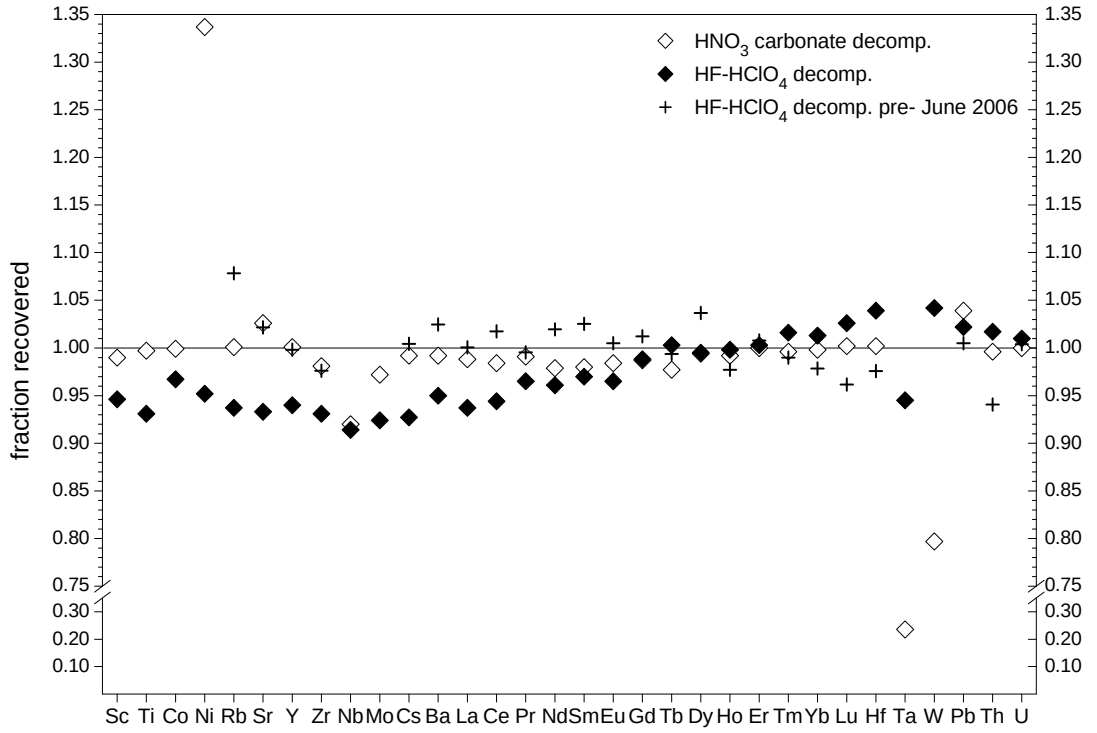

Figure 10. Multi-element analytical recoveries for the carbonate and HF-$HClO_4$ decomposition methods, expressed as a ratio of the measured element concentration divided by the spike concentration. Note break in the y-axis between 0.35-0.75. Spike solutions contained 10 µg/kg of the standard 32 elements analyzed, except for the pre-June 2006 HF-$HClO_4$ decomposition, which contained 1 µg/kg of the 24 elements routinely measured prior to June, 2006. Recoveries for most elements are between 95-105%, particularly for the carbonate and pre-June 2006 decompositions. Notable exceptions are Ni, Ta, and W for the carbonate digestion, which suggests contamination/interferences (Ni) and loss (Ta and W) during the decomposition, perhaps as a result of the filtering step. The large spread and general increase as a function of mass, in the fraction recovered for the 32 element HF-$HClO_4$ decomposition is attributed to effects arising from the utilization of the internal standards ^{101}Ru and ^{187}Re (see text for details).

and analytical recovery generally increases with increasing mass, though Ta does not follow this trend (Fig. 10). However, a test of analytical recovery performed prior to June 2006, conducted with the 24 elements originally analyzed by ICPMS within the JUB Geochemistry Lab, resulted in recovery percentages significantly better for many elements, particularly for elements with atomic masses below 138 (Ba). The exact reason for the more variable recovery observed for the full 32 element analysis currently conducted is not clear, though it is likely related to the internal standard correction. The generally constant analytical recovery of ~95% for elements with masses below 100, followed by the monotonic increase in recovery between masses 133 (Cs) and 183 (W), is mirrored by the IS correction factor for this analysis, which was 0.95 for all masses below ^{133}Cs, before linearly increasing to 0.98 for ^{183}W, and then decreasing to 0.96 for Pb, Th, and U.

For the more recent, full 32 element test of analytical recovery, the 10 μg/kg spike solution was analyzed in the middle of an ICPMS run containing Fe-rich carbonates that had a dilution factor of only 250, and these carbonates displayed extreme IS correction factors as high as 2.0, reflective of the high TDS content of these solutions. In contrast, the analytical recovery as determined from the pre-June 2006 analysis was not included within part of an ICPMS run, and was conducted following routine cleaning and optimization of the ICPMS. It therefore seems that the discrepancy between the two tests of analytical recovery for the HF-$HClO_4$ decomposition method, one using a 24 element spike and the other a 32 element spike, reflects details of the individual tests, including such factors as sample deposition within the ICPMS interface region affecting signal intensities (i.e., signal suppression or enhancement).

Based on the few data, it is therefore concluded that for the HF-$HClO_4$ decomposition analytical recoveries for the majority of elements are typically within 2-3% of their predicted concentrations, similar to that observed for the carbonate decomposition method. This variability may represent the optimum analytical recovery possible, as it is comparable to the inherent precision of ~2% observed for most element measurements (see above discussion regarding precision). However, in view of the limited data, more tests of analytical recovery are warranted, particularly using the HF-$HClO_4$ decomposition method and complete, 32 element spike solutions.

7. Analytical accuracy

7.1. Reference values and major element interferences

The best measure of the suitability of the analytical methods employed within the JUB Geochemistry Lab is if these methods can accurately (and reproducibly) quantify the elements of interest in certified reference materials. As mentioned previously, the CRMs used as routine quality assurance standards are chosen to match the rock types most commonly analyzed within the JUB Geochemistry Lab. If the measured CRM concentration data for a given sample decomposition is consistent with the certified data, then this provides the best measure of conservative element behavior and overall accuracy for the ICPMS methods employed.

The concentration data for CRMs are generally reported as either *recommended* values or *preferable/informational* values, with recommended values

considered more accurate and possessing lower degrees of uncertainty. Concentration data for most major and some trace elements in CRMs are typically provided by the issuing organization (Table 1). However, for many trace metals (particularly the REE, Nb, Mo, Ta, and W), values are either not provided by the issuing organization or are considered informational or preferred values, indicating that higher degrees of uncertainty surround these data. Therefore, for a significant number of the 32 elements analyzed at JUB, concentration data in CRMs may only be obtained from combinations of separate studies and compilations.

One of the most comprehensive and widely referenced compilations of geoanalytical data was assembled by Govindaraju (1994), which combines data produced using different analytical methods from a multitude of sources. However, for the CRMs listed in Table 1 much of the minor and trace metal data in Govindaraju (1994) is highly variable, particularly for the REE and other metals present at low concentrations such as Ti, Nb, Ta, Hf, Th, and U. Additionally, for some of the CRMs data has been published since 1994 using newer analytical methods such as laser ablation and/or high resolution multi-collector ICPMS. A thorough study of numerous CRMs, including the ones relevant to this discussion, was conducted by Dulski (2001), whose data closely match results from this study. Newer data (e.g., Baker et al., 2002; Bohlar et al., 2004) are consistent with the results presented here and the values of Dulski (2001), suggesting that the highly variable trace metal concentrations observed in older compilations of CRM data do not result from sample heterogeneity, but rather from limitations of older analytical methods.

The reference values for the CRMs used in this study are presented in Appendix 1, along with average concentration data for these CRMs as measured within the JUB Geochemistry Lab. The literature data presented are not intended to reflect an exhaustive or comprehensive survey of all available data for the various CRMs, and were selected according to three criteria: 1) data published by the CRM issuing organization, which usually are compilations of data produced by different laboratories using different methods; 2) studies that provided data for a large number of the 32 elements considered for this study; and/or 3) work that utilized similar analytical methods, particularly ICPMS techniques. This approach is intended to facilitate comparison between the CRM values measured at JUB with worldwide laboratories using similar analytical methods. Recently, Jochum et al. (2005) produced a thorough compilation of published major element, trace element, and

isotopic data for geologic CRMs, available as an electronic database (GeoReM), and the reader is referred to this resource for a complete survey of available CRM data.

Analytical accuracy will be discussed individually for each CRM. However, some general observations can be made regarding the JUB data and the reference values. The first is that the JUB data typically display greater precision compared to the average reference values, which is ascribed to the greater number of different methods and analytical techniques employed in the production of the reference values. The second is that poor precision and/or accuracy in the JUB data for specific elements, particularly those with masses <100, can often be predicted by the major element chemistry of the CRM (or sample). Poor results for elements with masses <100 are often due to metal-oxide and metal-chloride interferences arising from high concentrations of Mg, Al, Ca, Mn, and Fe in the CRMs (or sample).

For example, Figure 11 illustrates that concentrations of Mg and Ca above ~1% (wt.) in carbonate rock samples will produce measurable MgCl and CaO(H) interferences at mass 59, hindering accurate determinations for monoisotopic Co. The observed interferences on ^{59}Co are dominated by ^{24}Mg^{35}Cl for samples analyzed in 0.5 M HCl, and by ^{42,43}Ca^{16}O(^{1}H) species for samples analyzed in 0.5 M HNO_3. The interferences from Ca and Mg are significant enough to prevent the accurate determination of Co in the reference dolomite JDo-1, which contains 34.0% CaO and 18.4% MgO. Figure 11a indicates that Mg and Ca in JDo-1 would be expected to produce a combined interference on mass 59 equivalent to ~0.9 mg/kg Co, which is significantly greater than the reported Co concentration of ~0.2 mg/kg (App. 1). The use of 0.5 M HNO_3 in ICPMS analyses effectively removes the MgCl interference on ^{59}Co for JDo-1 (Fig. 11b), yet has little effect on interferences due to CaO(H), which are also similar in magnitude (~0.2 mg/kg) to the literature Co values. The data presented in Fig. 11 permits the estimation of interferences on ^{59}Co as a function of Ca and Mg contents in different samples (not only carbonate). It is concluded that reasonably accurate Co determinations in the presence of significant amounts of Mg and Ca are only possible if Co >10 mg/kg, i.e., when Co concentrations are at least one order of magnitude greater than the interferences typically expected in Mg- and Ca-rich rocks.

For other elements of interest with atomic masses <100, Table 4 lists interferences due to the major rock forming elements Mg, Ca, Al, Mn, and Fe. Note that while some interferences can be clearly identified (e.g., MgCl), other

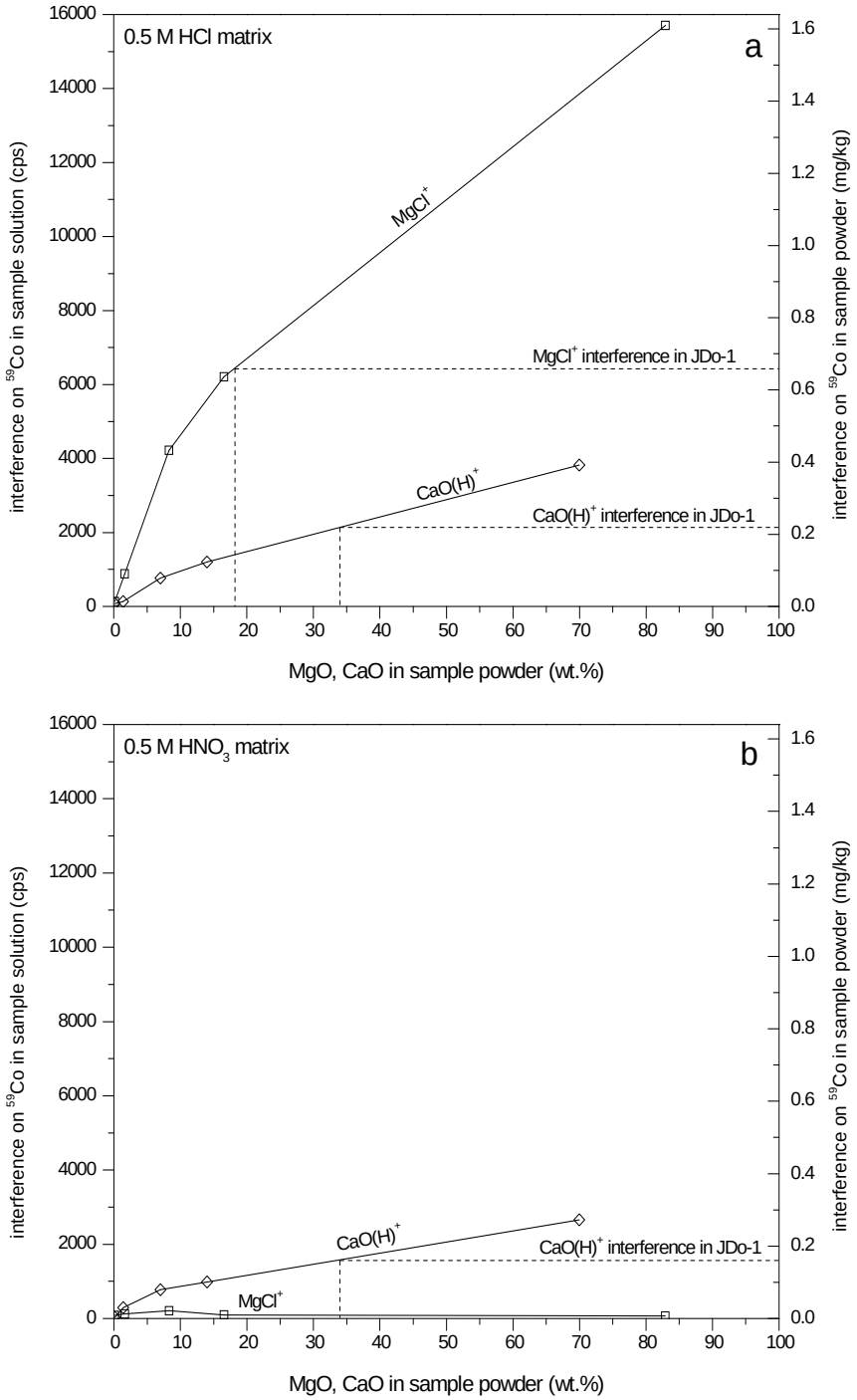

Figure 11. Mg and Ca interferences on ^{59}Co as functions of MgO and CaO content in sample powders. MgO and CaO are calculated as wt.% assuming the sample powders have been diluted by a factor of 1000, which is a typical dilution factor for Mg- and Ca-rich carbonate rocks (primarily dolomites). Top figure (a) shows interferences observed in HCl matrix, and the MgCl interference on mass 59 predicted for JDo-1 (18.4% MgO) is >0.6 mg/kg, significantly greater than literature Co values of ~0.2 mg/kg (see App. 1). Bottom figure (b) illustrates that MgCl interferences are eliminated when samples are analyzed in HNO_3, yet significant $CaO(H)^+$ interferences predicted for JDo-1 (34.0% CaO) still preclude accurate determinations of Co. It appears that reasonable Co determinations may only be possible for typical carbonate samples (MgO, CaO of 5-40%), when Co contents in the rock are at least one order of magnitude higher than the predicted interference concentrations (i.e., >10 mg/kg).

Table 4. Interferences observed for elements of interest with atomic masses <100.

monitored isotope	interfering element(s)	interfering molecule(s)*	comments
^{45}Sc	C, O	$^{12}C^{16}O^{17}O$, $^{12}C^{16}O_2{}^{1}H$	unavoidable; responsible for high Sc IQLs
^{47}Ti	C, N, O, Cl	$^{12}C^{35}Cl$, $^{14}N^{16}O^{17}O$	^{47}Ti best choice, particularly in HCl matrix
^{49}Ti	N, Cl	$^{14}N^{35}Cl$	^{49}Ti appropriate only in HNO_3 matrix
^{59}Co	Mg, Ca	**$^{24}Mg^{35}Cl$**, **$^{42,43}Ca^{16}O(^{1}H)$**	Co likely not quantifiable in carbonate or high-Mg/low-Co samples
^{60}Ni	Mg, Ca	$^{14}N_2{}^{16}O_2$, **$^{25}Mg^{35}Cl$, $^{44}Ca^{16}O$**,	^{60}Ni not appropriate in carbonate samples
^{62}Ni	Mg, Al	**$^{25}Mg^{37}Cl$, $^{27}Al^{35}Cl$**	^{62}Ni best choice for Mg-, Ca-rich samples, particularly in HNO_3 matrix
^{85}Rb	Ca	$^{48}Ca^{37}Cl$	insignificant interference due to low ^{48}Ca abundance (0.19%)
^{88}Sr	Ca	$^{48}Ca^{40}Ar$, $^{44}Ca_2$	insignificant interference at Ca/Sr ≤ 2000 (~JDo-1 ratio)
^{89}Y	Fe	$^{54}Fe^{35}Cl$	insignificant interference for Fe-rich CRMs
^{90}Zr	Mn	**$^{55}Mn^{35}Cl$**	interference ~10^{-4}(MnO), e.g., 15% MnO produces ~1.5 mg/kg interference
^{91}Zr	Ca, Fe	**$^{40}Ca^{16}O^{35}Cl$, $^{54,56}Fe^{37,35}Cl$**	^{91}Zr not appropriate in Ca-, Fe-rich samples
^{93}Nb	Ca, Fe	**$^{40}Ca^{16}O^{37}Cl$, $^{56}Fe^{37}Cl$**	significant interference, particularly in Fe-rich samples
^{95}Mo	Ca, Mn	$^{44}Ca^{16}O^{35}Cl$, **$^{55}Mn^{40}Ar$**	$^{55}Mn^{40}Ar$ significant regardless of acid matrix, ^{95}Mo not appropriate if MnO/Mo >1000
^{97}Mo	Ca	$^{44}Ca^{16}O^{37}Cl$	insignificant interference

* all interfering molecular species presumed to exist in a +1 valence state, and bold text indicates dominant species.

interferences must be inferred, as the total interference at a given mass may represent combinations of multiple interfering species, and examples would include CO_2, CO_2H, NO_2, CCl, and NCl. For the major elements Mg, Ca, Al, Mn, and Fe, high concentrations in rock samples are not observed to produce significant interferences for atomic masses >100. The practice of diluting samples with HCl following decomposition and the subsequent formation of metal-chloride molecular species (MCl(O)$^+$) is responsible for many of the interferences listed in Table 4, and these MCl(O)$^+$ interferences are insignificant for samples decomposed using the carbonate decomposition method. Samples decomposed using the HF-$HClO_4$ method may be diluted with 0.5 M HNO_3 to reduce or eliminate MCl(O)$^+$, assuming that all HCl used during the HF-$HClO_4$ decomposition is evaporated prior to diluting with HNO_3.

This suggests that use of HCl should be avoided in order to minimize MCl(O)$^+$ interferences. However, some elements, particularly the HFSE Nb and Ta, are not stable in low molarity HNO_3 solutions, and require HCl or HF to prevent apparent

'loss' of these elements in dissolved rock solutions due to adsorption/precipitation reactions in sample containers (Münker, 1998). For trace concentrations of Nb and Ta, Münker (1998) suggested diluting dissolved rock samples in 0.3 M HNO_3 and 0.06 M HCl for stabilizing these metals for ≥24 h, and the addition of 0.02 M HF when Nb and Ta in the diluted solution exceeded approximately 100 μg/kg and 4 μg/kg, respectively. The consistent use of 0.5 M HCl and the formation of $^{M}Cl(O)^{+}$ interferences does not appear to have adversely affected analytical precision or accuracy for the majority of the ICPMS analyses discussed here. However, for samples rich in Mg, Mn, and/or Fe that also have very low trace metal concentrations, it would be useful to more fully investigate mixtures of HNO_3 and HCl in order to maximize the sensitivity of the ICPMS method.

Some interferences persist regardless of the acid matrix used and result from analyzing aqueous solutions (e.g., $^{44}Ca^{16}O^{+}$ on ^{60}Ni), or from sample ionization in an Ar plasma. The latter effect is illustrated by presumed $^{44}Ca_2^{+}$ and $^{48}Ca^{40}Ar^{+}$ interferences on ^{88}Sr, which may erroneously increase measured Sr concentrations by 1-3 mg/kg as CaO contents in sample powders approach 40%. Another example is $^{55}Mn^{40}Ar^{+}$, which produces a 2-5 mg/kg interference on ^{95}Mo in sample powders that contain 10-15% MnO. Figures illustrating the significant interferences observed for Ni, Sr, Y, Zr, Nb, and Mo are presented in Appendix 2, and permit estimates of the magnitude of these interferences in various rock samples. It should be stated, however, that interferences observed in this study may not significantly affect analytical accuracy, provided the magnitude of the interference is small relative to the concentration of the trace metal of interest. An example is Nb, which cannot be determined accurately in Fe-rich, Nb-poor samples (<5 mg/kg Nb), but that is readily quantifiable in Fe-rich, Nb-rich rocks (>20 mg/kg Nb).

Analytical accuracy, as defined by the agreement between the average reference value and the measured JUB concentrations (App. 1), is presented in the following figures as a ratio of (JUB data/reference value), with a ratio of one indicating perfect agreement between the JUB data and the average CRM reference value. However, significant uncertainties in reference values exist for some elements, and some CRMs are more poorly characterized than others. This uncertainty in the CRM reference values can produce a wide range in the calculated ratio of (JUB data/reference value). Therefore, the range in calculated ratios due *solely to reference*

value uncertainty (as %RSD) is represented graphically in the following figures by means of vertical grey bars. A cursory examination indicates this range can be quite large, as illustrated in Fig. 12 for Mo (0.63–1.33) in FeR-2.

7.2. High Fe content rocks

Banded iron-formations (IFs) are a rock type frequently analyzed within the JUB Geochemistry Lab, and these samples are typically more than 90% SiO_2 and Fe_2O_3 in varying proportions, with NaO, MgO, Al_2O_3, and CaO all commonly present at low concentrations (<5%). For this discussion, and throughout this study, total Fe concentrations in rocks have been converted (where necessary) and reported as Fe_2O_3, as Fe in some CRMs has originally been determined as FeO or as combinations of FeO and Fe_2O_3. As expected, analytical interferences due to Fe dominate trace metal determinations in IFs, and analytical difficulties are expected primarily for ^{91}Zr and ^{93}Nb (Table 4). Fortunately, ^{90}Zr is not affected by high Fe contents, and is the preferred isotope for quantifying Zr in all Fe-rich samples. Monoisotopic Nb unfortunately offers no alternative isotope for analysis, and measured Nb concentrations for all iron-formation CRMs studied are significantly higher than literature reference values (App. 1). The discrepancy is attributed to interference on ^{93}Nb due to the high Fe content and generally low Nb concentrations in IFs. The low Nb contents are typical of the low trace metal concentrations in IFs, particularly for samples with relatively high Si/Fe ratios, as SiO_2 is a poor host mineral for trace metals. Therefore, it is necessary to employ very low dilution factors (≤500) for some IF samples (e.g., when SiO_2/Fe_2O_3 ~3), and even though much (if not all) of the Si is lost as volatile SiF_4 during the HF-$HClO_4$ decomposition, the remaining high Fe metal content in these samples can strongly suppress ICPMS signal intensities. As a result, IFs with high Si/Fe and very low aluminosilicate contents represent one of the more analytically challenging types of geologic samples commonly characterized within the JUB Geochemistry Lab.

FeR-2

The FeR-2 iron-formation is predominantly SiO_2 (49.2%), Fe_2O_3 (39.4%), and Al_2O_3 (5.1%). The rather high Al content benefits the determination of many trace metals such as Hf, Ta, and Th, as these elements are associated with refractory aluminosilicate phases, and are therefore present at relatively higher concentrations in

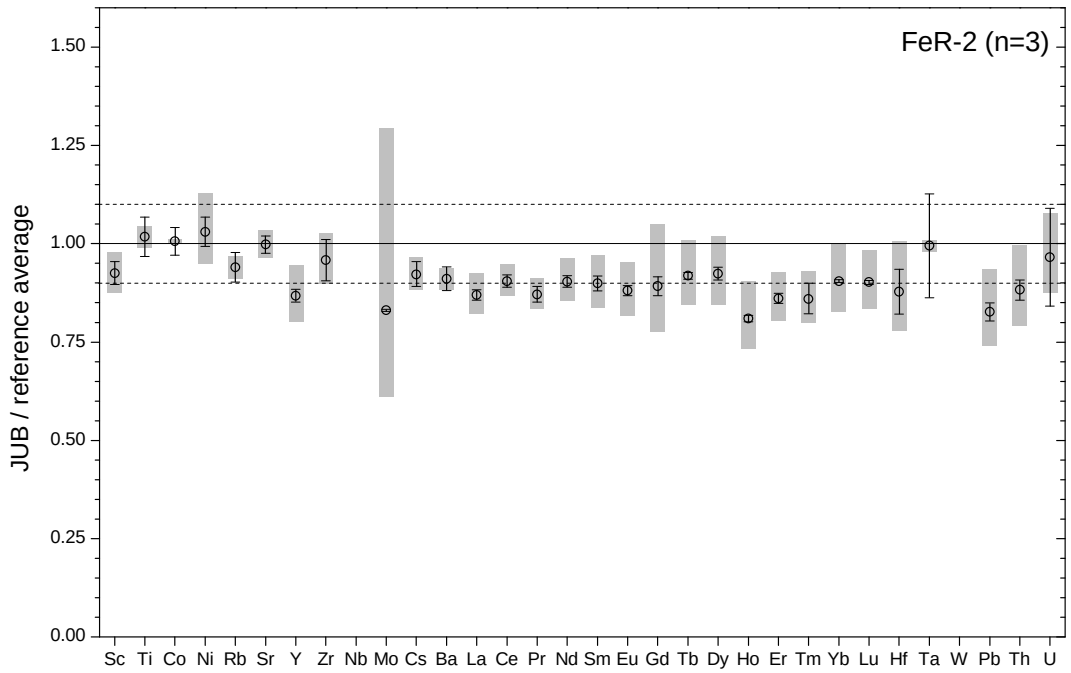

Figure 12. Accuracy estimation for ICPMS analysis of iron-formation FeR-2, where *n* equals the number of separate HF-$HClO_4$ sample decompositions and ICPMS analyses in 0.5 M HCl. Grey bars represent variability in the calculated ratio that is due solely to uncertainty in the *reference average.* Vertical lines represent the variability in the calculated ratio due to the uncertainty of the JUB data, and all data are presented in App. 1. Precision of JUB data is generally better than that observed for the average reference values, particularly for elements with atomic masses >100 amu (i.e., heavier than Mo). Measured JUB data for higher mass elements are generally lower than the reference average, though this reference average is skewed to higher values by the data of Yu et al. (2001) (see text for details and App. 1). Data for Nb not included due to probable FeCl interferences and large uncertainty in JUB data for Nb measurements (70% RSD).

FeR-2 compared to very Al-poor IFs. For FeR-2, the standard deviation of the JUB data is typically 1-3%, considerably better than the range observed in the literature data (App. 1). The JUB data tends to be somewhat lower than the reference value average, with 25 of the 32 elements analyzed displaying concentrations between 85–100% of the literature data (Fig. 12). However, the average reference values for many elements are skewed towards higher numbers by the data of a single study (Yu et al., 2001), and if the data from Yu et al. (2001) are not considered, then measured JUB concentrations for 24 of 32 elements are within 90-110% of reference values (see App. 1).

FeR-4

The FeR-4 iron-formation has very similar SiO_2 (50.1%) and Fe_2O_3 (39.2%) contents compared to FeR-2, but only one-third as much Al_2O_3 (1.70%).

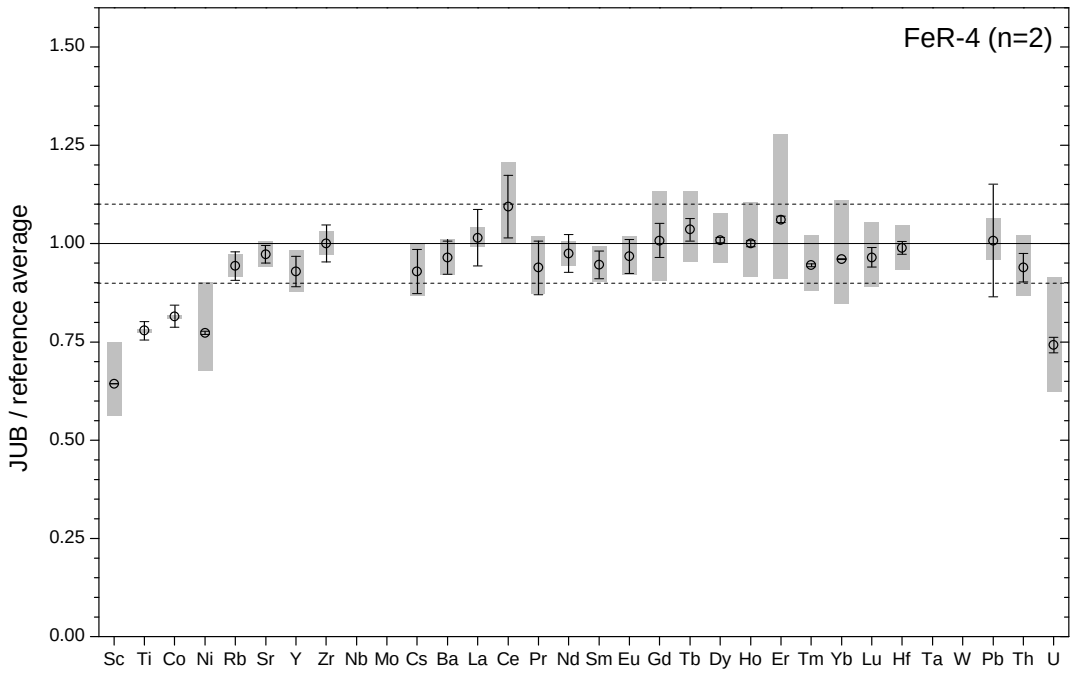

Figure 13. Accuracy estimation for ICPMS analysis of iron-formation FeR-4, where *n* equals the number of separate HF-$HClO_4$ sample decompositions and ICPMS analyses in 0.5 M HCl. Grey bars represent variability in the calculated ratio that is due solely to uncertainty in the *reference average.* Vertical lines represent the variability in the calculated ratio due to the uncertainty of the JUB data, and all data are presented in App. 1. Good agreement is observed for most elements, with exceptions being Sc, Ti, Co, Ni and U. Reference data for Nb, Mo, and Ta are not shown, and are available only from a single published study by Yu et al. (2001), who found highly variable results for these elements when comparing two different sample decomposition methods (HF-$HClO_4$ versus HF-H_2SO_4). See text for details.

Consequently, many trace metals have significantly lower concentrations in FeR-4 (e.g., Sc, Zr, Nb, the REE, Hf, Th). The precision of the JUB data is poorly constrained by the limited number of analyses, though it seems comparable to, if not significantly better than, the variation observed in literature reference values. The relative accuracy of the FeR-4 data is presented in Figure 13, and is somewhat better than that observed for FeR-2, except for elements with the lowest and highest masses (Sc, Ti, Co, Ni, and U). Poor results for Sc are not unexpected as Sc literature values for FeR-4 range from 1.1-1.5 mg/kg, which is similar in magnitude to the IQL observed for Sc (~0.8 mg/kg, Table 2).

However, Ti, Co, and Ni are all present in FeR-4 at concentrations well above their respective IQLs using the ICPMS methods described here (Fig. 4), so low signal-to-noise ratios are not expected to adversely affect determinations of these elements. For Co and Ni, the literature data are reported to only one significant digit and concentrations of these two elements are apparently low (2 and 8 mg/kg,

respectively). Previous workers have observed that many metals with very low abundances in CRMs are likely present at concentrations lower than initially reported, and that early data compilations frequently overestimate the true abundance of these elements (e.g., Dulski, 2001; Yu et al., 2001), perhaps due to older, less sensitive analytical techniques. It is therefore suggested that the apparent 'low' concentrations for Co and Ni determined at JUB may reflect this observation, though the limited published data and few JUB analyses of FeR-4 indicate that more work regarding these elements is necessary.

The Ti concentration determined in this study and the literature reference value (327 mg/kg and 420 mg/kg, respectively), both seem high enough to suggest that accurate Ti analyses in FeR-4 are possible. However the Ti reference value is compiled from analyses utilizing sample fusion and X-ray fluorescence (XRF) measurements (Abbey et al., 1983), which may suffer from relatively high blanks from the flux used during sample fusion, and/or poor detection/quantification limits compared to ICPMS measurements. It is therefore possible that the true Ti abundance in FeR-4 is lower than 420 mg/kg, and the discrepancy between the JUB data and the compiled reference average rather reflects the limited sensitivity and precision of many of the Ti analyses of FeR-4.

IF-G

The IF-G iron-formation is the most Fe-rich and Al-poor IF utilized as a CRM within the Geochemistry Lab, with 55.9% Fe_2O_3, 41.2% SiO_2, and 0.15% Al_2O_3. Unfortunately, IF-G as prepared by the issuing organization (IWG-GIT, Table 1) during the original processing run (first lot) is no longer available, and subsequently a second lot of IF-G was prepared by IWG-GIT. For many of the earliest IF analyses performed within the Geochemistry Lab, IF-G was the preferred CRM, and as a result the aliquot of the original first lot IF-G powder was completely consumed. In June 2007 an aliquot of the second lot of IF-G powder was obtained from IWG-GIT, which subsequently has been analyzed several times. As reported by IWG-GIT, the only differences between the two IF-G lots regard the concentrations of Cr, Co, and W. As Co and W are relevant to this discussion, it is noted that Co and W concentrations in the second IF-G lot are significantly lower than those originally reported for the first IF-G lot, due to different crushing methods utilized during preparation of the two lots.

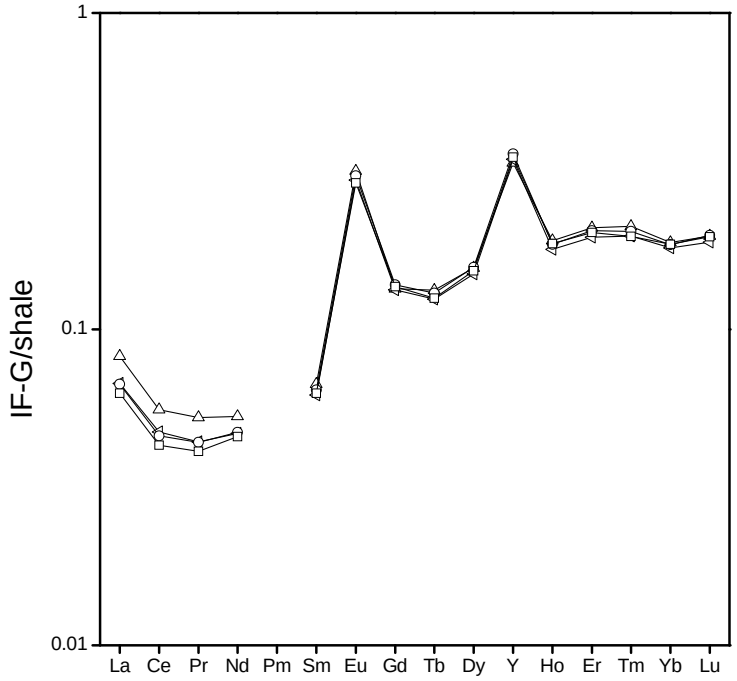

Fig 14. Rare earth and element and yttrium data from four separate HF-$HClO_4$ decompositions of the new, second lot of the iron-formation IF-G as prepared and issued by IWG-GIT. Data normalized to Post Archean Australian Shale (PAAS, McLennan, 1989). The majority of the REE data are consistent, with exceptions for the light REE (La, Ce, Pr, and Nd).

As a consequence of the above events, most analyses performed at JUB of the original IF-G lot used the pre-June 2006 ICPMS method, which quantified 24 trace metals. Only two analyses of this original IF-G lot were performed using the current 32 element ICPMS method, whereas the second IF-G lot has been analyzed several times using the 32 element method. Unfortunately, results for analyses of the second IF-G lot are not entirely consistent, and suggest that heterogeneities may exist within the sample powder. This is illustrated in Figure 14, which is a REE-yttrium (REY) diagram depicting data from four separate HF-$HClO_4$ decompositions for the second lot of IF-G powder. For the majority of the REE (Sm through Lu), the data for the separate decompositions are quite consistent, whereas La, Ce, Pr, and Nd are much more variable. This behavior is not well understood at this time. Fractionation across the REE series for small aliquots of rock samples is often a function of mineralogical controls on REE distributions within the bulk rock, and the data in Fig. 14 are preliminarily interpreted to reflect small mineralogical heterogeneities in the second lot of IF-G.

In consideration of the above observations, the discussion of analytical accuracy is restricted to the two decompositions of the *original lot* of IF-G that were

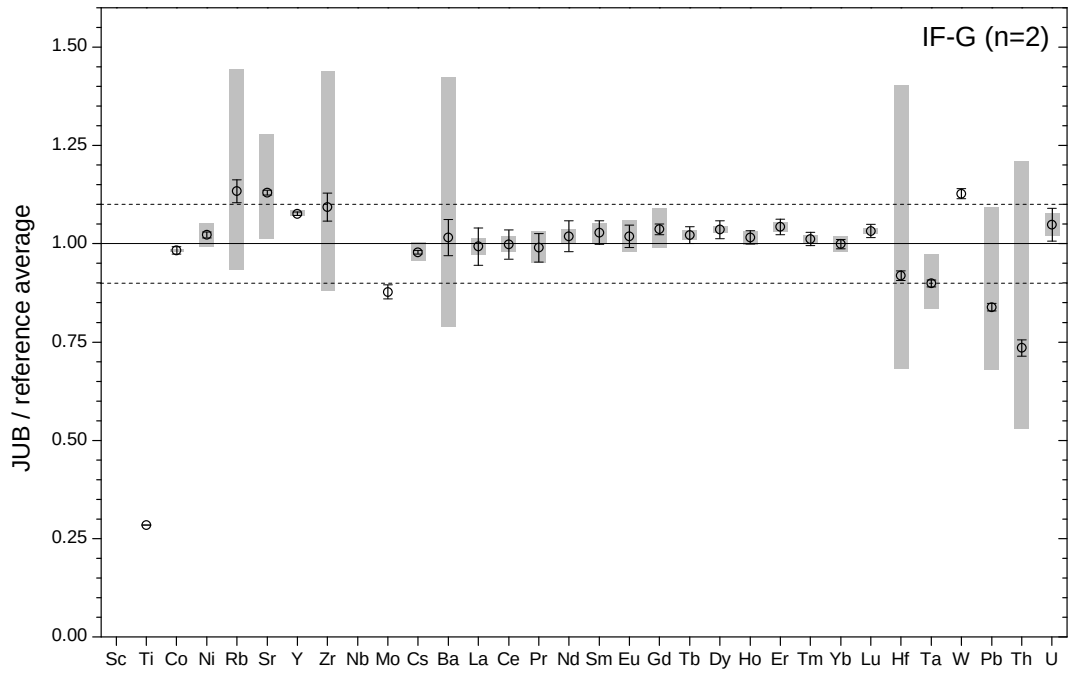

Figure 15. Accuracy estimation for ICPMS analysis of iron-formation IF-G, where *n* equals the number of separate HF-$HClO_4$ sample decompositions and ICPMS analyses in 0.5 M HCl. Grey bars represent variability in the calculated ratio that is due solely to uncertainty in the *reference average.* Vertical lines represent the variability in the calculated ratio due to the uncertainty of the JUB data, and all data are presented in App. 1. Data for Sc not reported due to high IQL, and Nb not reported due to significant FeCl interference. Reasons for poor observed Ti accuracy are considered to be similar to those proposed for FeR-4 (see text for details). Lower JUB concentrations for Hf, Ta, Pb, and Th are not considered anomalous, as it is likely that these elements are present at concentrations lower than originally reported for IF-G, an observation supported by the data of Dulski et al. (2001) and Bohlar et al. (2004).

performed using the current 32 element ICPMS analysis (see App. 1). Results from these analyses are presented in Figure 15, and JUB data for 23 of 32 elements are between 90–100% of the average reference values. Data for Sc and Nb are not shown, as Sc concentrations in IF-G (~0.3 mg/kg) are below the IQL for Sc (Fig. 4), and literature Nb concentrations of ~0.1 mg/kg are significantly lower than the predicted FeCl interferences on ^{93}Nb of ~0.6 mg/kg (Apps. 1 and 2).

The apparent poor accuracy of the JUB determination for Ti is considered to arise from reasons similar to those proposed for Ti determinations in FeR-4, i.e., a combination of low concentration (84 mg/kg) and analytical methodology for determination of the reference values (e.g., sample fusion and XRF analyses). The wide discrepancy observed for the Hf, Ta, Pb, and Th data of this study is primarily due to the inclusion of values from Govindaraju (1994) when calculating the reference average for these elements. Compared to more recent ICPMS analyses by Dulski (2001) and Bohlar et al. (2004), JUB data for these elements are quite

consistent (App. 1), and similar to FeR-4, it is concluded that older data compilations frequently overestimate the abundance of many trace elements that are present at very low concentrations.

7.3. Shales and clastic sediments

Fine-grained clastic rocks and sediments commonly analyzed during geochemical research at JUB include shales and river sediments. Shales and clastic sediments may have Al_2O_3 concentrations as high as ~15%, and the high aluminosilicate mineral content of these samples produces a relative enrichment in many trace metals. For example, the REY are incompatible trace metals that behave similarly to Al in crustal processes, and the REY are good proxies for the Al-rich continental crust that erodes to form river sediments and shales. In SCo-1, a shale CRM issued by the USGS, the summed REY concentrations are approximately 170 mg/kg, whereas the IF-G iron-formation discussed above contains ~22 mg/kg of REY.

This trace metal enrichment facilitates geochemical analyses of shales and clastic sediments in two ways, with the first being that reference values are better constrained, as older, less sensitive analytical methods can produce precise and accurate data for many trace metals. The second advantage arises from the ability to significantly dilute shale and sediment samples for ICPMS analyses while remaining well above the IQLs for many trace metals, thereby reducing matrix effects and major element interferences. This latter effect is illustrated using SCo-1 and IF-G, which, as mentioned above, have very different REY concentrations. Assuming SCo-1 was diluted by a factor 7-8 times greater than the dilution factor used for IF-G, then similar ICPMS signal intensities would be expected for the REY when analyzing these two CRMs.

SCo-1

The SCo-1 shale CRM (Cody shale) contains 13.7% Al_2O_3, 5.14% Fe_2O_3, approximately 2.6% each MgO and CaO, and only trace amounts of Mn (410 mg/kg). Figure 16 depicts the analytical accuracy observed for SCo-1. Of the 32 elements analyzed, 27 are within ±10% of the reference value, with lower masses displaying the greatest deviation, as the JUB data are significantly higher for these elements (Sc, Ti, Co, Ni). Some of the discrepancy observed for Sc, Ti, Co, and Ni can be ascribed

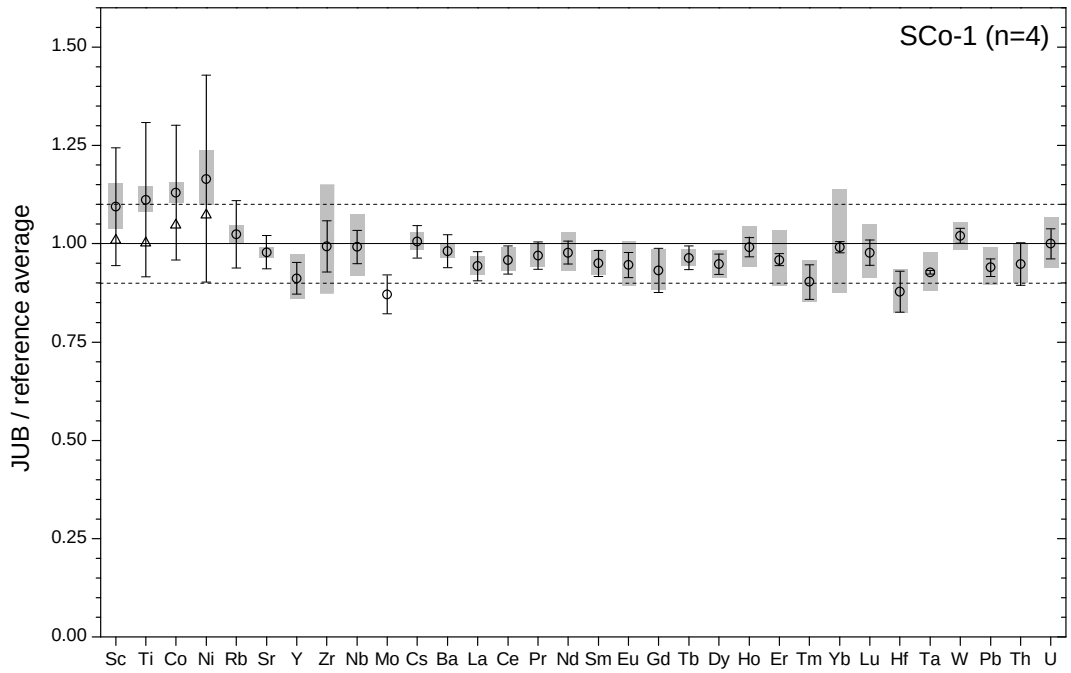

Figure 16. Accuracy estimation for ICPMS analysis of shale SCo-1, where *n* equals the number of separate HF-$HClO_4$ sample decompositions and ICPMS analyses in 0.5 M HCl. Grey bars represent variability in the calculated ratio that is due solely to uncertainty in the *reference average*. Vertical lines represent the variability in the calculated ratio due to the uncertainty of the JUB data, and all data are presented in App. 1. The triangles for Sc, Ti, Co, and Ni represent average JUB data that excludes a single analysis that determined anomalously high values for these four elements, and when the 'anomalous' data are not considered the JUB averages more closely match the reference values for Sc, Ti, Co, and Ni.

to a single JUB analysis of SCo-1 that determined much higher concentrations for these elements, and when these 'anomalous' data are not considered (see Fig. 16), the measured concentrations for 30 of 32 analyzed elements are between 90–110% of the reference value.

Potential major element interferences on trace metal determinations in SCo-1 would include $^{27}Al^{35}Cl$ on ^{62}Ni, and FeCl on ^{93}Nb (Table 4). The impact of Al-chloride interferences on ^{62}Ni is significant enough that it is recommended that ^{62}Ni not be used for Ni determinations in shales (or sediments) that contain more that a few percent Al_2O_3 and that are diluted in HCl (see App. 2). Note that the Ni data presented in App. 1 and Fig. 16 reflect concentrations for SCo-1 that were determined solely by monitoring of ^{60}Ni. As for Nb, the presence of ~5% Fe_2O_3 in SCo-1 would be predicted to increase Nb concentrations by roughly 0.1 mg/kg, which is insignificant when compared to the SCo-1 reference Nb value of 11.9 mg/kg. It is therefore concluded that Fe_2O_3 concentrations in shales (or sediments) of 3-7% are

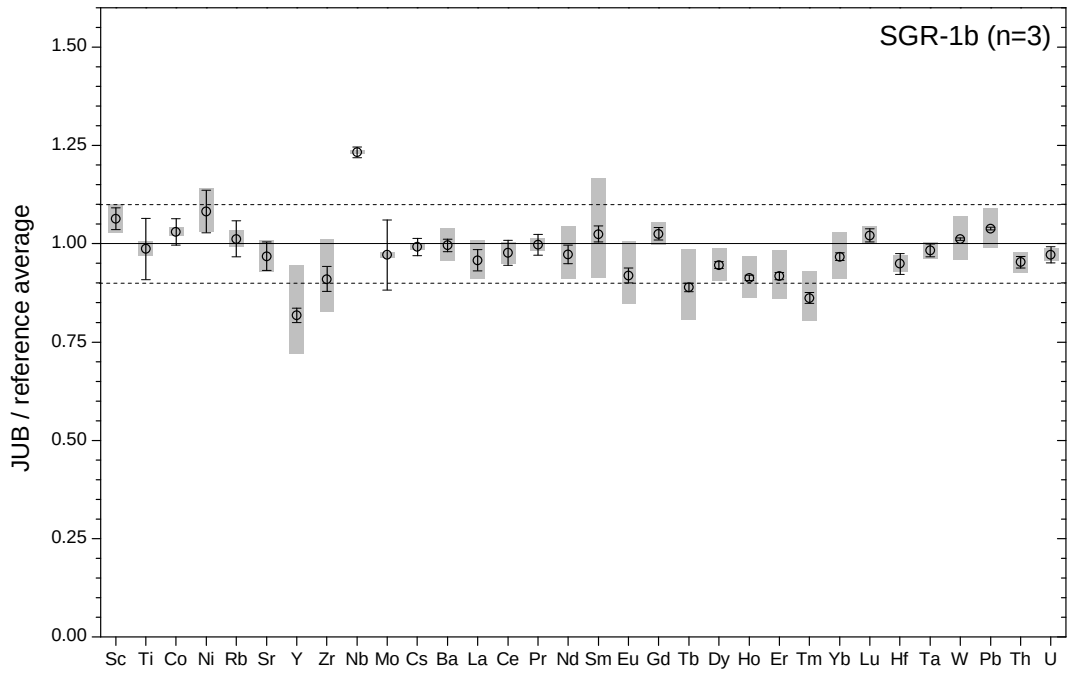

Figure 17. Accuracy estimation for ICPMS analysis of shale SGR-1b, where *n* equals the number of separate HF-$HClO_4$ sample decompositions and ICPMS analyses in 0.5 M HCl. Grey bars represent variability in the calculated ratio that is due solely to uncertainty in the *reference average.* Vertical lines represent the variability in the calculated ratio due to the uncertainty of the JUB data, and all data are presented in App. 1. The measured concentrations for Ni, Y, Tb, and Tm are not necessarily considered anomalous, and likely represent small interferences (Ni) and relatively large uncertainties in the reference data (Y, Tb, Tm; see text and App. 1).

not likely to adversely affect Nb determinations, assuming Nb is present in the sample at concentrations of several mg/kg or higher.

SGR-1b

The SGR-1b (Green River) shale is a petroleum and carbonate rich CRM issued by the USGS. The SGR-1b shale is identical to the original SGR-1 shale (S.A. Wilson, USGS, personal communication) and contains 6.5% Al_2O_3, 4.4% MgO, 8.4% CaO, 3.0% Fe_2O_3, and minor amounts of Mn (267 mg/kg). While the Al content of SGR-1b is low compared to the SCo-1 shale, it is still high enough to produce significant Al-chloride interferences on ^{62}Ni. As a result Ni concentration data reported for SGR-1b are determined solely from analyses of the ^{60}Ni isotope. For the remaining major elements, significantly higher MgO and CaO in SGR-1b compared to SCo-1 would be expected to erroneously increase measured signal intensities for ^{60}Ni, due to MgCl and CaO(H) inteferences. The combined magnitude of these Mg and Ca interferences on ^{60}Ni is estimated to be ~2 mg/kg (App. 2), and this is

consistent with the average Ni concentration for SGR-1b measured at JUB of 30.3 mg/kg, which is slightly higher than the Ni reference average of 28 mg/kg (App. 1).

Figure 17 compares measured JUB trace element data with reference values, and 28 of the 32 analyzed elements are within ±10% of the average reference value. Measured concentrations for Y, Tb, and Tm are 10-20% lower than the average reference value, whereas measured Nb concentrations are >20% higher than the literature Nb values. The discrepancies for Y, Tb, and Tm may arise from the wide range observed in reference values, and/or the aforementioned higher trace metal contents frequently reported by compilations of older data, as concentrations for these elements as reported by Dulski (2001) are indistinguishable from the JUB data (App. 1). The higher Nb content in SGR-1b as determined at JUB is unlikely to result from FeCl interferences (see above discussion for SCo-1), and is not necessarily anomalous considering that literature Nb values solely reflect older data compilations.

7.4. High Si content rocks (cherts)

Occasionally, trace metal analyses are required for rocks which are almost exclusively composed of quartz (SiO_2). Examples of such rocks include micro-crystalline SiO_2 chemical precipitates (cherts), and relatively pure quartz clastic sediments (e.g., sandstones). To date, little research has been performed at JUB concerning quartz-dominated clastic rocks, and therefore this section focuses on very pure SiO_2 chemical precipitates. These cherts are similar to the Si-rich, Fe-poor iron-formations discussed earlier, though for this discussion the term chert refers to a SiO_2 chemical precipitate that contains very little (≤0.5%) Al_2O_3, MgO, and CaO. Concentrations of Fe_2O_3 may range between 1-5%, and as Fe contents increase beyond this range the previous discussion regarding iron-formations is considered more appropriate.

The only chert CRM analyzed within the JUB Geochemistry Lab is JCh-1 (Geological Survey of Japan), which is 98% SiO_2, 0.73% Al_2O_3, >0.10% MgO and CaO, and only 0.36% Fe_2O_3. The microcrystalline quartz that dominates cherts is a poor host for most metals, and as a consequence these rocks tend to have very low total trace metal contents. This is illustrated by JCh-1, which has a total REY content of 11.9 mg/kg, roughly half that observed in IF-G (21.8 mg/kg). Trace metal determinations for JCh-1 relative to literature reference values are presented in Figure 18. At first glance, few of the JUB data are similar to the average reference value,

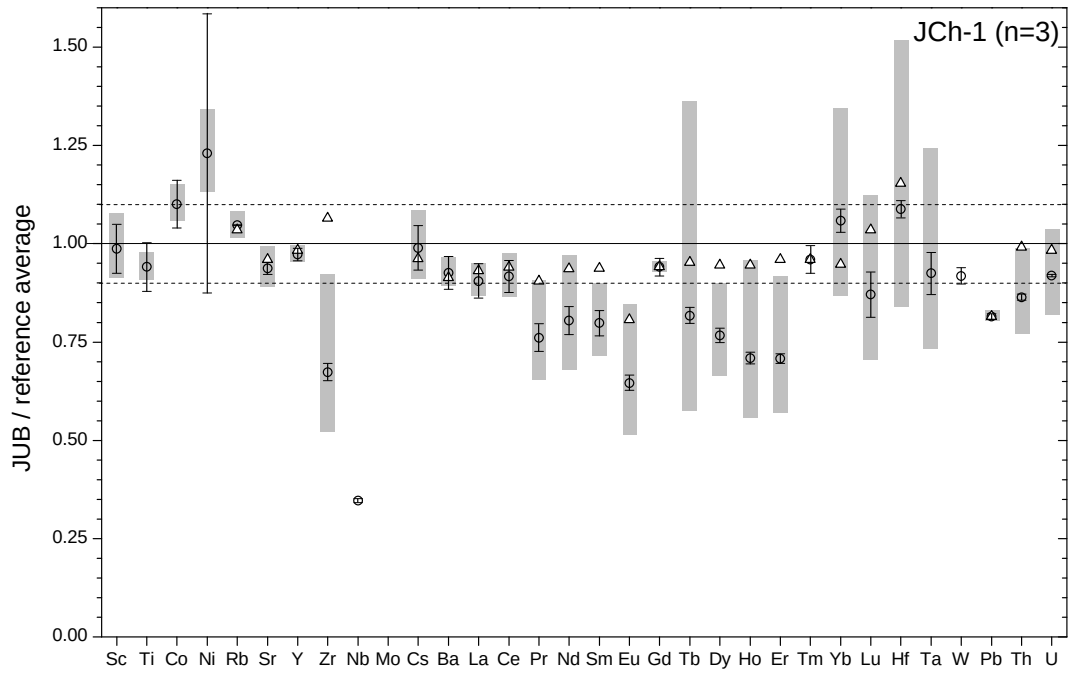

Figure 18. Accuracy estimation for ICPMS analysis of chert JCh-1, where *n* equals the number of separate HF-$HClO_4$ sample decompositions and ICPMS analyses in 0.5 M HCl. Grey bars represent variability in the calculated ratio that is due solely to uncertainty in the *reference average.* Vertical lines represent the variability in the calculated ratio due to the uncertainty of the JUB data, and all data are presented in App. 1. The JUB data are quite consistent and reproducible, with the exception of Ni. The reference data for higher mass elements have a wide range of values (i.e., larger grey bars), with JUB data generally lower. Considering the uncertainty in the reference data, and the very low trace metal contents, the JUB data have additionally been normalized to the data of Dulski (2001), who has published the only complete REY dataset for JCh-1 (App. 1). The JUB/Dulski (2001) values are plotted as white triangles, and the majority of these ratios are close to 1.

with measured concentrations for many metals significantly lower than reference data. However, the JUB data tend to be much more precise, particularly for higher mass elements. The exception is Ni, and the large variation in Ni measured at JUB results from one analysis, which determined a concentration of 14.0 mg/kg. The remaining two analyses at JUB determined Ni of 7.41 and 8.59 mg/kg, similar to the average reference value of 8.13 mg/kg (App. 1), and it is concluded that the single, 14.0 mg/kg Ni analysis is likely anomalous.

The large uncertainty in the average reference values for many elements may be due to the difficulty in determining the very low trace metal contents in JCh-1, and few reference data exist for some elements (e.g., the monoisotopic REE Pr, Tb, Ho, and Tm). One of the most complete trace element datasets yet published for JCh-1 is from Dulski (2001), whose data compare favorably with the concentrations determined at JUB, and these data are presented in Fig. 18.

7.5. Carbonate rocks

A common type of rock analyzed at JUB are carbonates, which are chemical precipitates generally containing low trace metal contents, similar to cherts. Carbonate rocks are dominated by $(Ca,Mg)CO_3$ minerals, and Ca and Mg may exist in solid solution within the carbonate mineral structure. As a result, carbonate rock samples typically analyzed may range from limestones ($CaCO_3$), through dolomites ($(Ca,Mg)CO_3$), to pure magnesites ($MgCO_3$). All of these carbonate rock types are effectively decomposed using the HNO_3 carbonate decomposition method, though, as noted previously, any accessory aluminosilicate minerals and refractory organic carbon are relatively unaffected by dissolution with HNO_3.

This section discusses the application of both decomposition methods (HF-$HClO_4$ and HNO_3) to carbonate rocks, and describes the applicability and accuracy of these methods with respect to specific elements of interest. As the literature reference values are generally determined by analytical methods capable of thoroughly characterizing the whole-rock abundance of elements, the inability of the carbonate decomposition method to dissolve refractory silicate minerals results in 'poor' analytical results for elements typically hosted within these minerals (e.g., Zr, Nb, Hf, Ta, Th, among others). It is therefore necessary to first examine data obtained using the HF-$HClO_4$ whole-rock decomposition method, as these data are most comparable to the average reference value calculated from literature sources.

The most commonly utilized carbonate CRM is the dolomite JDo-1, issued by the Geological Survey of Japan (GSJ). The JDo-1 dolomite is 34.0% CaO and 18.5% MgO, with only trace amounts of Al, Mn, or Fe. Therefore, major element interferences would be expected from the high Ca and Mg contents, and should primarily affect determinations of Co, Ni, Zr, and Nb. Figure 19 presents comparisons between concentrations determined at JUB using the HF-$HClO_4$ decomposition method with the average reference values. Determinations of Co and Ni are not shown in Fig. 19, as the elements are severely compromised in HCl acid matrices by interferences generated from Mg and Ca (Table 4). The JUB measured Co of 1.46 mg/kg is several times higher than the average reference value of 0.234 mg/kg, and measured Ni is 11.1 mg/kg, also several times higher than the reference value of 2.9 mg/kg.

Of the remaining elements Ti, Sr, Y, the REE, and W show good agreement with the average reference values, and the reference values themselves are consistent

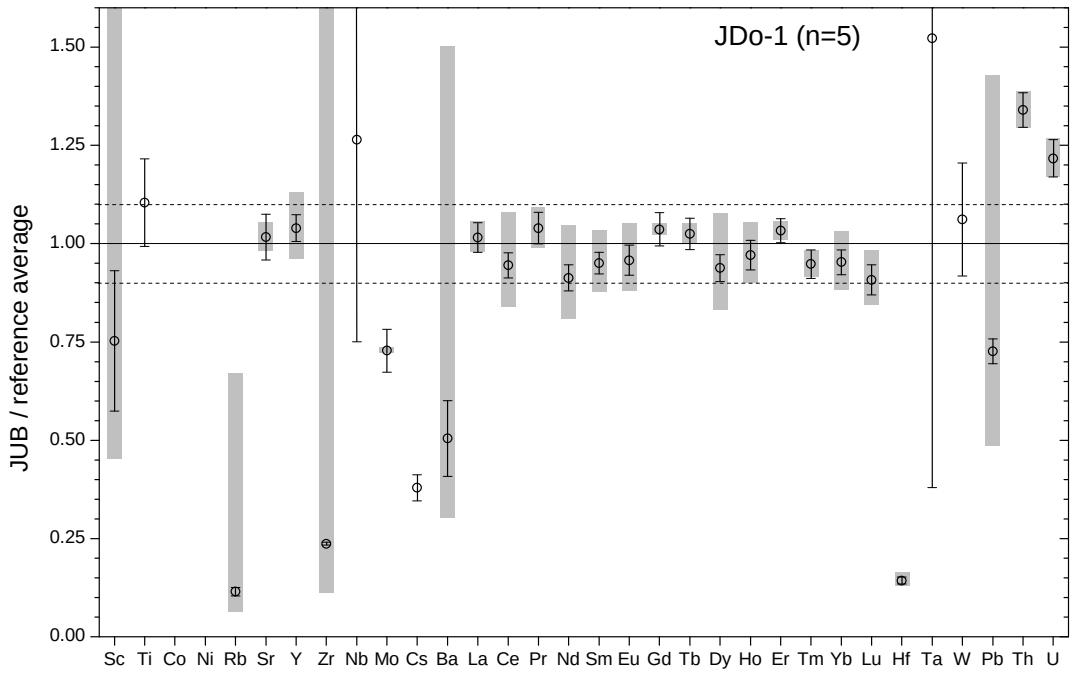

Figure 19. Accuracy estimation for ICPMS analysis of dolomite JDo-1, where *n* equals the number of separate HF-$HClO_4$ sample decompositions and ICPMS analyses in 0.5 M HCl. Grey bars represent variability in the calculated ratio that is due solely to uncertainty in the *reference average.* Vertical lines represent the variability in the calculated ratio due to the uncertainty of the JUB data, and all data are presented in App. 1. Data for Co and Ni not shown due to large MgCl and CaO(H) interferences. The reference averages for several elements display very large uncertainties (Sc, Rb, Zr, Ba, and Pb, see App. 1). The JUB data for Sc is close to the IQL (Fig. 4), and Sc measurements at the concentration levels reported for JDo-1 are unlikely to be reliable.

and calculated from a relatively large number of published studies (App. 1). Exceptions are Ti and W, as previously published data are only available from Imai et al. (1996), with Ti reported as 0.00133% TiO_2. The observed discrepancies for other elements are variously attributed to either anomalously high reference data from individual studies that skew the average reference value (Sc, Rb, Zr, and Ba), or to a lack of published reference data (Nb, Cs, Ta). For Sc, concentrations in JDo-1 are similar to the IQL in 0.5 M HCl (Table 4), indicating that accurate Sc measurements in JDo-1 are likely to prove difficult. With respect to Zr and Ba the measured JUB concentrations agree well with at least two other published studies (see App. 1).

The elements which display the greatest discrepancies, either as uncertainty in reference values or as deviation of the measured JUB concentration from the average of published data, are generally incompatible in carbonate minerals. As the JDo-1 dolomite is a very pure marine chemical precipitate, these incompatible elements (e.g., Sc, Rb, Zr, Nb, Cs, Hf, Ta, Th) are likely to be concentrated in discrete,

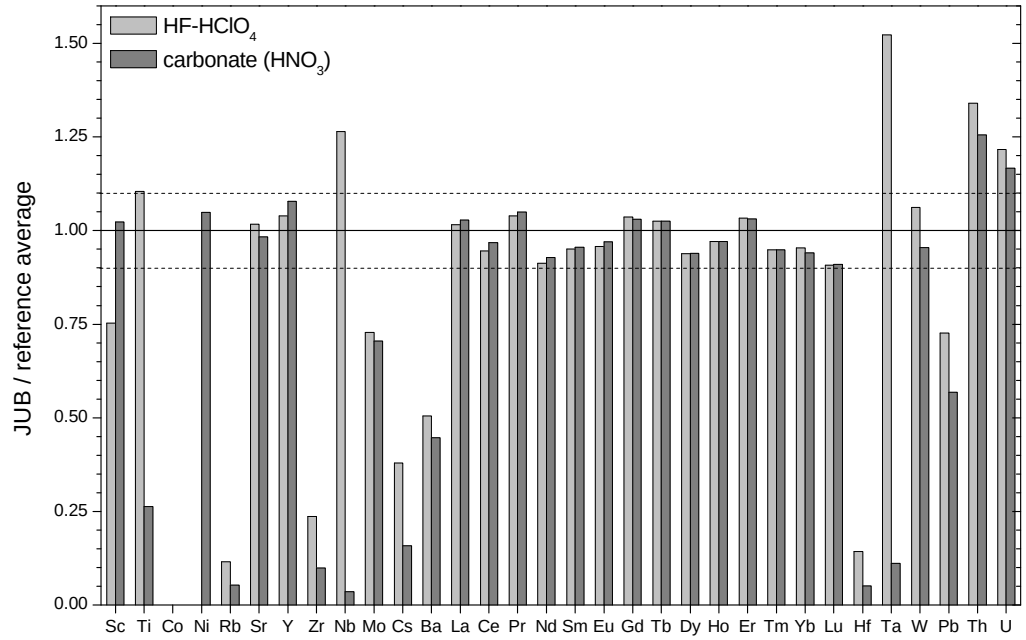

Figure 20. Comparison of analytical accuracy relative to average reference values for both HF-$HClO_4$ and carbonate (HNO_3) decompositions of the JDo-1 dolomite. Based upon similar results for the two decomposition methods, Sr, Y, the REE, W, Th, and U are considered to be quantifiable using the carbonate decomposition method. Additionally, note the excellent results for Ni determined from the carbonate decomposition method, which were calculated using the ^{62}Ni isotope. Elements likely to be hosted in refractory aluminosilicate phases that resist complete dissolution using the carbonate decomposition include Ti, Rb, Zr, Nb, Cs, Hf, and Ta.

refractory mineral phases. If that is the case, then these refractory minerals may not be homogenously distributed within the JDo-1 powder, offering a possible explanation for the wide variation in reported concentrations for incompatible elements.

Compared to the HF-$HClO_4$ decomposition method the carbonate decomposition method is not expected to completely dissolve all mineral phases (e.g., aluminosilicates), and data for JDo-1 obtained using the two different decomposition methods are presented in Figure 20. Regarding the carbonate decomposition of JDo-1, and many other carbonate samples as well, a black residue is commonly filtered out of the sample solution, and this residue is presumed to be refractory organic carbon. The black solid retained during the filtering step does not appear to be of significance for the determination of Ni, Sr, Y, the REE, W, Th, and U, and it is concluded that these elements are hosted primarily by carbonate minerals, and therefore are quantifiable using the carbonate decomposition method. The accurate quantification of Ni using the carbonate method is notable, as this is only possible in an HNO_3 acid matrix and by monitoring the ^{62}Ni isotope. Unlike ^{60}Ni, which is generally not suitable for Ni

determinations in carbonate rocks regardless of the acid matrix, concentration determinations using ^{62}Ni provide excellent results for samples that are diluted in HNO_3, primarily through a reduction in the $^{25}Mg^{37}Cl$ interference.

Elements that appear to be hosted primarily in refractory mineral phases resistant to decomposition using the HNO_3 carbonate method include Ti, Rb, Zr, Nb, Cs, Hf, and Ta, which would be expected for these incompatible elements. Two elements that may be concentrated in different mineral phases are Ba and Pb (C- and S-rich minerals?), for which the carbonate decomposition recovers approximately 90% and 80%, respectively, of the concentrations observed for the HF-$HClO_4$ decomposition method.

As stated above, it appears that the carbonate decomposition provides satisfactory results for W. However, W is one of three elements apparently 'lost' during the analytical recovery test of the carbonate decomposition method, along with Ta, and to a lesser extent Nb (see Section 6, Fig. 10). The low analytical recovery for Nb, Ta, and W are attributed to the filtering step of the carbonate decomposition. For Nb and Ta, the poor analytical recoveries during the carbonate decomposition method are inconsequential, as regardless, sample dissolution in HNO_3 is not expected to provide accurate determinations of these elements. In the case of W, the observed loss during the filtering step is estimated at ~0.002 mg/kg (Fig. 10), which is also inconsequential when considering the reference concentration of W in the JDo-1 dolomite of ~0.260 mg/kg. It is therefore unlikely that any loss of W during the filtering step for the carbonate decomposition would significantly affect W determinations, assuming W is present at concentrations ≥0.050 mg/kg in the sample powder. This is particularly true when considering the uncertainty in the JUB measured W data for JDo-1 (~15% RSD).

7.6. Marine ferromanganese nodules and crusts

Samples which comprise a large fraction of the geochemical research performed with the Geochemistry Lab at JUB are marine ferromanganese nodules and crusts (referred to collectively as Fe-Mn crusts). These Fe-Mn crusts are typically 13-15% SiO_2, 3-5% Al_2O_3, ~3% each CaO and MgO, 33-38% MnO, and 8-15% Fe_2O_3. Therefore, the high metal content and interferences from Mn and Fe are expected to provide the greatest obstacles to accurate trace metal determinations. However, unlike other metal-rich rocks such as iron-formations, Fe-Mn crusts are highly enriched in

many trace metals, and therefore may be diluted significantly following decomposition. For example, the combined REY concentration within the Fe-Mn crust JMn-1 is >800 mg/kg, whereas the iron-formation IF-G contains only ~22 mg/kg REY. While IF samples typically may not be diluted by a factor greater than 1000, Fe-Mn crust analyses may benefit from higher dilution factors (≥5000).

Several Fe-Mn crust CRMs are available for geochemical studies at JUB, and include JMn-1 (Table 1), NOD-A-1 and NOD-P-1 (USGS), and GSPN-2 and GSPN-3 (Institute of Rock and Mineral Analysis, People's Republic of China). For this discussion only the JMn-1 ferromanganese crust issued by the Geological Survey of Japan is considered, though additional information regarding analyses at JUB of other Fe-Mn crust CRMs is available from K. Schmidt.

Figure 21 displays comparisons between measured JUB trace metal concentrations in JMn-1 with the average reference value. Measured concentrations are lower than the average reference value for all analyzed elements, with JUB data for 24 of 32 elements between 80-95% of the reference value. The precision of the JUB is generally quite good (2-3 % RSD), suggesting that the low measured values are reproducible and do not result from a single anomalous analysis. As discussed earlier, at high TDS contents samples may suffer from signal suppression effects (Section 4.2), which may result in low measured concentrations. However, this does not appear to be the case with JMn-1, as all of the JUB analyses were performed at dilution factors of 2500-5000, and the internal standard correction factors for these analyses were typically between 0.90–1.10.

Rather, it is hypothesized that absorption of water vapor by JMn-1 sample powder is primarily responsible for the low measured concentrations. For this study, the JMn-1 powder was not dried prior to analysis, as for most CRMs drying the rock powder (e.g., overnight at 105-110°C) has not proven to significantly affect the measured concentrations of the elements of interest. However, Fe-Mn crusts are microcrystalline marine precipitates composed of poorly ordered mineral phases that, unlike other rock CRMs, have never undergone mineral recrystallization during diagenesis and lithification. As a result it is possible that powdered Fe-Mn crusts may more readily absorb water from ambient laboratory air (even though all CRMs are stored in dessicators until ready for use), and any increase in sample mass due to this effect would drive measured concentrations of trace metals towards lower values. This hypothesis is supported by detailed studies of Fe-Mn crusts by K. Schmidt

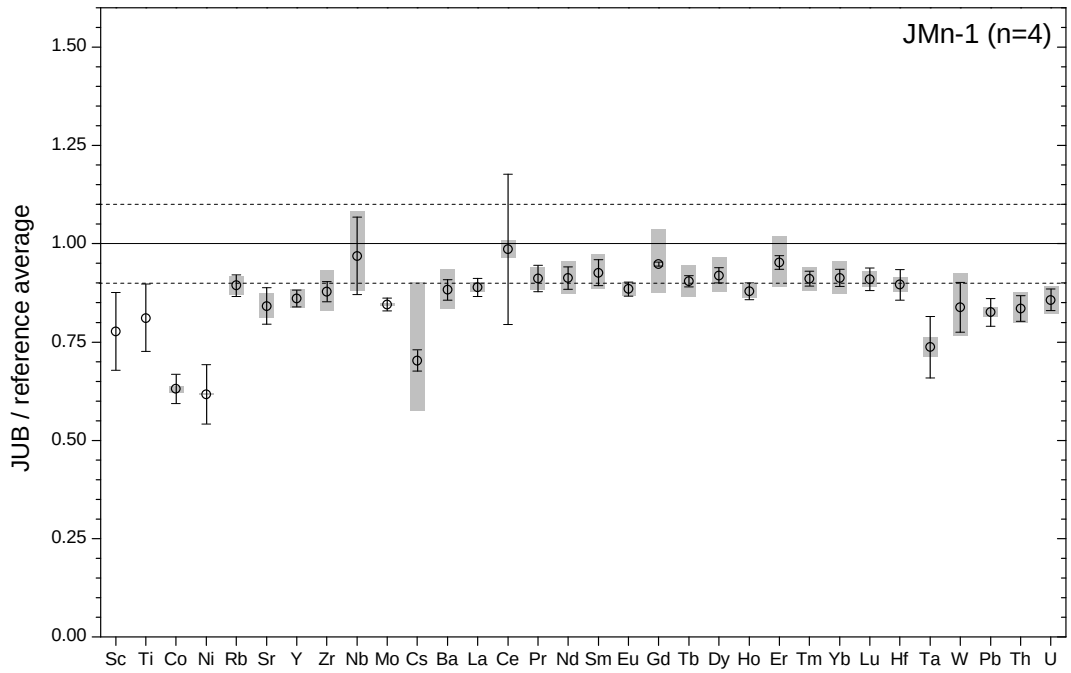

Figure 21. Accuracy estimation for ICPMS analysis of Fe-Mn nodule JMn-1, where *n* equals the number of separate HF-$HClO_4$ sample decompositions and ICPMS analyses in 0.5 M HCl. Grey bars represent variability in the calculated ratio that is due solely to uncertainty in the *reference average.* Vertical lines represent the variability in the calculated ratio due to the uncertainty of the JUB data, and all data are presented in App. 1. The generally low concentrations for many elements as measured at JUB are hypothesized to result from the adsorption of water vapor by the JMn-1 powder, which would effectively dilute the sample and lower the measured concentrations (see text for details).

(personal communication), who observed that concentrations measured in non-dried JMn-1 powders were typically 10-20% lower than concentrations determined for dried JMn-1 powders.

7.7. Basalts

The last rock type frequently used in geochemical studies at JUB is basalt, which is representative of oceanic crust. Basaltic rocks are relatively Al-poor, Mg- and Fe-rich igneous rocks that have formed throughout Earth's history, and have been the focus of numerous geochemical studies related to crustal differentiation, hot spot volcanism, seawater-crust interaction, etc. As a result of this research attention basaltic CRMs are very well characterized, with numerous published studies reporting data for a large number of trace metals.

One of the best characterized basalt CRMs is BHVO-2, a Hawaiian basalt issued by the USGS. The BHVO-2 basalt is 13.5% Al_2O_3, 7.2% MgO, 11.4% CaO, 0.17% MnO, and 12.3% Fe_2O_3. Based on these major element abundances,

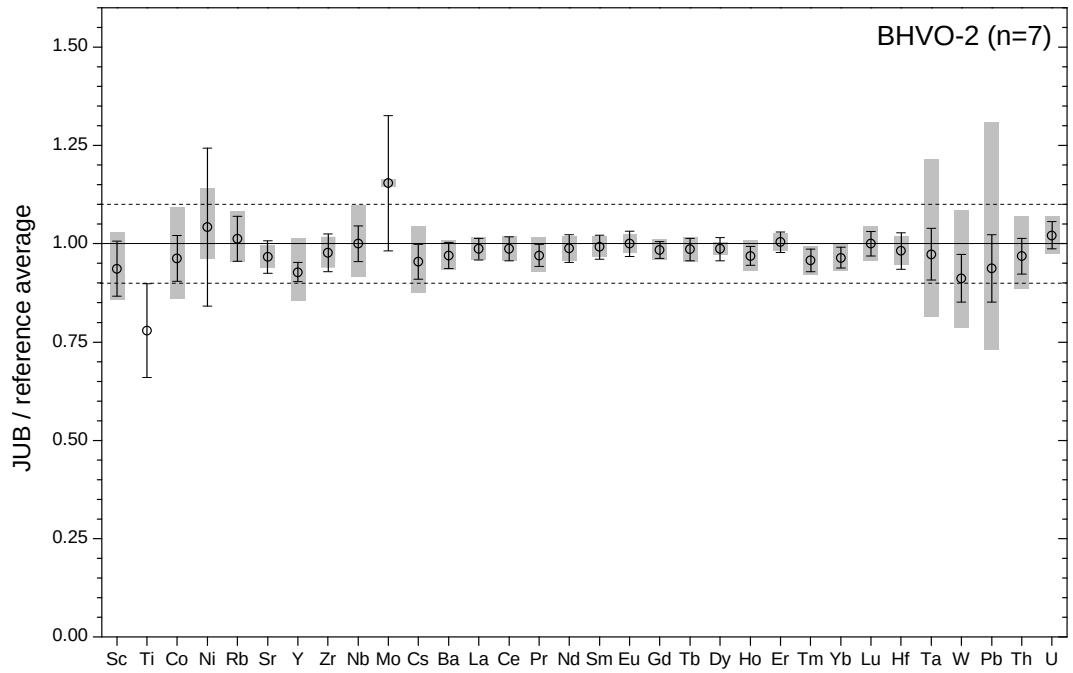

Figure 22. Accuracy estimation for ICPMS analysis of basalt BHVO-2, where *n* equals the number of separate HF-$HClO_4$ sample decompositions and ICPMS analyses in 0.5 M HCl. Grey bars represent variability in the calculated ratio that is due solely to uncertainty in the *reference average*. Vertical lines represent the variability in the calculated ratio due to the uncertainty of the JUB data, and all data are presented in App. 1. Of all the CRMs analyzed at JUB, data for BHVO-2 basalt most closely matches the average reference values, and does so for the greatest number of elements.

interferences would be expected on Co and Ni (from MgCl, AlCl, and CaO(H)), and to a lesser extent on Nb from FeCl. However, concentrations of Co, Ni, and Nb in BHVO-2 are significant (46.0, 119, and 17.5 mg/kg, respectively), and major element interferences do not appear to affect analytical accuracy for Co, Ni, and Nb (Figure 22).

Of the various CRMs analyzed at JUB, data for BHVO-2 most closely matches the average reference values, and does so for the greatest number of elements. Of the 32 elements measured, 30 are within ±10% of the reference value, and 26 are within ±5% (Fig. 22). The excellent agreement between measured and reference data is attributed to the fact that BHVO-2 contains significantly higher concentrations of many elements that display 'poor' accuracy for a number of CRMs (e.g., Co, Ni, Zr, Nb, Hf, Ta, Th), and these higher concentrations facilitate geochemical analyses. Additionally, the numerous published studies for a large number of trace metals in BHVO-2 ensures a robust dataset for calculating an average

reference value. The result is that for many elements the uncertainty in the average reference value is similar to that observed for the JUB data (2-5% RSD, App. 1).

The close agreement illustrated for most elements in Fig. 22 is not observed for Ti in BHVO-2, which has consistently produced low measured values in the JUB data compared to the compiled literature value (App. 1). The reason for this behavior is not yet clear, yet it is hypothesized that it may result from a combination of the high Ti content in BHVO-2 and the relatively low 10 μg/kg Ti calibration standard used for determination of Ti concentrations. The ionization efficiency of Ti is quite low, and the 10 μg/kg Ti calibration standard produces an ICPMS signal intensity of only 8000-10,000 cps, relative to rather high blank intensities of 500-800 cps due to CCl and NO_2 interferences (Table 4). In comparison, the abundance of Ti in BHVO-2 routinely produces 7-9 *million* cps at dilution factors of 1000. A benefit of ICPMS instruments is that they frequently offer linear signal responses for many elements at concentration ranges that exceed six orders of magnitude. However, in the case of Ti, the combination of blank intensities roughly one order of magnitude less than the calibration standard intensities, which are themselves approximately three orders of magnitude less than the sample intensity, may produce a non-linear instrument response. The fact that good results are observed in those CRMs that contain ~1000-1500 mg/kg Ti (FeR-2 and SGR-1b), with poorer results at higher Ti abundances (e.g., >6000 mg/kg as in JMn-1), offers indirect support of this hypothesis. However, further investigation is warranted, and an approach of higher dilution factors for BHVO-2 (2500-5000), coupled with an increase in the Ti concentration of the calibration standard (50 μg/kg?) is recommended.

7.8. Rare earth element ratios

A significant emphasis of much of the research conducted within the Jacobs University Geochemistry Lab regards the behavior of the rare earth elements and yttrium in geological samples, including rocks and minerals, as well as natural water samples such as seawater, hydrothermal fluids, and ground and river waters. Analytical studies of the REY are generally more focused upon the relative distribution of these elements within any given sample, rather than their concentrations, and the REY plot in Fig. 14 is a typical manner of presenting REY data. Frequently, the shape of REY patterns for interpreting geological samples are

Table 5. Select REY ratios and chondrite-normalized REE anomalies as calculated from reference data and JUB data for BHVO-2 basalt.

REY ratio	avg. ref. data[1]	JUB data	JUB/ref. avg.
Pr/Sm	0.8885	0.8691	0.978
Pr/Dy	1.017	1.000	0.983
Pr/Yb	2.711	2.726	1.006
Sm/Dy	1.145	1.151	1.005
Sm/Yb	3.051	3.137	1.028
Dy/Yb	2.665	2.726	1.023
Y/Ho	26.44	25.31	0.957
Ce/Ce*[2]	1.00	1.01	0.99
Ce/Ce*[3]	0.933	0.964	0.97
Eu/Eu*[4]	1.00	1.01	0.99
Eu/Eu*[5]	1.01	1.02	0.99

[1] average reference data (see Appendix 1).
[2] calculated as Ce/Ce* = Ce/(0.5La+0.5Pr).
[3] calculated as Ce/Ce* = Ce/(2Pr-1Nd) after Bolhar et al. (2004).
[4] calculated as Eu/Eu* = Eu/(0.5Sm+0.5Gd).
[5] calculated as Eu/Eu* = Eu/(0.67Sm+0.33Tb).

more useful than the absolute REY abundances, because fractionation between REY elements (and the specific REY patterns that result), may offer clues to the processes responsible for the formation and subsequent history of many geological samples.

Since the relative distribution of the REY is often more informative for interpreting geochemical data, it is useful to examine the ability of the described analytical methods in accurately determining the REY patterns in geological materials. As this study has focused upon the analyses of CRMs, and the BHVO-2 basalt is considered the best characterized reference material with respect to the REY, the discussion is limited to relative REY ratios in BHVO-2.

Table 5 lists REY ratios that characterize the relative distributions of the light rare earth elements (Pr/Sm), the middle rare earth elements (Sm/Dy), and the heavy rare earth elements (Dy/Yb) for the BHVO-2 basalt. Ratios that include La, Ce, Gd, Eu, and Lu are not used, as these elements may display anomalous behavior in some geological samples (e.g., La and Ce in seawater, and Eu in hydrothermal fluids and plagioclase-rich rocks). Data used for calculating all REY ratios are tabulated in Appendix 1. No consideration of the relative errors in determining the concentrations of individual REY elements as reported in Appendix 1 is present in the data of Table 5, as for many of the elements the %RSD is very similar between the average

reference value and the measured JUB data (e.g., 3.5% and 2.7% for Yb, respectively). Relative to the REY ratios calculated from the average reference data, the JUB ratios are accurate to within 1% for Pr/Yb, 2% for Pr/Dy, 3% for Pr/Sm, Sm/Yb, and Dy/Yb, and to within 5% for Y/Ho. Considering the well-characterized nature of the BHVO-2 basalt and the large number of highly precise ICPMS analyses reported for this CRM, these values are considered the best estimates of the accuracy of the JUB analytical methods in determining REY ratios.

Also presented in Table 5 are examples of calculated REE anomalies for chondrite-normalized data of Ce and Eu, two rare earth elements that may be fractionated from neighboring REE in natural systems (e.g., in seawater for Ce, and in high-temperature hydrothermal systems for Eu). Normalized REE data that is anomalous is commonly quantified by means of X/X^* ratios, where X is the normalized measured concentration for a particular rare earth element, and X^* is the predicted normalized concentration for that element. The predicted REE concentration X^* may be calculated in various ways (e.g., Bolhar et al., 2004), and X^* is commonly obtained by interpolating between adjacent REE, as in the calculation of Eu* by means of (0.5Sm + 0.5Gd). Alternatively, X^* may be obtained by extrapolating from adjacent REE, as in the case of Ce* by means of (2Pr - 1Nd). Different methods for calculating chondrite-normalized Ce/Ce* and Eu/Eu* are presented in Table 5, and demonstrate that REE anomalies calculated from measured JUB data accurately reproduce the anomalies as determined from the average reference data of the BHVO-2 basalt.

8. Summary and conclusions

The ICPMS analytical methods utilized within the JUB Geochemistry Lab are capable of reproducibly determining accurate concentrations of many trace metals in a variety of rock types. The relative precision of the ICPMS measurements is primarily controlled by the inherent ICPMS instrument precision, and not by sample preparation and decomposition techniques. On average, for *all* rock types decomposed using the HF-$HClO_4$ decomposition method, the ICPMS instrument precision (RSD) is better than 3% for eleven elements (Ti, Co, Sr, Y, Zr, Ba, La, Ce, Pr, Nd, Pb), between 3-5% for sixteen elements (Sc, Ni, Rb, Nb, Sm, Eu, Gd, Tb, Dy, Ho, Er, Tm, Yb, Lu, Th, U), and between 5-8% for only five elements (Mo, Cs, Hf, Ta, W). Certainly, the poorer precision observed for some elements is due to low

concentrations of these elements in many rock types (e.g., Cs and Hf in JDo-1), and/or possible inhomogeneities in the CRM sample powders.

The sample decomposition methods employed appear to conservatively retain all 32 elements analyzed throughout the dissolution procedures, with the only exceptions being Ni, Ta, and W during the carbonate decomposition. Greater than expected recoveries of Ni in spike solutions during the carbonate decomposition suggest a Ni contamination of 2-5 μg/kg occurs, likely during filtration of the dissolved sample solution. Analytical recoveries of Ta and W are low (24% and 80%, respectively), and observed to a lesser extent for Nb (92% recovery), and appear to reflect retention of these elements on the 0.2 μm cellulose acetate filters used during the carbonate decomposition.

Some analyzed elements are significantly affected by interferences generated by high major element contents in certain rock types. The affected elements have atomic masses <100, and interferences primarily result from oxide and chloride species of the major rock-forming elements Mg, Ca, Al, Fe, and Mn. The best example is Co, which is unlikely to be measurable in carbonate samples due to MgCl and CaO(H) interferences, unless present at significant concentrations in the sample powder (>10 mg/kg). Determination of low Nb contents (less than ~20 mg/kg) in Fe-rich samples is also likely to prove difficult, and Appendix 2 provides a thorough treatment of observed major element interferences and recommendations regarding analyses of specific rock types. The potential for reducing chloride-derived interferences that arise from the use of HCl during sample dilutions should be investigated more thoroughly. Diluting samples prior to ICPMS analyses in mixtures of HNO_3 and HCl may satisfactorily mitigate many major element interferences on low mass trace metals such as Co, Ni, Zr, Nb, and Mo.

The analytical accuracy of the ICPMS measurements is considered excellent, though accuracy assessments are hampered by the lack of well constrained reference values for many trace metals in the CRMs discussed. It appears that older data compilations frequently overestimate the abundances of many trace metals, and for some elements very few published data exist (e.g., Nb, Mo, Ta, W). The best constrained CRM is the BHVO-2 basalt, for which the data produced at JUB is in excellent agreement. Based upon multiple analyses of BHVO-2 it is concluded that the JUB methods described here provide accurate element determinations for 31 of

the 32 analyzed elements, with Ti being the only exception. Element concentrations in CRMs measured at JUB also agree well with recent published studies that focused on similar trace metals, and that used similar analytical methods. While the task of ensuring accuracy in analytical data is a continuous process, it is concluded that the ICPMS methods described here are suitable for reproducibly determining highly precise and accurate trace element data in a variety of geologic materials.

References

Abbey S., McLeod C.R., and Liang-Guo W. (1983) FeR-1, FeR-2, FeR-3, and FeR-4 four Canadian iron-formation samples prepared for use as reference materials. Geol. Sur. Canada paper 83-19.

Baker J.A., Waight T., and Ulfbeck D. (2002) Rapid and highly reproducible analysis of rare earth elements by multiple collector inductively coupled plasma mass spectrometry. *Geochim. Cosmochim. Acta*, 66, 3635-3646.

Barrat J.A., Boulègue J.J., Tiercelin J.-J., and Lesourd M. (2000) Strontium isotopes and rare-earth element geochemistry of hydrothermal carbonate deposits from Lake Tanganyika, East Africa. *Geochim. Cosmochim. Acta*, 64, 287-298.

Bédard L.P. and Barnes S.-J. (2002) A comparison of N-type semi-planar and coaxial INAA detectors for 33 geochemical reference samples. J. *Radioanalytical Nuclear Chem.*, 254, 485-497.

Bolhar R., Kamber B.S., Moorbath S., Fedo C.M., and Whitehouse M.J. (2004) Characterisation of early Archaean chemical sediments by trace element signatures. *Earth Planet. Sci. Lett.*, 222, 43-60.

Dai Kin F., Prudêncio M.I., Gouveia M.A., and Magnusson E. (1999) Determination of rare earth elements in geological reference materials: A comparative study by INAA and ICP-MS. *Geostand. Newsletter*, 23, 47-58.

Doherty W. (1989) An internal standardization procedure for the determination of yttrium and the rare earth elements in geological materials by inductively coupled plasma-mass spectrometry. *Spectrochim. Acta*, 44B, 263-280.

Dulski P. (1994) Interferences of oxide, hydroxide and chloride analyte species in the determination of rare earth elements in geological samples by inductively coupled plasma-mass spectrometry. *Fresenius J. Anal. Chem.*, 350, 194-203.

Dulski P. (2001) Reference materials for geochemical studies: new analytical data by ICP-MS and critical discussion of reference values. *Geostand. Newsletter*, 25, 87-125.

Eggins S.M. (2003) Laser ablation ICP-MS analysis of geological materials prepared as lithium borate glasses. *Geostand. Newsletter*, 27, 147-162.

Faure G. (1986) *Principles of Isotope Geology*. John Wiley and Sons, New York.

Flem B. and Bédard L.P. (2002) Determination of trace elements in BCS CRM 313/1 (BAS) and NIST SRM 1830 by inductively coupled plasma-mass spectrometry and instrumental neutron activation analysis. *Geostand. Newsletter*, 26, 287-300.

Garbe-Schönberg C.-D. (1993) Simultaneous determination of thirty-seven trace elements in twenty-eight international rock standards by ICP-MS. *Geostand. Newsletter*, 17, 81-97.

Govindaraju K. (1994) 1994 compilation of working values and sample descriptions for 383 geostandards. *Geostand. Newsletter*, 18, 1-158.

Govindaraju K. (1995) 1995 working values with confidence limits for twenty-six CRPG, ANRT and IWG-GIT geostandards. *Geostand. Newsletter*, 19 (special), 1-95.

Huang S. and Frey F.A.(2003) Trace element abundances of Mauna Kea basalt from phase 2 of the Hawaii Scientific Drilling Project: Petrogenetic implications of correlations with major element content and isotopic ratios. *Geochem. Geophys. Geosys.*, 4, 1-43.

Imai N., Terashima S., Itoh S., and Ando A. (1996) 1996 compilation of analytical data on nine GSJ geochemical reference samples: "Sedimentary Rock Series". *Geostand. Newsletter*, 20, 165-216.

Imai N., Terashima S., Itoh S., and Ando A. (1999) 1998 compilation of analytical data for five GSJ geochemical reference samples: The "Instrumental Analysis Series". *Geostand. Newsletter*, 23, 223-250.

Jochum K.P., Nohl U., Herwig K., Lammel E., Stoll B., and Hofmann A.W. (2005) GeoReM: A New Geochemical Database for Reference Materials and Isotopic Standards. *Geostand. Geoanalytical. Res*, 29, 333-338.

Korotev R.L. (1996) A Self-Consistent compilation of elemental concentration data for 93 geochemical reference samples. *Geostand. Newsletter*, 20, 217-245.

MacDougall D., Crummett W.B., and et al. (1980) Guidelines for Data Acquisition and Data Quality Evaluation in Environmental Chemistry. *Anal. Chem.*, 52, 2242–2249.

McLennan S. (1989) Rare earth elements in sedimentary rocks: influence of provenance and sedimentary processes. in Geochmemstry and Mineralogy of the Rare Earth Elements (eds. B.R. Lipin and G.A. McKay). Reviews in Mineralogy, Vol. 21.

Meisel T., Schöner N., Paliulionyte V. and Kahr E. (2002) Determination of rare earth elements, Y, Th, Zr, Hf, Nb and Ta in geological reference materials G-2, G-3, SCo-1 and WGB-1 by sodium peroxide sintering and inductively coupled plasma-mass spectrometry. *Geostand. Newsletter*, 26, 53-61.

Münker C. (1998) Nb/Ta fractionation in a Cambrian arc/back arc system, New Zealand: source constraints and application of refined ICPMS techniques. *Chem. Geol.*, 144, 23-45.

Plumlee G. (1998) USGS Certificate of Analysis Basalt, Hawaiian Volcanic Observatory, BHVO-2, USGS, Boulder CO.

Polat A., Li Jianghai, Fryer B.J., Kusky T., Gagnon J., and Zhang S. (2006) Geochemical characteristics of the Neoarchean (2800-2700 Ma) Taishan greenstone belt, North China Craton: Evidence for plume-craton interaction. *Chem. Geol.*, 230, 60-87

Ryder C.H., Gill J., Tepley III F., Ramos F., and Reagan M. K. (2006) Closed- to open-system-differentiation at Arenal volcano (1968-2003). *J. Volcano. Geotherm. Res.*, 157, 75-93.

Schramm B., Devey C.W., Gillis K.M., and Lackschewitz K. (2005) Quantitative assessment of chemical and mineralogical changes due to progressive low-temperature alteration of East Pacific Rise basalts from 0 to 9 Ma. *Chem. Geol.*, 218, 281-313.

Shafer J.T., Neal C.R., and Regelous M. (2005) Petrogenesis of Hawaiian postshield lavas: Evidence from Nintoku Seamount, Emperor Seamount Chain. *Geochem. Geophys. Geosys.*, 6, Q05L09, doi:10.1029/2004GC000875.

Smith D.B. (1995) USGS Certificate of Analysis Cody Shale, SCo-1, United States Geologic Survey, Boulder, CO.

Terashima S., Usui A., and Imai N. (1995) Two new GSJ geochemical reference samples: Syenite JSy-1 and manganese nodule JMn-1. *Geostand. Newsletter*, 19, 221-229.

Thomas R. (2003) *Practical Guide to ICPMS*. Practical Spectroscopy Series, Taylor and Francis, London.

Thompson J.J and Houk R.S. (1987) A Study of Internal Standardization in Inductively Coupled Plasma-Mass Spectrometry. *Appl. Spectroscopy*, 41, 801-806.

Willbold M. and Jochum K.P. (2005) Multi-element isotope dilution sector field ICP-MS: A precise technique for the analysis of geological materials and is application to geological reference materials. *Geostand. Geoanalytical. Res.*, 29, 63-82.

Wilson S.A.(2001) USGS Certificate of Analysis Green River Shale, SGR-1. United States Geologic Survey, Boulder CO.

Yamamoto Koshi, Itoh N., Matsumoto T., Tanaka Tsuyoshi, and Adachi M. (2004) Geochemistry of Precambrian carbonate intercalated in pillows and its host basalt: implications for the REE composition of circa 3.4Ga seawater. *Precam. Res.*, 135, 331-344.

Yu Z., Robinson P., and McGoldrick P. (2001) An evaluation of methods for the chemical decomposition of geological materials for trace element determination using ICP-MS. *Geostand. Newsletter*, 25, 199-217.

Appendix 1. Analytical data

Appendix 1 contains the literature data used to calculate the average CRM reference values discussed in Section 7 regarding analytical accuracy. The average measured trace metal concentrations as determined within the JUB Geochemistry Lab for the various CRMs are also presented. As discussed within the main text of this study, some isotopes with atomic masses <100 are not suitable for quantifying elemental concentrations, and the data presented in this appendix reflect this observation.

Two elements have isotopes that are routinely monitored during ICPMS analyses, but not necessarily used for purposes of quantifying the element. These elements are Ni and Zr, which are monitored for the following isotopes; ^{60}Ni and ^{62}Ni, and ^{90}Zr and ^{91}Zr. For samples low in Mg and Ca, ^{60}Ni is the preferred isotope for quantification, as ^{60}Ni is more abundant (26.22%) than ^{62}Ni (3.63%). The exception to this occurs only for samples that are diluted in 0.5 M HNO_3 (i.e., the carbonate decomposition), and in these cases high Ca and Mg contents are not problematic. Diluting samples in HNO_3 eliminates the $^{25}Mg^{37}Cl$ interference on ^{62}Ni, and in these instances ^{62}Ni is the most appropriate choice for Ni determinations.

However, rocks that are low in Mg and Ca (and Ni) may produce anomalous results for ^{62}Ni, primarily for those samples with more than a few percent Al_2O_3. This behavior is observed for the iron-formations FeR-2 and IF-G, which have very different Al_2O_3 contents of 5.1% and 0.15%, respectively, yet similar Ni concentrations (~23 mg/kg). For FeR-2, use of the ^{62}Ni isotope is not appropriate as it results in Ni concentrations several mg/kg higher than the reference value, whereas ^{60}Ni accurately reproduces the literature data. However, for IF-G both ^{60}Ni and ^{62}Ni are in excellent agreement and match the reference value, and the Ni data for IF-G presented here were quantified using both Ni isotopes. It is therefore recommended that ^{62}Ni not be used for quantifying Ni unless Mg, Ca, and Al are present at very low concentrations, and/or the sample is diluted in HNO_3. It should be noted that in addition to IF-G, Ni in the ferromanganese nodule JMn-1 is also determined using both Ni isotopes, and that ^{62}Ni returns a Ni concentration ~10-20% higher than that observed using ^{60}Ni. This discrepancy is somewhat surprising considering the very high Ni abundance in JMn-1 (~1.2%). However, the somewhat poor analytical results

for JMn-1 as described in Section 7.6 preclude definitive statements as to the reason for this discrepancy, and further studies of this effect in JMn-1 are recommended.

Concentrations of Zr as reported for all CRMs in this study have been determined solely using ^{90}Zr. Interferences on the ^{91}Zr isotope primarily result from $^{56}M^{35}Cl$ interferences, where *M* can be Fe, CaO(H), or ArO, and the use of HNO_3 for diluting samples will reduce these interferences. Good results using ^{91}Zr in an HCl acid matrix appear to be limited to samples which contain more than ~40 mg/kg Zr, and that contain less than ~10% Fe_2O_3. The use of ^{91}Zr for quantifying Zr should be used with caution, and is likely to prove most useful only for samples diluted in HNO_3, or for those samples diluted in HCl for which the Mn content is high enough to produce significant $^{55}Mn^{35}$ interferences that preclude the use of ^{90}Zr for quantifying Zr (see App. 2).

Appendix 1. Literature reference values and measured element concentration data for CRMs analyzed within JUB Geochemistry Lab. Data in mg/kg.

	FeR-2								FeR-4								IF-G[4]									
	Govindaraju (1994)	Dulski (2001)	Yu et al. (2001)	Abbey et al. (1983)			*this study*		Govindaraju (1994)	Dulski (2001)	Yu et al. (2001)	Abbey et al. (1983)			*this study*		Govindaraju (1995)	Dulski (2001)	Barrat et al. (2000)	Baker et al. (2002)	Bohlar et al. (2004)			*this study*	
method[1]	compiled	ICPMS	ICPMS	compiled	ref. avg.[2]	*%RSD*	JUB avg.[3] (n=3)	*%RSD*	compiled	ICPMS	ICPMS	compiled	ref. avg.	*%RSD*	JUB avg. (n=2)	*%RSD*	compiled	ICPMS	ICPMS	ID MC-ICPMS	ICPMS	ref. avg.	*%RSD*	JUB avg. (n=2)	*%RSD*
Sc	6		5.31	6	5.77	*5.6*	5.34	*3.2*	1.5		1.09	1.5	1.36	*14.2*	0.875		0.3				0.2846	0.2923	*2.6*	<IQL	
Ti	1140			1080	1110	*2.7*	1130	*4.9*	420			420	420	*0.0*	327	*3.0*	84					84		23.9	
Co	7			7	7	*0.0*	7.04	*3.5*	2			2	2	*0.0*	1.63	*3.4*	29					29		28.5	*0.9*
Ni	25			21	23	*8.7*	23.7	*3.6*	8			6	7	*14.3*	5.41	*0.5*	22.5				23.856	23.178	*2.9*	23.7	*0.7*
Rb	67	65	61.8	66	65.0	*3.0*	61.1	*4.0*	16	16.1	14.9	16	15.8	*3.1*	14.9	*3.8*	0.4	0.5			0.2909	0.3970	*21.5*	0.450	*2.6*
Sr	58	63	60.9	58	60.0	*3.5*	59.9	*2.2*	62	66	60.4	62	62.6	*3.3*	60.9	*2.3*	3	4			3.61	3.54	*11.6*	4.00	*0.5*
Y	16	13.3	13.2	15	14.4	*8.2*	12.5	*1.8*	9	7.9	7.87	8	8.19	*5.7*	7.61	*4.2*	9	9.1			9.135	9.078	*0.6*	9.77	*0.4*
Zr	39	41	45.8	39	41.2	*6.7*	39.5	*5.5*	18	19.3	18.4	18	18.4	*2.9*	18.4	*4.7*	1	1.0			0.5637	0.8546	*24.1*	0.934	*3.3*
Nb			3.95		3.95		5.76*	*70.5*			0.776		0.776		1.91*	*14.4*	0.1				0.0989	0.0995	*0.6*	0.764*	*19.6*
Mo	3		6.05	3	4.02	*35.8*	3.34	*0.3*			0.142		0.142		1.03		0.7					0.7		0.614	*2.0*
Cs	4.5	4.61	4.95	5	4.77	*4.5*	4.40	*3.4*	0.7	0.7	0.667	0.8	0.717	*7.0*	0.666	*6.0*	0.06	0.059			0.0623	0.0604	*2.3*	0.0591	*0.5*
Ba	230	226	243	240	235	*3.0*	214	*3.3*	39	39	38.3	43	39.8	*4.7*	38.4	*4.4*	1.5	3			2.024	2.175	*28.6*	2.21	*4.5*
La	12	12.8	13.6	14	13.1	*5.9*	11.4	*1.5*	8	8.1	8.47	8	8.14	*2.4*	8.26	*7.1*	2.8	2.7	2.67	2.626	2.706	2.700	*2.1*	2.68	*4.8*
Ce	25	26	27.8		26.3	*4.4*	23.8	*1.8*	11	13.3	13.7		12.7	*9.4*	13.9	*7.3*	4	4	3.93	3.801	3.902	3.927	*1.9*	3.92	*3.7*
Pr	3	3.2	3.35		3.18	*4.5*	2.77	*2.3*	2	1.69	1.72		1.80	*7.7*	1.69	*7.3*	0.4	0.45	0.427	0.4098	0.4302	0.4234	*4.1*	0.419	*3.7*
Nd	12	12	13.6		12.5	*6.0*	11.3	*1.7*	8	7.6	8.22		7.94	*3.2*	7.74	*4.9*	1.8	1.75	1.74	1.709	1.731	1.746	*1.7*	1.78	*3.9*
Sm	2.5	2.6	3.02	2.6	2.68	*7.5*	2.41	*2.1*	2.1	2.2	2.39	2.2	2.22	*4.7*	2.10	*3.7*	0.4	0.39	0.375	0.3859	0.399	0.3900	*2.4*	0.401	*2.9*
Eu	1.25	1.28	1.48		1.34	*7.6*	1.18	*1.4*	0.74	0.7	0.79		0.74	*5.0*	0.716	*4.5*	0.39	0.37	0.348	0.3554	0.3621	0.3651	*3.9*	0.372	*2.8*
Gd	2	2.33	2.88		2.40	*15.1*	2.14	*2.7*	1.1	1.22	1.44		1.25	*11.2*	1.26	*4.3*	0.74	0.71	0.65	0.6671	0.6669	0.6868	*4.8*	0.712	*1.3*
Tb	0.32	0.354	0.398		0.357	*8.9*	0.328	*0.9*	0.15	0.173	0.185		0.169	*8.6*	0.175	*2.8*	0.11	0.111	0.109		0.1123	0.1106	*1.1*	0.113	*2.1*
Dy	2	2.2	2.51		2.24	*9.4*	2.07	*1.7*	1	1.05	1.16		1.07	*6.2*	1.08	*0.7*	0.8	0.81	0.805	0.799	0.7914	0.8011	*0.8*	0.830	*2.2*
Ho	0.6	0.463	0.545		0.536	*10.5*	0.434	*1.0*	0.2	0.22	0.251		0.224	*9.4*	0.224	*0.8*	0.2	0.203	0.209		0.2066	0.2047	*1.7*	0.208	*1.7*
Er	1.5	1.38	1.64		1.51	*7.1*	1.30	*1.5*	0.5	0.65	0.761		0.637	*16.8*	0.676	*0.8*	0.63	0.64	0.636	0.6345	0.6188	0.6319	*1.2*	0.659	*1.9*
Tm	0.2	0.207	0.237		0.215	*7.5*	0.185	*4.5*		0.093	0.108		0.101	*7.5*	0.0954	*0.4*	0.09	0.091			0.0923	0.0911	*1.0*	0.0922	*1.7*
Yb	1.25	1.35	1.59	1.3	1.37	*9.5*	1.24	*0.4*	0.7	0.63	0.717	0.5	0.637	*13.4*	0.612	*0.1*	0.6	0.58	0.573	0.5646	0.5802	0.5796	*2.0*	0.579	*1.2*
Lu	0.2	0.203	0.239		0.214	*8.3*	0.193	*0.6*	0.1	0.091	0.112		0.101	*8.5*	0.0975	*2.6*	0.09	0.091	0.091	0.08939	0.0904	0.0904	*0.7*	0.0933	*1.6*
Hf	1	1.1	1.35		1.15	*12.8*	1.01	*6.5*	0.5	0.52	0.572		0.531	*5.7*	0.525	*1.6*	0.04	0.023			0.0182	0.0271	*34.6*	0.0249	*1.3*
Ta	0.2		0.194		0.197	*1.5*	0.196	*13.3*			0.051		0.051		0.0900	*3.6*	0.2				0.1715	0.1858	*7.7*	0.167	*1.0*
W							1.59	*34.9*							1.65	*1.8*	220					220		248	*1.1*
Pb	11	9	8.48	11	9.87	*11.6*	8.16	*2.7*	8	7.3	7.14	8	7.61	*5.2*	7.67	*14.2*	4	2.5			2.518	3.006	*23.4*	2.52	*1.1*
Th	2.4	2.6	3.22	3	2.81	*11.5*	2.48	*2.9*	0.8	0.87	0.976		0.882	*8.2*	0.828	*3.9*	0.1	0.05			0.0434	0.0645	*39.2*	0.0474	*2.9*
U	1.2	1	1.29		1.16	*10.4*	1.12	*12.9*	0.5	0.8	0.641		0.647	*18.9*	0.480	*2.7*	0.02	0.021			0.0213	0.0208	*2.7*	0.0218	*4.0*

[1] data sources, whether compiled from studies or from single analytical method, and arranged chronologically: ID MC-ICPMS = isotope dilution multi-collector-ICPMS.

[2] reference average reported to number of significant digits observed in most precisely measured data from literature sources.

[3] JUB average calculated from number of sample decompositions reported in Table 1 and reported to three significant digits only for illustrative purposes (see Section 5 regarding analytical precision).

[4] IF-G data from analyses of original (first lot) IF-G powder as distributed by IWG-GIT; see Table 1 and Section 7 in text for details.

* values greater than reference average considered to include significant contributions from interfering molecular species, arising from high major element contents (Mg, Al, Ca, Mn, Fe).

Appendix 1 continued. Data in mg/kg.

	SCo-1											SGR-1b									JCh-1								
	Smith (1995)	Korotev (1996)	Dai Kin (1999)	Dulski (2001)	Bédard and Barnes (2002)	Meisel et al. (2002)	Eggins (2003)			*this study*		Govindaraju (1994)	Korotev (1996)	Dai Kin (1999)	Wilson (2001)	Dulski (2001)			*this study*		Govindaraju (1994)	Imai et al. (1996)	Dulski (2001)	Flem and Bédard (2002)			*this study*	
method[1]	compiled	INAA	ICPMS	ICPMS	INAA	ICPMS	LA-ICPMS	ref. avg.[2]	*%RSD*	JUB avg.[3] (n=4)	*%RSD*	compiled	INAA	ICPMS	compiled	ICPMS	ref. avg.	*%RSD*	JUB avg. (n=3)	*%RSD*	compiled	compiled	ICPMS	INAA	ref. avg.	*%RSD*	JUB avg. (n=3)	*%RSD*
Sc	11	11.57			11.53		12.7	11.70	*5.3*	12.8	*13.7*	4.6	4.94		4.6		4.71	*3.4*	5.01	*2.6*	0.85	0.979		1	0.943	*7.0*	0.931	*6.3*
Ti	3776						3561	3669	*2.9*	4080	*17.6*	1580			1520		1550	*1.9*	1530	*7.9*	180	189			185	*2.4*	174	*6.5*
Co	11	11.13			11.6			11.24	*2.3*	12.7	*15.1*	11.8	11.73		12		11.84	*1.0*	12.2	*3.3*	15	15.5		14.4	15.0	*3.0*	16.5	*5.5*
Ni	27	24						26	*5.9*	30.3	*22.6*	29	26		29		28	*5.1*	30.3*	*5.0*	7.5	8.76			8.13	*7.7*	10.0	*28.9*
Rb	110	111.5		113	106		111.7	110.4	*2.2*	113	*8.4*	83	79			80	81	*2.1*	82.0	*4.5*	8.5	8.61	8.6	8.3	8.50	*1.5*	8.90	*0.1*
Sr	170	175		169			172.7	171.7	*1.4*	168	*4.3*	420	393		420	381	404	*4.2*	391	*3.7*	4.6	4.2	4.2		4.3	*4.4*	4.03	*1.6*
Y	26			22.8		24.2	26.8	25.0	*6.2*	22.8	*4.4*	13			13	9.6	11.9	*13.5*	9.74	*2.2*	1.84	1.81	1.8		1.82	*0.9*	1.77	*1.6*
Zr	160	166		153	116	165	188.6	158.1	*13.8*	157	*6.6*	53	45		53	42	48	*10.1*	43.7	*3.5*	11.7	11.5	6.2		9.8	*26.0*	6.60	*3.2*
Nb	11					11.6	13.2	11.9	*7.8*	11.8	*4.3*	5.2			5.2		5.2	*0.0*	6.41	*1.1*		1.7			1.7		0.590	*1.5*
Mo	1.4							1.4		1.22	*5.7*	35.1			35		35.1	*0.1*	34.1	*9.2*							0.245	*10.5*
Cs	7.8	7.77		7.7	7.4		7.46	7.63	*2.2*	7.67	*4.1*	5.2	5.19		5.2	5.1	5.17	*0.8*	5.13	*2.2*	0.3	0.243	0.288	0.29	0.280	*7.8*	0.277	*5.7*
Ba	570	559		578	567		592	573	*2.0*	562	*4.3*	290	270		290	265	279	*4.1*	278	*1.6*		302	302	291	298	*1.7*	276	*4.5*
La	30	29.3	28.9	29	30.3	29.7	31.1	29.8	*2.4*	28.1	*3.9*	20.3	18.4	18.2	20	18	19.0	*5.1*	18.2	*2.8*	1.5	1.52	1.44	1.44	1.48	*2.4*	1.34	*4.8*
Ce	62	56.7	57.3	57	60.3	57.5	58.8	58.5	*3.1*	56.1	*3.7*	36	34.4	34	36	33.8	34.8	*2.8*	34.0	*3.3*	4.72	5.21	4.7	4.66	4.82	*4.7*	4.42	*4.5*
Pr	6.6		6.7	7.1		7		6.9	*3.0*	6.69	*3.6*	3.9		3.85		4	3.92	*1.6*	3.91	*2.7*	0.5		0.37		0.44	*14.9*	0.335	*4.6*
Nd	26	25.4	28.4	26	24	27	27.3	26.3	*5.0*	25.7	*3.0*	15.5	13.8	13.7	16	13.8	14.6	*6.8*	14.2	*2.4*	1.7	2.05	1.41	1.4	1.64	*16.2*	1.32	*4.4*
Sm		5.14	5.2	5.0	5.12	5.31	5.52	5.22	*3.2*	4.96	*3.5*	2.7	2.6	1.9	2.7	2.42	2.46	*12.2*	2.52	*2.0*	0.4	0.359	0.30	0.35	0.352	*10.1*	0.281	*4.0*
Eu		1.088	1.3	1.13	1.11	1.17	1.18	1.163	*5.9*	1.10	*3.4*	0.56	0.466	0.48	0.56	0.47	0.507	*8.5*	0.466	*2.1*	0.08	0.0594	0.060	0.1	0.0749	*22.3*	0.0484	*3.0*
Gd			5.3	4.6		4.72	4.8	4.86	*5.5*	4.53	*6.0*	2		1.9	2	2.05	1.99	*2.7*	2.04	*1.5*			0.304		0.304	*0.0*	0.286	*2.4*
Tb		0.675	0.72	0.69	0.69	0.7		0.70	*2.1*	0.675	*3.1*	0.36	0.297	0.37		0.3	0.332	*10.1*	0.295	*1.2*	0.09	0.0385	0.046	0.04	0.0536	*39.5*	0.0438	*2.5*
Dy			4.2	4.0		4.3	4.43	4.23	*3.7*	4.01	*2.7*	1.9		1.8	1.9	1.71	1.83	*4.3*	1.73	*0.9*	0.4	0.378	0.289		0.356	*13.5*	0.273	*2.4*
Ho			0.76	0.8		0.86		0.81	*5.1*	0.803	*2.5*	0.38		0.38	0.4	0.34	0.38	*5.8*	0.347	*0.7*	0.1		0.060		0.080	*25.0*	0.0567	*2.1*
Er			2.2	2.38		2.53	2.68	2.45	*7.3*	2.35	*1.6*	1.11		1.2	1.1	0.99	1.10	*6.8*	1.01	*1.0*	0.3	0.233	0.174		0.236	*21.8*	0.167	*1.8*
Tm			0.4	0.35		0.36		0.37	*5.8*	0.334	*4.8*	0.17		0.18	0.17	0.147	0.167	*7.3*	0.144	*1.6*			0.025		0.025		0.0240	*3.6*
Yb		2.27	1.7	2.34		2.37	2.57	2.25	*13.0*	2.23	*1.4*	0.94	0.966	1.1	0.94	0.96	0.981	*6.1*	0.949	*1.0*	0.1	0.182	0.171	0.16	0.153	*20.7*	0.162	*2.8*
Lu		0.341	0.31	0.36	0.35	0.37	0.388	0.353	*6.9*	0.345	*3.3*	0.14	0.146	0.14		0.146	0.143	*2.1*	0.146	*1.7*	0.04	0.0344	0.026	0.023	0.0309	*21.8*	0.0269	*6.6*
Hf		4.75		4.3	4.4	4.8	5.1	4.67	*6.2*	4.10	*5.9*	1.39	1.371		1.4	1.32	1.370	*2.2*	1.30	*2.8*	0.2	0.195	0.15	0.09	0.159	*27.8*	0.173	*2.0*
Ta		0.804			0.9	0.84	0.921	0.866	*5.4*	0.803	*0.5*	0.42	0.402				0.411	*2.2*	0.404	*1.6*		0.182		0.11	0.146	*24.7*	0.135	*5.8*
W	1.4	1.5						1.5	*3.4*	1.53	*1.9*	2.57	2.3		2.6		2.49	*5.4*	2.52	*0.3*		92.3			92.3		84.7	*2.3*
Pb	31			30.0			33.7	31.6	*5.0*	29.7	*2.4*	38			38	42	39	*4.8*	40.5	*0.3*	2	2	2.0		2.0	*0.0*	1.63	*0.9*
Th	9.7	9.01		9.5	8.72	9.3	10.23	9.41	*5.2*	8.92	*5.7*	4.78	4.48		4.8	4.64	4.68	*2.7*	4.46	*1.6*		0.735	0.56	0.63	0.642	*11.2*	0.555	*0.9*
U		3		3.1	2.7		3.22	3.01	*6.4*	3.01	*3.8*	5.4	5.31		5.4	5.2	5.33	*1.5*	5.18	*2.1*		0.736	0.60	0.59	0.642	*10.4*	0.590	*0.3*

[1] data sources, whether compiled from studies or from single analytical method, and arranged chronologically: INAA = instrumental neutron activation analysis, LA-ICPMS = laser ablation-ICPMS.

[2] reference average reported to number of significant digits observed in most precisely measured data from literature sources.

[3] JUB average calculated from number of sample decompositions reported in Table 1 and reported to three significant digits only for illustrative purposes (see Section 5 regarding analytical precision).

***** values greater than reference average considered to include significant contributions from interfering molecular species, arising from high major element contents (Mg, Al, Ca, Mn, Fe).

Appendix 1 continued. Data in mg/kg.

	JDo-1										JMn-1						
	Garbe-Schönberg (1993)	Govindaraju (1994)	Imai et al. (1996)	Dulski (2001)	Yamamoto (2004)			*this study* HF-$HClO_4$		*this study* carbonate[4]	Terashima et al. (1995)	Imai et al. (1999)	Dulski (2001)			*this study*	
method[1]	ICPMS	compiled	compiled	ICPMS	ICPMS HF-$HClO_4$	ref. avg.[2]	*%RSD*	JUB avg.[3] (n=5)	*%RSD*	JUB avg.[3] (n=7)	*%RSD*	ICPMS	compiled	ICPMS	ref. avg.	*%RSD*	JUB avg. (n=4)	*%RSD*
Sc	0.5	0.14	0.136			0.259	*66.0*	0.195	*23.7*	0.265	*6.8*		13		13		10.1	*12.7*
Ti			7.97			7.97		8.80	*10.1*	2.10	*8.9*		6360		6360		5160	*10.5*
Co	0.3		0.168			0.234	*28.2*	1.46*	*29.6*	0.689*	*16.9*	1692	1732		1712	*1.2*	1080	*5.9*
Ni		2.9	2.9			2.9	*0.0*	11.1*	*2.8*	3.04	*5.9*	12552	12632		12592	*0.3*	7770	*12.1*
Rb			1.5	0.14		0.82	*82.9*	0.0940	*9.1*	0.0434	*25.0*	11.04	10.9	11.6	11.18	*2.7*	9.99	*3.1*
Sr	108	119	116	117		115	*3.6*	117	*5.7*	113	*2.6*	737	792	800	776	*3.6*	653	*5.5*
Y	8.9	11.2	10.3	10.4		10.2	*8.1*	10.6	*3.3*	11.0	*3.0*	106.49	111	114	110.50	*2.8*	95.1	*2.5*
Zr	0.4		6.21	0.56		2.39	*113.1*	0.567	*1.4*	0.237	*12.8*	350	344	392	362	*5.9*	318	*2.9*
Nb			0.2			0.2		0.253	*40.6*	0.0072	*12.5*	27.42	22.3		24.86	*10.3*	24.1	*10.2*
Mo	0.4		0.4			0.4	*0.0*	0.291	*7.5*	0.282	*34.3*	316	318		317	*0.3*	268	*2.0*
Cs			0.019			0.019		0.0072	*8.8*	0.0030	*19.8*	0.41	0.604	0.37	0.461	*22.2*	0.324	*3.8*
Ba	24		6.14	7		12.4	*66.4*	6.26	*19.1*	5.54	*2.5*	1702	1714	1511	1642	*5.7*	1450	*2.9*
La	7.1	7.87	7.93	7.7	7.56	7.63	*3.9*	7.75	*3.7*	7.84	*2.8*	124.88	122	121	122.63	*1.3*	109	*2.6*
Ce	1.85	2.54	2.49	2.02	2.06	2.19	*12.5*	2.07	*3.4*	2.12	*2.3*	286	277	271	278	*2.2*	274	*19.4*
Pr	0.97	0.9	0.956	1.05	0.986	0.972	*5.0*	1.01	*3.9*	1.02	*2.5*	29.72	31.4	32	31.04	*3.1*	28.3	*3.7*
Nd	4	5.33	5.25	4.09	4.21	4.58	*12.8*	4.18	*3.6*	4.25	*2.4*	127.88	137	123	129.29	*4.5*	118	*3.1*
Sm	0.73	0.84	0.788	0.68	0.686	0.745	*8.2*	0.708	*2.9*	0.712	*2.7*	29.25	30.2	27	28.82	*4.7*	26.7	*3.6*
Eu	0.15	0.19	0.176	0.162	0.154	0.166	*8.9*	0.159	*4.0*	0.161	*3.0*	7.26	7.58	7.53	7.46	*1.9*	6.60	*2.0*
Gd	0.87		0.87	0.9	0.872	0.878	*1.4*	0.910	*4.1*	0.904	*3.5*	26.05	29.8	32.1	29.32	*8.5*	27.8	*0.5*
Tb	0.12	0.12	0.116	0.12	0.113	0.118	*2.4*	0.121	*3.9*	0.121	*3.3*	4.42	4.81	4.92	4.72	*4.5*	4.27	*1.6*
Dy	0.71	1	0.814	0.75	0.747	0.804	*12.9*	0.754	*3.6*	0.755	*3.4*	25.65	28.3	28.6	27.52	*4.8*	25.3	*2.1*
Ho	0.17	0.2	0.164	0.167	0.164	0.173	*7.9*	0.168	*3.9*	0.168	*3.6*	5.49	5.76	5.58	5.61	*2.0*	4.93	*2.4*
Er	0.44		0.44	0.46	0.462	0.451	*2.3*	0.466	*3.0*	0.465	*3.2*	13.26	14.6	15.6	14.49	*6.6*	13.8	*1.8*
Tm	0.06	0.06	0.058	0.056	0.055	0.058	*3.5*	0.0550	*3.8*	0.0550	*3.9*	2.04	2.14	2.21	2.13	*3.3*	1.94	*2.1*
Yb	0.29	0.36	0.323	0.305	0.303	0.316	*7.7*	0.301	*3.3*	0.297	*3.5*	12.86	13.8	14.4	13.69	*4.6*	12.5	*2.4*
Lu	0.05	0.05	0.0494	0.043	0.042	0.0469	*7.7*	0.0426	*4.2*	0.0427	*3.9*	2.06	2.07	2.16	2.10	*2.1*	1.91	*3.1*
Hf	0.12	0.1	0.0897			0.1032	*12.2*	0.0148	*5.9*	0.0053	*16.7*	6.1	6.23	6.4	6.24	*2.0*	5.59	*4.3*
Ta			0.009			0.009		0.0137	*75.1*	0.0010	*0.0*	0.68	0.635		0.658	*3.4*	0.485	*10.6*
W			0.26			0.26		0.276	*13.5*	0.248	*17.5*	37.49	45.3		41.40	*9.4*	34.7	*7.5*
Pb	0.5	1	0.19	0.77		0.62	*49.2*	0.450	*4.4*	0.352	*23.7*	444	430	434	436	*1.4*	360	*4.3*
Th	0.04		0.0429			0.0415	*3.5*	0.0556	*3.3*	0.0521	*6.1*	11.93	11.7	13	12.21	*4.6*	10.2	*3.9*
U	0.8		0.858	0.88		0.846	*4.0*	1.03	*3.9*	0.987	*6.1*	4.81	5.01	5.3	5.04	*4.0*	4.32	*3.2*

	BHVO-2											
	Plumlee (1998)	Huang and Frey (2003)	Willbold and Jochum (2005)	Shafer et al. (2005)	Schramm et al. (2005)	Ryder (2006)	Polat et al. (2006)			*this study*		
method[1]	compiled	ICPMS	ICPMS	ICPMS	ICPMS	ICPMS	ICPMS	ref. avg.	*%RSD*	JUB avg. (n=7)	*%RSD*	
Sc	32			38	30.1	32		33.0	*9.0*	30.9	*7.4*	
Ti	16300							16300		12700	*15.3*	
Co	45			56.2	41	45.7	42	46.0	*11.8*	44.3	*6.0*	
Ni	119			137	107	115	115	119	*8.4*	124	*19.3*	
Rb	9.8	9.48	8.56	10.1	8.71	9.77	8.69	9.30	*6.3*	9.42	*5.6*	
Sr	389	399	394	407	389	396	368	392	*2.9*	379	*4.3*	
Y	26	28.3	29	25.8	23.2	28	23	26.2	*8.5*	24.3	*2.6*	
Zr	172	178	172	174	168	181	158	172	*4.0*	168	*4.9*	
Nb	18	19	18.9	19.2	16.6	15.8	15	17.5	*9.0*	17.5	*4.5*	
Mo	4			3.94				3.97	*0.8*	4.58	*14.9*	
Cs	0.1			0.11	0.09	0.11	0.09	0.10	*8.9*	0.0954	*4.6*	
Ba	130	135	131	142	129	133	125	132	*3.8*	128	*3.4*	
La	15	15.2	15.3	15.5	14.5	15.3	14.23	15.00	*2.9*	14.8	*2.8*	
Ce	38	38.4	37.6	38.4	35.3	37.5	35.73	37.28	*3.1*	36.8	*3.1*	
Pr	5.35	5.57	5.31	5.72	5.1	5.39	4.96	5.34	*4.5*	5.18	*2.9*	
Nd	25	24.9	24.5	24.8	23.4	24.6	22.8	24.3	*3.2*	24.0	*3.6*	
Sm	6.2	6.16	6.04	5.99	5.9	6.12	5.69	6.01	*2.7*	5.96	*3.1*	
Eu	2.07	2.03	2.05	2.07	1.96	2.07	1.96	2.03	*2.3*	2.03	*3.2*	
Gd	6.3	6.13	6.23	6.48	5.9	6.32	6.13	6.21	*2.7*	6.11	*2.1*	
Tb	0.9	0.963	0.933	0.9	0.9	0.959	0.89	0.921	*3.1*	0.908	*2.9*	
Dy	5.31	5.3	5.29	5.25	5.2	5.34	5.07	5.25	*1.6*	5.18	*3.0*	
Ho	1.04	1.01	0.964	1.03	0.95	1.01	0.93	0.991	*4.0*	0.960	*2.5*	
Er	2.54	2.5	2.49	2.49	2.4	2.53	2.39	2.48	*2.2*	2.49	*2.6*	
Tm	0.33	0.35	0.321	0.34	0.32	0.34	0.31	0.330	*3.9*	0.316	*3.0*	
Yb	2	2.05	1.95	2.01	1.91	2.03	1.84	1.97	*3.5*	1.90	*2.7*	
Lu	0.28	0.286	0.269	0.28	0.26	0.278	0.25	0.272	*4.4*	0.272	*3.1*	
Hf	4.1	4.42	4.2	4.58	4.4	4.38		4.35	*3.6*	4.27	*4.7*	
Ta	1.4	1.22	1.08	1.23	1.09	0.686	0.92	1.089	*19.8*	1.06	*6.7*	
W	0.21			0.29				0.25	*16.0*	0.228	*6.7*	
Pb	1.6	1.53	1.8	1.22	1.58	2.89	1.58	1.74	*28.4*	1.63	*9.2*	
Th	1.2	1.3	1.13	1.32	1.2	1.22	1.53	1.27	*9.5*	1.23	*4.7*	
U	0.403	0.446	0.403	0.45	0.42	0.425	0.4	0.421	*4.6*	0.430	*3.4*	

[1] data sources, whether compiled from studies or from single analytical method, and arranged in chronologically.

[2] reference average reported to number of significant digits observed in most precisely measured data from literature sources.

[3] JUB average calculated from number of sample decompositions reported in Table 1 and reported to three significant digits only for illustrative purposes (see Section 5 regarding analytical precision), with exception of some elements for JDo-1 carbonate decomposition method.

[4] data for JDo-1 includes measured concentrations as determined using both the HF-$HClO_4$ and carbonate (HNO_3) sample decomposition methods (see Fig. 1). Note that Ni data for carbonate decomposition solely determined from the ^{62}Ni isotope.

* values greater than reference average considered to include significant contributions from interfering molecular species, arising from high major element contents (Mg, Al, Ca, Mn, Fe).

Appendix 2. Interferences due to major elements

Appendix 2 contains figures illustrating significant molecular interferences for atomic masses <100 that arise from high concentrations of the major rock forming elements Mg, Al, Ca, Mn, and Fe. Interferences observed for Ni, Sr, Y, Zr, Nb, and Mo are discussed. Data are presented following the format used in Fig. 11 of the main text, which describes significant interferences observed for ^{59}Co due to high Mg and Ca.

The identification of interfering molecular species was accomplished by analyzing artificial solutions that contained a single element over a range of concentrations (1-500 mg/kg). Analyzed concentrations of Mg, Al, Ca, Mn, and Fe were 1, 10, 50, and 100 mg/kg. Using a typical dilution factor of 1000 for many dissolved rock samples, the 1-500 mg/kg concentration range chosen for the artificial solutions represents rock powders that would contain 0.1-50% of the major elements. Studies of interferences due to Mg, Ca, and Fe included an additional 500 mg/kg solution, as these three elements may routinely approach concentrations of 20-80% (wt.% oxide) in many geologic samples. The Mg, Al, Ca, Mn, and Fe solutions were produced in two different acid matrices, 0.5 M HCl and 0.5 M HNO_3, as these are the acid concentrations used for diluting dissolved rock powders. Data indicate that different acid matrices can have a profound effect upon the magnitude of potential interfering molecular species.

Whereas interferences were identified using solutions that contained 1-500 mg/kg of the major elements, data are presented as functions of the concentration of Mg, Al, Ca, Mn, and Fe in weight percent oxides. This is because major element concentrations are frequently determined on solid samples by analytical methods such as XRF, and these data are typically reported as oxide wt.%. For any given plot in Appendix 2, the wt.% for major element concentrations is directly correlative with the Mg, Al, Ca, Mn, and Fe solution concentrations of 1-500 mg/kg.

The measured interferences at a given atomic mass are presented as both raw data in cps (left vertical axis), and as calculated concentration in mg/kg (right vertical axis). The raw data in cps reflects uncorrected ICPMS intensities, and it should be noted that these intensities will vary as a function of daily instrument performance, frequently by as much as 20% (RSD). The raw cps data also varies as a function of

the concentration of the major element being considered, since as concentrations increase (e.g., to 500 mg/kg) the high TDS content of the solution begins to suppress analyte intensities, similar to that observed for rock samples that are only minimally diluted before analysis.

The quantification of the observed interferences as concentrations in mg/kg allows predictions to be made regarding the potential impact these interferences might have upon trace metal determinations. For example, as the CaO content in a carbonate rock increases from 10% to 40%, then Ni concentrations determined in an HCl acid matrix would be expected to increase from ~2.5 mg/kg to ~6 mg/kg, due to Ca interferences on ^{60}Ni (Fig. A2.1). These calculated interferences in concentration units of m/kg are obtained from the long term average instrument response as determined from the 10 µg/kg calibration standard (described in Fig. 2, Section 4). For example, the ^{60}Ni isotope has an average instrument response of 2158 cps/µg·kg^{-1} in 0.5 M HCl, and a sample containing 14% CaO and diluted 1000x would be expected to generate an CaO(H) interference of ~6700 cps on mass 60. Therefore, Ni quantified in this sample using measurement of the ^{60}Ni isotope would be erroneously overestimated by approximately 3.1 µg/kg (i.e., 2158/6700 = 3.1).

It should be noted that, similar to estimates of interferences based upon raw data (cps), interference estimates reported as concentrations (mg/kg) will vary with instrument performance. As the long term average instrument response for the 10 µg/kg calibration standard varies by as much as 30% (RSD), and this is the basis for the calculation of the interference magnitude in mg/kg, then these calculated concentrations will vary similarly.

Data for interferences are presented for the following isotopes in the order; ^{60}Ni, ^{62}Ni, ^{88}Sr, ^{89}Y, ^{90}Zr, ^{91}Zr, ^{93}Nb, and ^{95}Mo. Regardless of the element of interest, or the specific interferences that inhibit accurate concentration measurements of these elements, the key factor is always the relative abundance of the interfering species to the isotope of interest. In other words, the greatest analytical difficulties arise when trying to quantify small concentrations of an element in the presence of large concentrations of interfering elements. As a result, while some interferences may be large, e.g., several mg/kg in the case of Ca_2 and ArCa on Sr, the effect of these interferences is minor if the element being measured is abundant in the sample (e.g., 115 mg/kg Sr in the JDo-1 dolomite).

The case of Ni determinations in carbonates has been mentioned previously, and the conclusion is that accurate Ni determinations in Ca- and Mg-rich rocks are only possible in HNO_3 acid matrices and by utilizing the ^{62}Ni isotope. Figures A2.1 through A2.4 illustrate the numerous Ca and Mg interferences on ^{60}Ni and ^{62}Ni. Additionally, Figure A2.5 demonstrates that Al_2O_3 abundances typical for shales (10-15%) that are analyzed in 0.5 M HCl are expected to contribute 2-3 mg/kg to the measured Ni concentration. The data suggest that ^{62}Ni, when measured in a HNO_3 acid matrix, offers the best isotope for Ni determinations in Mg-,Ca-, and Al-rich samples. However, ^{62}Ni is a low abundance isotope of Ni (3.63%), and will produce a relatively low signal response during ICPMS measurements, and this factor must be considered during attempts to quantify Ni.

Figure A2.6 illustrates significant interferences on ^{88}Sr due to various Ca and presumed Ar species ($^{40}Ca^{48}Ca$, $^{40}Ar^{48}Ca$, and $^{44}Ca^{44}Ca$). These interferences exist regardless of the acid matrix used to prepare the samples for ICPMS analysis. Concentrations of Sr in many rocks are in the range of 50 to several hundred mg/kg (App. 1), and as Ca and Sr are both alkaline earth metals, their concentrations in many rocks vary proportionally. As a result, even though high Ca contents may produce an interference of 1-3 mg/kg on Sr, this frequently is of no great significance as Sr concentrations themselves may be high in the sample (e.g., ~115 mg/kg in the case of the JDo-1 dolomite).

Interferences on Y due to high Fe contents in samples are presented in Figure A2.7 for informative purposes only. The impact of these interferences is likely to be small (~0.10 mg/kg) relative to typical Y contents in rocks (~10-50 mg/kg, see App. 1), and will not be discussed further.

Figures A2.8 and A2.9 demonstrate that significant interferences due to Mn and Fe may adversely impact determinations of Zr. The ^{90}Zr isotope suffers an interference of several mg/kg in 0.5 M HCl due to $^{55}Mn^{35}Cl$ (Fig. A2.8). The effects of high Fe contents on measurements of ^{91}Zr are much greater due to $^{56}Fe^{35}Cl$, and interferences of 10-20 mg/kg would be expected in Fe-rich samples such as IFs (Fig. A2.9). Smaller, but still significant effects are noted for $^{40}Ca^{16}O^{35}Cl$ interferences on ^{91}Zr. These effects would be minimized by the use of HNO_3 as the diluting acid. Based upon these observations, the ^{91}Zr isotope is not recommended for most rock types, unless the use of HCl is avoided, or if Ca- and Fe-poor, Mn-rich samples require analysis.

Potential interferences on monoisotopic ^{93}Nb are presented in Fig. A2.10, and are very similar to those described for ^{91}Zr. This is due to the substitution of the ^{37}Cl isotope for ^{35}Cl in the Fe and Ca molecular species listed above (i.e., $^{56}Fe^{37}Cl$ and $^{40}Ca^{16}O^{37}Cl$). Unlike Zr, Nb offers no additional isotope for analysis, and the low natural abundance of Nb exacerbates the problem of interfering species due to major elements. Accurate Nb analyses are unlikely in Fe- and Ca-rich rock types, unless the use of HCl is avoided. However, as discussed in Section 7.1 of the main text, Nb is unstable in pure HNO_3 acid matrices, and the presence of HCl stabilizes Nb, as well as other HFSE like Ta, in solution long enough for accurate ICPMS measurements. As mentioned previously, future work examining the optimum acid matrix for ICPMS determinations of Nb and Ta is recommended.

The last element that appears to suffer from major element interferences is Mo, and in particular Mn interferences on the ^{95}Mo isotope (Fig. A2.11). Similarly to the Ca-Ar interferences on ^{88}Sr, Mn affects measured intensities for ^{95}Mo regardless of the acid matrix. This is apparently due to the $^{55}Mn^{40}Ar$ molecular species, which forms independently of the bulk solution composition. Whereas the use of HCl appears to suppress $^{55}Mn^{40}Ar$ formation (Fig. A2.11), the magnitude of the interference is significant regardless of the acid matrix (e.g., ~3-6 mg/kg at 20-30% MnO). It is therefore recommended that the ^{97}Mo isotope be used for Mo determinations in rock samples that contain more than a few percent MnO, unless Mo concentrations in the sample are the range of 50 to hundreds of mg/kg.

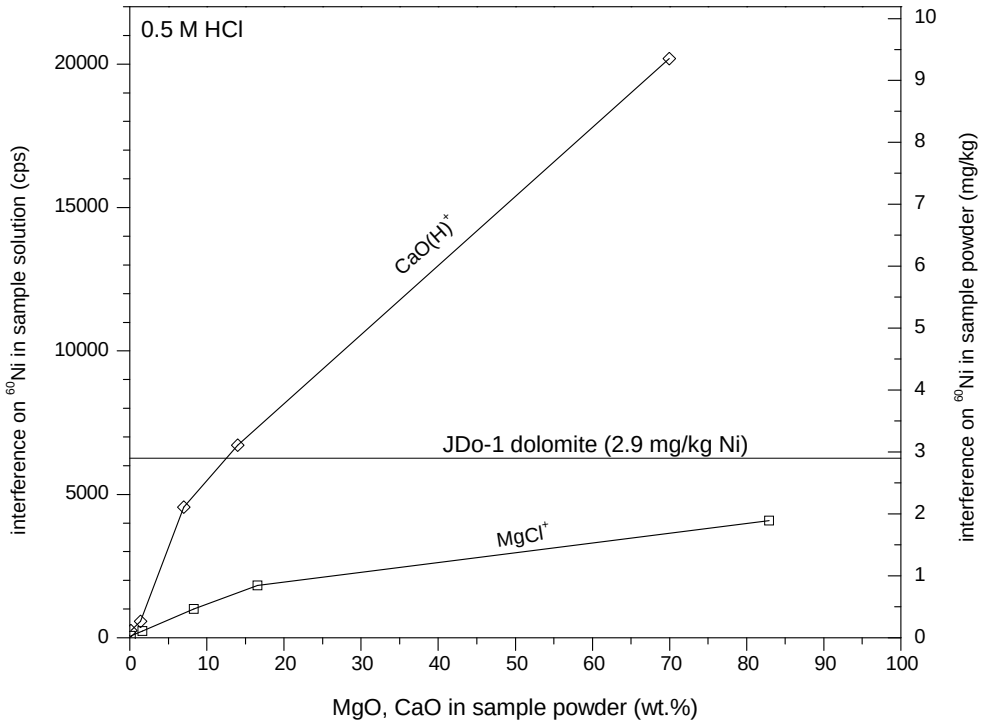

Figure A2.1. Interferences observed at mass 60 (Ni) in 0.5 M HCl due to sample Mg and Ca content. JDo-1 contains 18.4% MgO and 34.0% CaO, effectively prohibiting in carbonate rocks determinations of Ni concentrations that are similar to JDo-1 (2.9 mg/kg Ni).

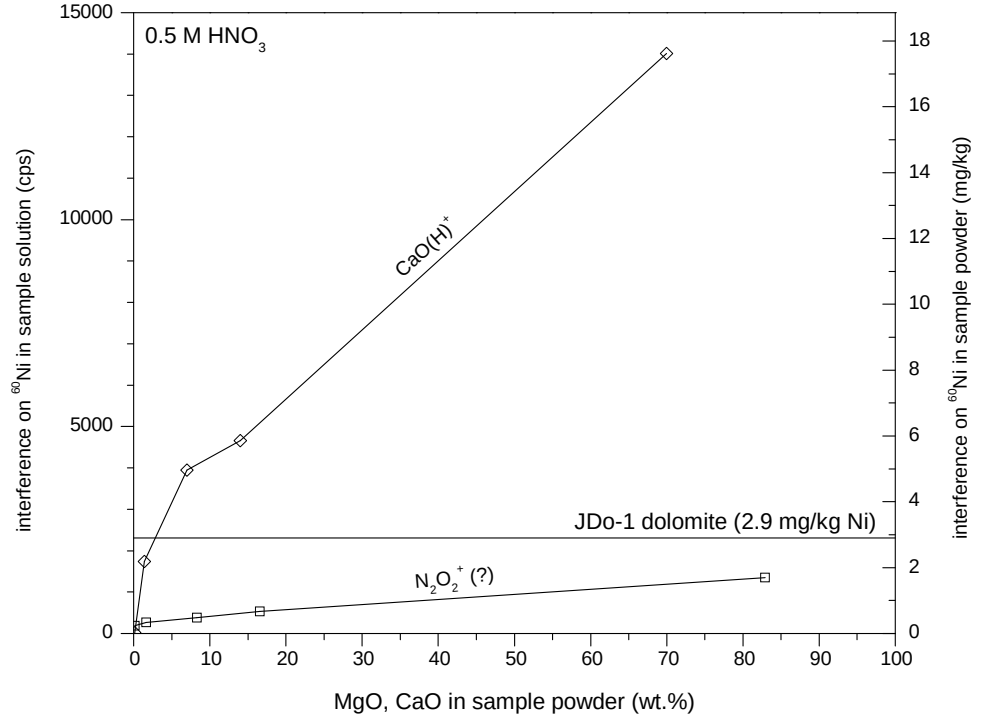

Figure A2.2. Interferences observed at mass 60 (Ni) in 0.5 M HNO_3 due to sample Mg and Ca content. Use of HNO_3 effectively removes MgCl interference, but does not affect the dominant CaO(H) interference.

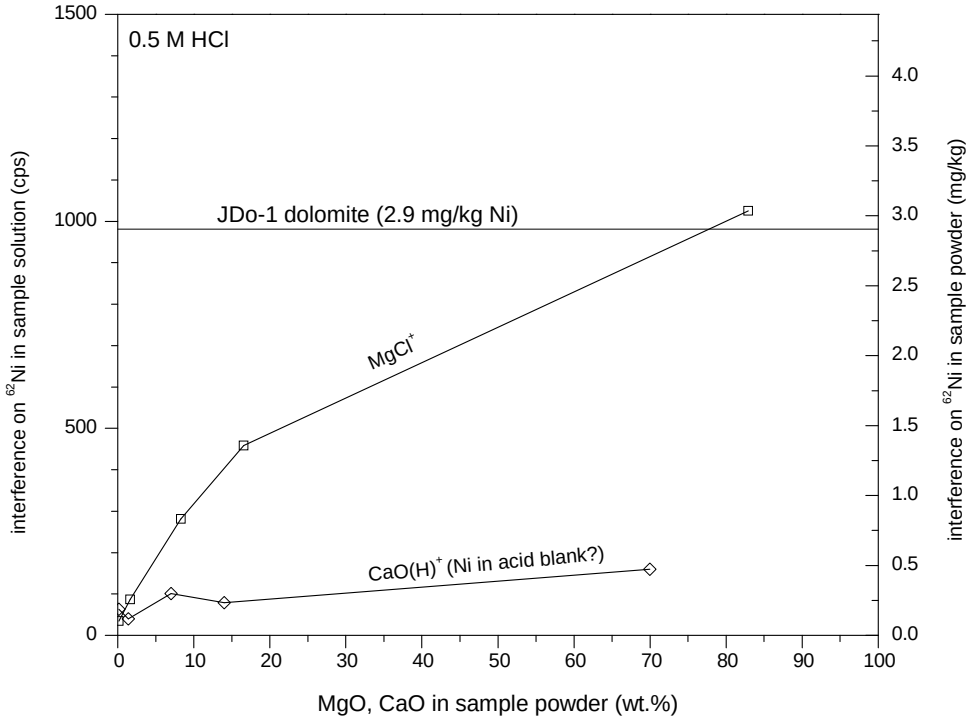

Figure A2.3. Interferences observed at mass 62 (Ni) in 0.5 M HCl due to sample Mg and Ca content. JDo-1 contains 18.4% MgO and 34.0% CaO, effectively prohibiting in carbonate rocks determinations of Ni concentrations that are similar to JDo-1 (2.9 mg/kg Ni).

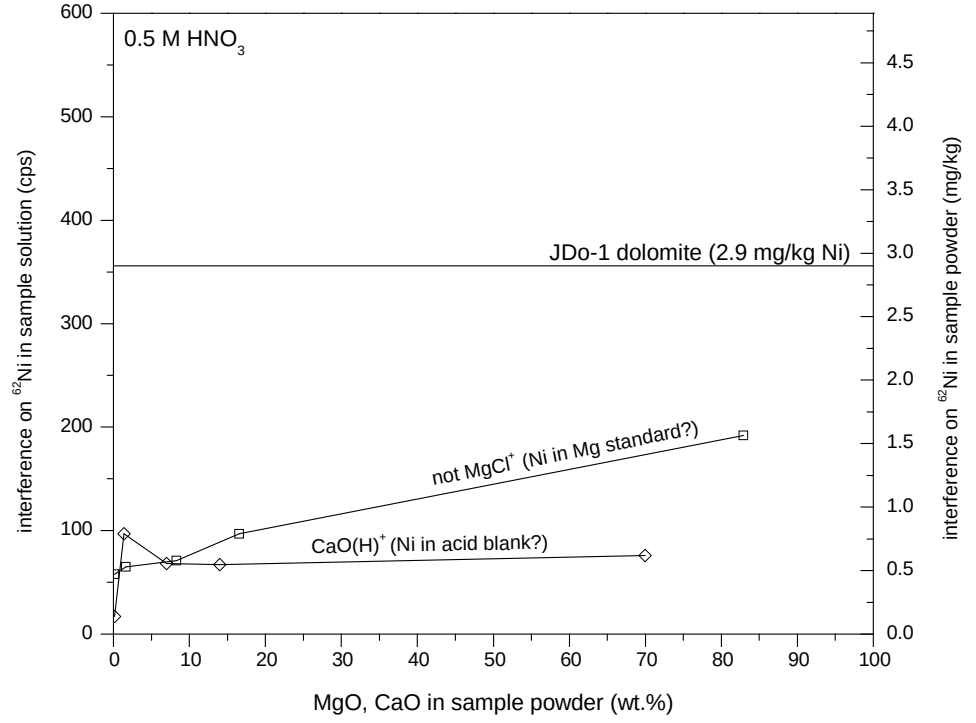

Figure A2.4. Interferences observed at mass 62 (Ni) in 0.5 M HNO_3 due to sample Mg and Ca content. When monitored in HNO_3 matrices, the ^{62}Ni isotope is likely the most useful for trace Ni determinations in carbonate rocks, though the low abundance of ^{62}Ni (3.63%), which generates low ICPMS signal intensities, must be considered.

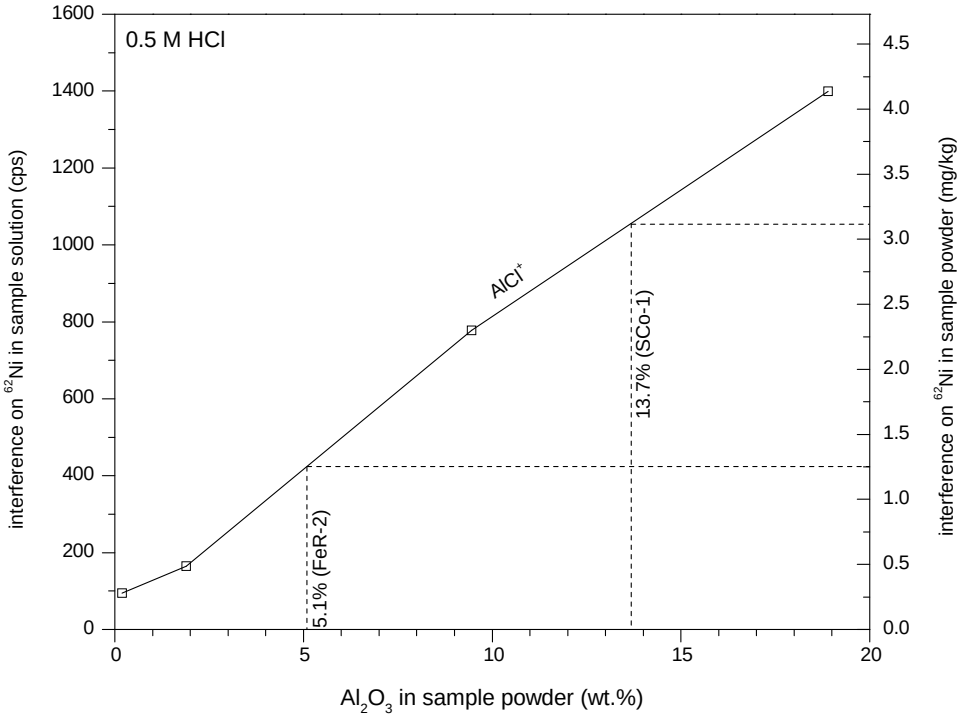

Figure A2.5. Interferences observed at mass 62 (Ni) in 0.5 M HCl due to sample Al content. Shown are Al contents of two common CRMs that contain similar Ni (23 mg/kg for FeR-2, and 26 mg/kg for SCo-1). The lower Al/Ni of FeR-2 is expected to allow reasonable Ni determinations using ^{62}Ni, however the poor agreement between ^{60}Ni and ^{62}Ni argues against this (see App. 1). The greater Al/Ni of SCo-1 significantly contributes to higher than expected Ni determinations in SCo-1 (see App. 1).

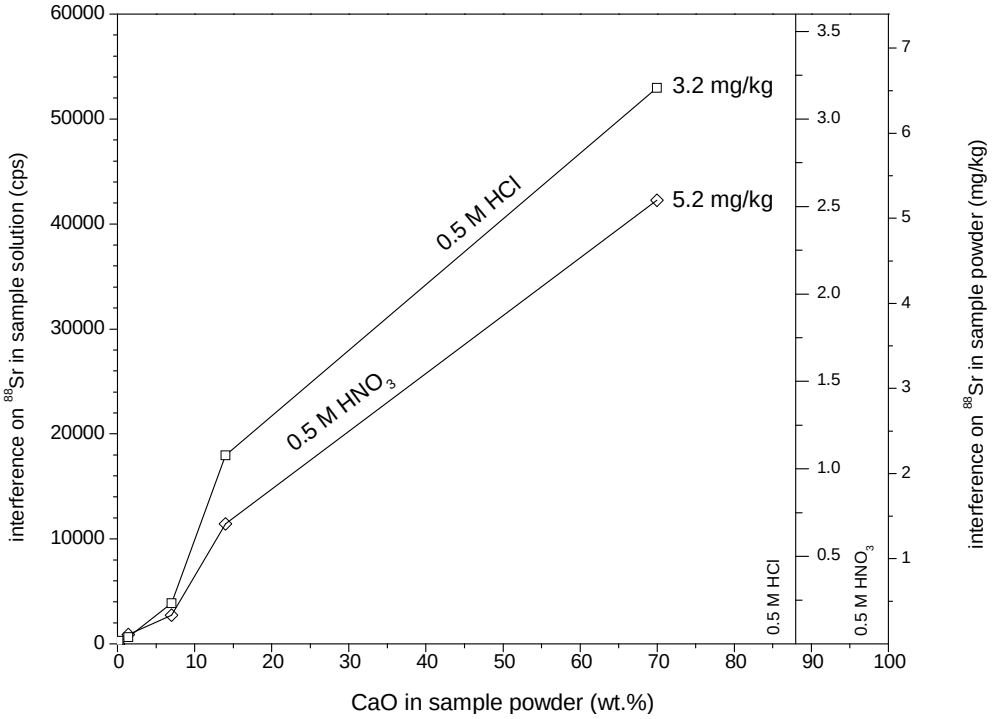

Figure A2.6. Interferences observed at mass 88 (Sr) in both 0.5 M HCl and HNO_3 as a function of Ca content. Note right vertical axis denotes two concentration scales, dependent upon acid matrix. Significant interferences due to probable combinations of ^{40}Ca^{48}Ca, ^{40}Ar^{48}Ca, and ^{44}Ca^{44}Ca exist regardless of acid matrix. Note that the discrepancy between acid matrices regarding the magnitude of the interference arises from different ICPMS signal response (sensitivity) in HCl and HNO_3. Caution should be exercised when interpreting Sr concentrations below ~75 mg/kg in samples with high Ca contents.

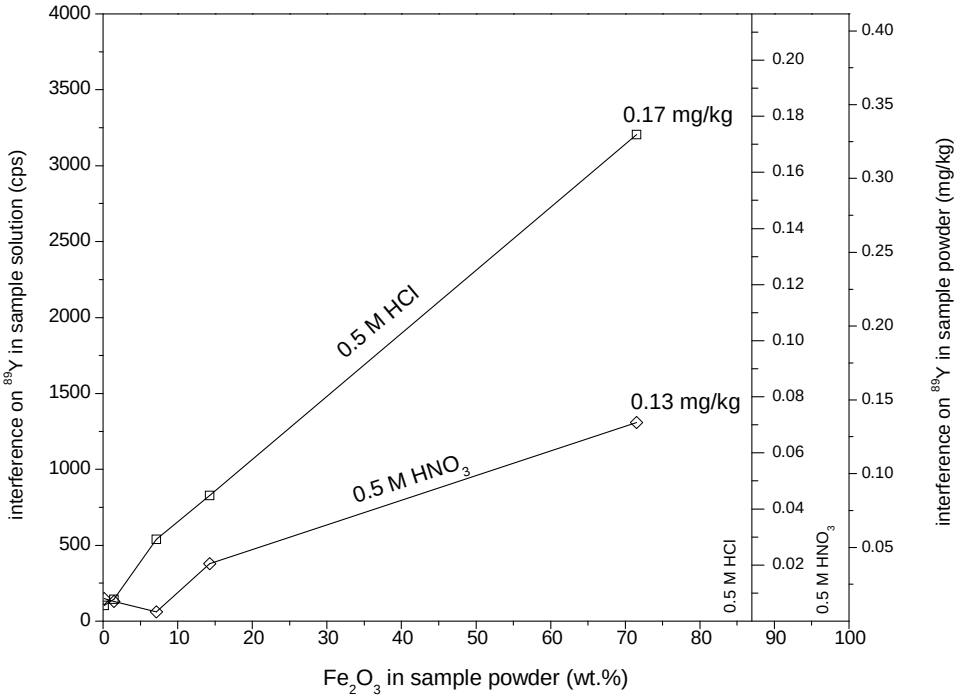

Figure A2.7. Interferences observed at mass 89 (Y) in both 0.5 M HCl and HNO_3 as a function of Fe content. Note right vertical axis denotes two concentration scales, dependent upon acid matrix. A minor $^{54}Fe^{35}Cl$ interference exists in 0.5 M HCl, and interferences are linear, though small, for both acid matrices, perhaps reflecting small Y contamination in artificial Fe solution. Concentrations of Y in all Fe-rich CRMs are 8-12 mg/kg, suggesting that Fe-interferences in these CRMs are not significant.

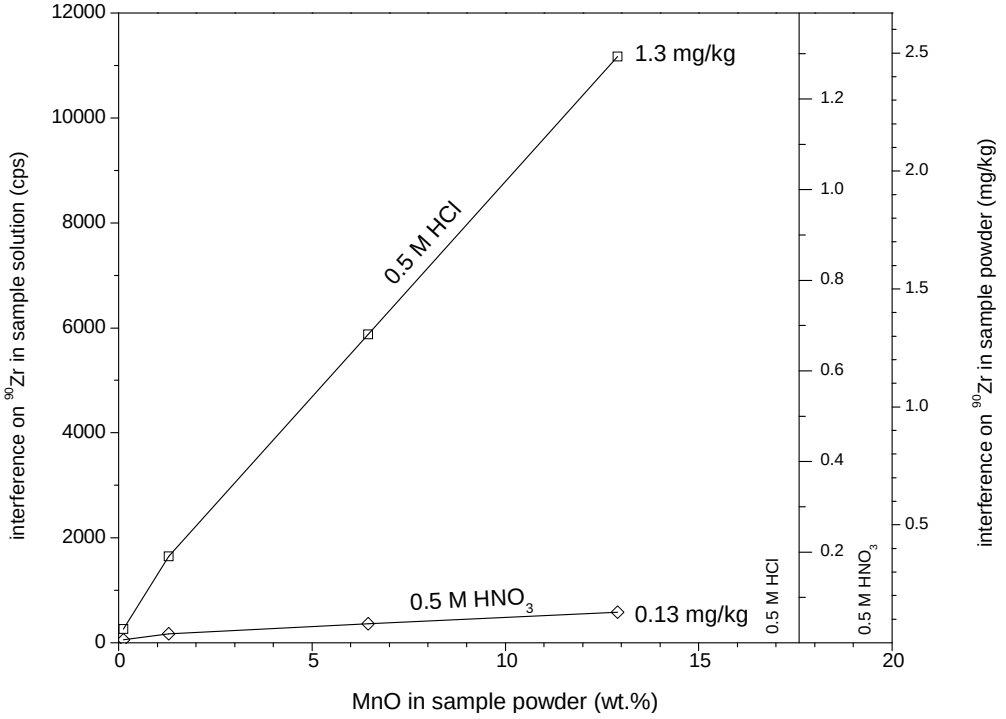

Figure A2.8. Interferences observed at mass 90 (Zr) in both 0.5 M HCl and HNO_3 as a function of MnO content. Note right vertical axis denotes two concentration scales, dependent upon acid matrix. A strong $^{55}Mn^{35}Cl$ interference exists in 0.5 M HCl. Concentrations of MnO in Fe-Mn crusts (and Mn ores) may exceed 30%, and extrapolation of the data suggest possible interferences on ^{90}Zr of several mg/kg.

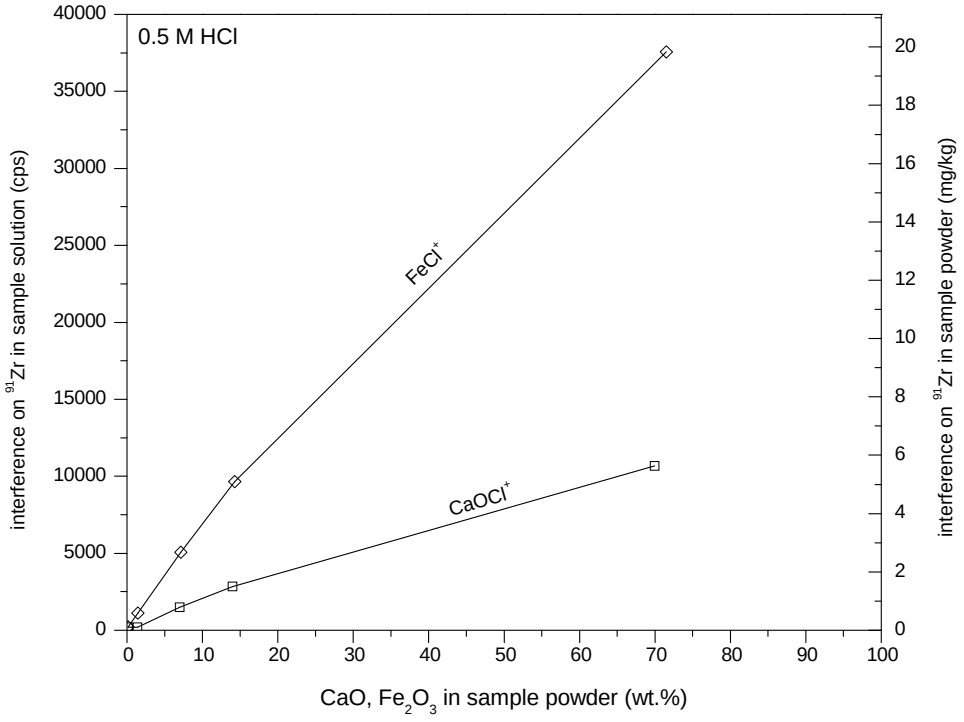

Figure A2.9. Interferences observed at mass 91 (Zr) in 0.5 M HCl as a function of both Ca and Fe content. Interferences in HNO_3 acid not observed. Significant interferences produced at low concentrations (<10%) for both Ca and Fe, precluding accurate Zr determinations using this isotope in iron-formations and many carbonate rocks. Use of ^{91}Zr for quantification likely useful only in samples with very low Fe and Ca contents, very high Zr abundances (100's of mg/kg), or for carbonate free Mn-rich samples (Mn-ores) where ^{90}Zr is unreliable (see Fig. A2.8).

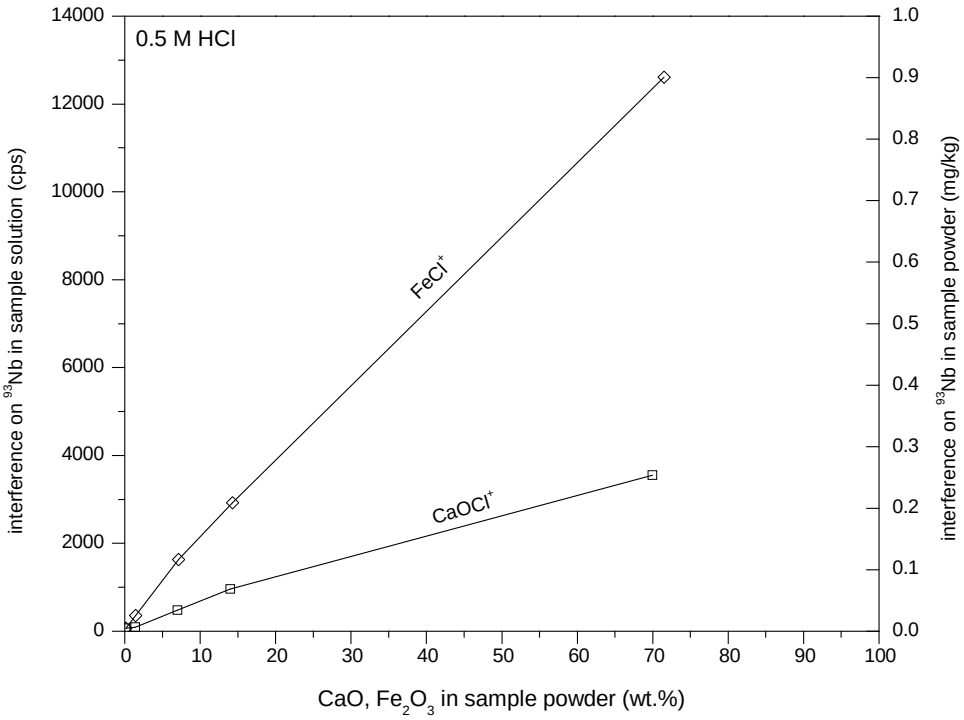

Figure A2.10. Interferences observed at mass 93 (Nb) in 0.5 M HCl as a function of both Ca and Fe content. Interferences in HNO_3 acid not observed. Interferences produced for both Ca and Fe, and though small, are significant for rocks with low Nb contents (e.g., the iron-formation IF-G and dolomite JDo-1).

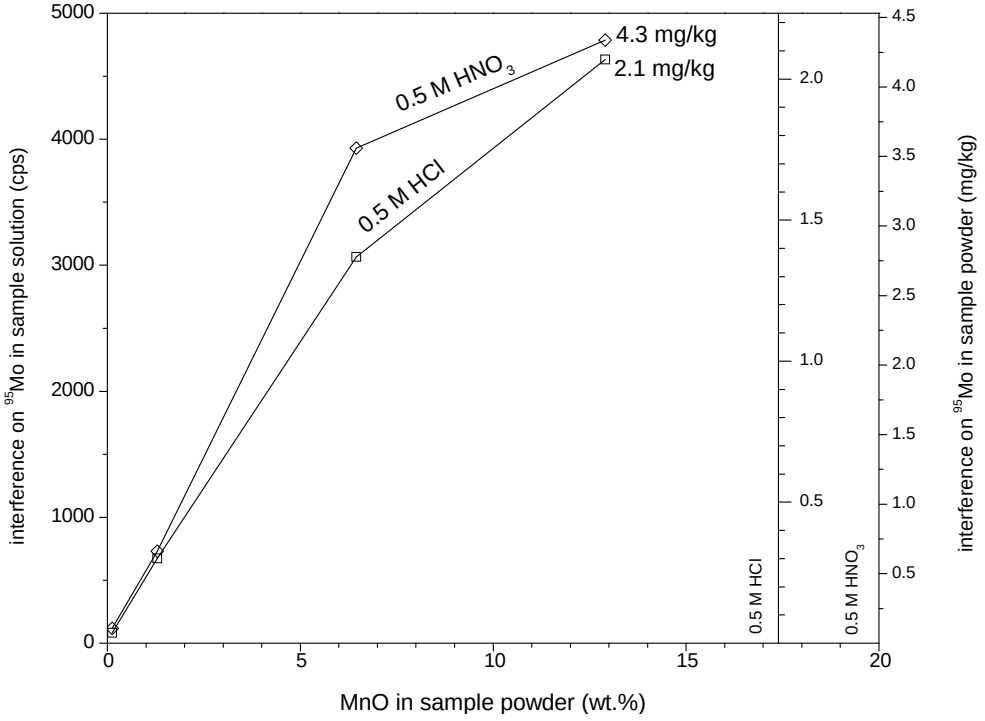

Figure A2.11. Interferences observed at mass 95 (Mo) in both 0.5 M HCl and HNO_3 as a function of MnO content. Note right vertical axis denotes two concentration scales, dependent upon acid matrix. Significant interferences produced for both HCl and HNO_3 acid matrices. For Mn-bearing (>5%), relatively Mo-poor (<10 mg/kg) samples, use of the ^{95}Mo isotope is cautioned for Mo concentration determinations, and use of ^{97}Mo, which suffers no apparent major element interferences, is recommended.